CERN–TH 6131/91
ISN 37/91

THE NON-RELATIVISTIC THREE-BODY PROBLEM FOR BARYONS

Jean–Marc Richard
CERN, Theory Division
CH 1211 Genève 23
and
Institut des Sciences Nucléaires
Université Joseph Fourier–CNRS–IN2P3
53, avenue des Martyrs
F–38026 Grenoble Cedex

Abstract

The non-relativistic quark model, when applied to baryons, involves an interesting 3-body problem where the constituents are bound by a confining potential. We review various possible methods which can be used for solving the 3-quark problem accurately and discuss selected applications to baryon spectroscopy. We also present the state of the art on the rigorous properties concerning the level order of the 3-body spectrum, the dependence of the binding energy on the quark masses, and the inequalities relating the 3-body to 2-body binding energies.

CERN–TH 6131/91
August 12, 1991.

Chapter 1

BARYONS AND THE THREE-BODY PROBLEM

1.1 Who is afraid of the three-body problem ?

The 3-body and, more generally, the few-body problem sometimes has the bad reputation of being a jungle where non-experts are quickly discouraged, whereas specialists enjoy endless debates on technical improvements concerning scattering or bound-state equations, with much attention paid to the computational consequences and very little concern about the underlying physics.

This is, of course, a wrong impression. To give just one example, many aspects of the nuclear forces have been discovered from the few-nucleon systems such as tritium or helium, and one of the most striking challenges in strong interaction physics remains the understanding of the 3-nucleon binding energy and form factor [1].

In the present review, I shall try to convince the reader that the non-relativistic quantum 3-body problem, as it appears in baryon spectroscopy, is reasonably easy to handle, involves amazing pieces of mathematics, and provides crucial tests of quark dynamics.

In fact, the 3-body problem which is needed for the non-relativistic models of baryons is relatively simple compared to most other 3-body problems encountered in atomic or nuclear physics: in the He atom ($\alpha\, e^- e^-$), or in the positronium ion ($e^+ e^- e^-$), asymmetry occurs already in the potential energy; in ^{3}H or ^{3}He nuclei, one should account, at the very beginning, for the complicated spin and isospin dependence of the internucleon potential. Three quarks in a baryon have an antisymmetric colour wave function and thus behave as bosons bound by a symmetric potential which does not depend much on spin. Such a simple situation occurs only for molecular clusters like $(^4\mathrm{He})^3$ with, however, a more sharply varying potential [2].

The quark model is a mine of exercises for those who have the chance of teaching quantum mechanics, once they have exhausted the charm of the Stark effect and other examples borrowed from atomic physics. The baryon sector is particularly rich. For instance, it illustrates how antisymmetrization is important, in a situation intermediate

between the trivial 2-body case and the limit of a large number of constituents, where second quantization techniques are applied. It is also amazing to show that, if (qqq) is bound by a pairwise potential, $V = \sum v(r_{ij})$, whose strength is half of that of the $q\bar{q}$ potential, i.e. $v(r) = \frac{1}{2} V_{q\bar{q}}(r)$, then the energies or masses of ground-state mesons and baryons fulfil the inequality $2(qqq) \geq 3(q\bar{q})$. This is a simple consequence of the variational principle, as shown in Chapter 9.

1.2 Old, present, and future baryon spectroscopy

The successful picture of the baryon spectrum was one of the most striking of the early achievements of the quark model and its precursors based on unitary symmetries [3]. Everyone remembers the prediction of the Ω^- particle, the strangeness $S = -3$ member of the decuplet of $J^P = (3/2)^+$ baryons. Simple formulae relate the masses of ground-state baryons of increasing strangeness. We shall come back to their microscopic grounds in Chapters 8 and 11.

Besides this "horizontal" scanning of the mass spectrum, the excitation patterns i.e. the "vertical" aspects of the spectrum were quite well described in terms of the harmonic-oscillator model [4]. More meson nucleon resonances have been identified meanwhile [5], all fitting quite well into the picture of the 3-quark model with spin, radial, or orbital excitations [6].

These "early" baryons approximately obey $SU(3)_F$ flavour symmetry: the wave function, including colour, spin, space, and flavour degrees of freedom, is antisymmetric under the exchange of any pair of quarks. The changes induced by the mass difference between the d and the u quarks or between the ordinary and the strange quarks can be treated as small corrections.

A large part of the present experimental activity concerns baryons with heavy flavours, Qqq or Qqs or Qss, where q means u or d . These states, with their helium-like structure, are much more asymmetric: the two light quarks are rotating rather fast around a flavoured quark which remains almost static.

In the near future, double-charm baryons QQq should provide interesting information on quark dynamics with the superposition, within the same hadron, of the slow motion of two heavy quarks experiencing the short-range QCD potential, and of the fast motion of a light quark around them [7, 8].

With triple-charm baryons, we will recover an exact antisymmetry of the wave function. The ccc baryons will exhibit an interesting spectrum of narrow levels [9, 10]. In quarkonium spectroscopy, excitations become broad only when they lie above the Zweig-allowed threshold $Q\overline{Q} \to Q\bar{q} + q\overline{Q}$. Likewise, triple-charm baryons are narrow until one reaches the threshold for flavour splitting: $QQQ \to QQq + \bar{q}Q$. The first excitations, which lie below this threshold, will be stable under strong interactions, with only electromagnetic decay $QQQ^* \to QQQ + \gamma$. Of course, each unit of charm added to a baryon implies a great suppression factor in the production rate and, a more dramatic effect, an increase of the eventual multiplicity of the decay and thus,

by orders of magnitude, an increase in the difficulty of reconstructing the events.

Although this is completely out of the scope of the present review, one may underline the fact that these flavoured baryons will provide extremely interesting information on weak interactions. The difference between the $D^+(c\bar{d})$ and $D^\circ(c\bar{u})$ lifetimes tells us that, while decaying, the charm quark does not ignore its environment. To test the role of W exchange or annihilation or "penguin" diagrams, it is crucial to measure the lifetimes and main branching ratios of the various species of charmed baryons [8].

In both charm and non-charm sectors, new problems have been raised in hadron spectroscopy. One question concerns the existence of localized "diquark" clusters inside baryons [11]. Another hot topic concerns the possible "hybrid" states qqqg with a valence gluon and, possibly, exotic quantum numbers. We find it important to analyse carefully the dynamics of "ordinary" qqq baryons before concluding the need for new configurations.

We shall adopt here the naming scheme of the Particle Data Group. In the charm strange sector, we denote by Ξ_c a csq state of "Λ type", i.e. whose light-quark pair is mostly in a spin $S = 0$ state; Ξ_c' the csq state of spin $\frac{1}{2}$ and of "Σ type", i.e. with the sq pair mostly in a spin $S = 1$ state; Ξ_c^* the spin $\frac{3}{2}$ state. Double star will be given to any radial and orbital excitations.

The ground state baryons made of ordinary, strange, or charmed quarks are listed in Table 1.1. The beauty analogues are easily extrapolated. The isospin wave functions will be given in Section 3.6.

1.3 Outline of the review

For pedagogical reasons, we shall start this review with very elementary reminders of the 2-body problem, followed by some mathematical developments on the 2-body Schrödinger equation, which will be useful for their 3-body analogues discussed in Chapters 8, 9 and 10.

The 3-body problem is introduced in Chapter 3 through the simple but powerful harmonic-oscillator model. A natural continuation is the perturbed oscillator where anharmonicity corrections are treated to first order, leading to interesting regularities of the energy shifts: this will be presented in Chapter 8.

In Chapter 4, we use the harmonic oscillator for the expansion of the wave function in the general case. This is the first of the variational methods we shall discuss.

Then we shall present in some detail the method of the hyperspherical expansion which, in many aspects, appears as a generalization of the harmonic oscillator, sharing most of its symmetries but relaxing the Gaussian character of the radial wave functions.

Chapter 6 deals with the alternative method based on the Faddeev equations in configuration space, which can be applied very successfully to confining interactions.

Next comes a discussion on the quark–diquark approximation which is suited for angular excitations of ordinary baryons, and a discussion on the Born–Oppenheimer approximation which provides a simple picture of double-charm baryons QQq .

Table 1.1: Ground-state baryons with ordinary, strange or charmed flavour. Here q denotes u or d, and qq or qqq stands for a properly symmetrized or antisymmetrized isospin wave function. Masses are in MeV.

Name	Content	Spin	Isospin	Mass
N	qqq	$\frac{1}{2}$	$\frac{1}{2}$	939
Δ	qqq	$\frac{3}{2}$	$\frac{3}{2}$	1232
Λ	sqq	$\frac{1}{2}$	0	1116
Σ	sqq	$\frac{1}{2}$	1	1192
Σ^*	sqq	$\frac{3}{2}$	1	1384
Ξ	ssq	$\frac{1}{2}$	$\frac{1}{2}$	1315
Ξ^*	ssq	$\frac{3}{2}$	$\frac{1}{2}$	1532
Ω	sss	$\frac{3}{2}$	0	1672
Λ_c	cqq	$\frac{1}{2}$	0	2281
Σ_c	cqq	$\frac{1}{2}$	1	2455
Σ_c^*	cqq	$\frac{3}{2}$	1	
Ξ_c	csq	$\frac{1}{2}$	$\frac{1}{2}$	2460
Ξ_c'	csq	$\frac{1}{2}$	$\frac{1}{2}$	
Ξ_c^*	csq	$\frac{3}{2}$	$\frac{1}{2}$	
Ω_c	css	$\frac{1}{2}$	0	2740
Ω_c^*	css	$\frac{3}{2}$	0	
Ξ_{cc}	ccq	$\frac{1}{2}$	$\frac{1}{2}$	
Ξ_{cc}^*	ccq	$\frac{3}{2}$	$\frac{1}{2}$	
Ω_{cc}	ccs	$\frac{1}{2}$	0	
Ω_{cc}^*	ccs	$\frac{3}{2}$	0	
Ω_{ccc}	ccc	$\frac{3}{2}$	0	

While discussing several variational expansions or possible approximation schemes, we shall present numerical illustrations based on the simple potential model $\sum r_{ij}^{\beta}$, with selected values of β and the same quark masses, so that the merits of the various methods can easily be compared.

In Chapter 8, we summarize the existing rigorous results on the level order of the 3-body problem with confining interactions. We treat nearly harmonic potentials and nearly hyperscalar potentials and study how the zero-order degeneracy is broken. Then we compare the first radial and the first orbital excitations for a large class of local potentials.

Chapter 9 deals with mass inequalities. First, we analyse the mass dependence of the binding energy and derive inequalities between baryons of different flavour content which are bound by the same potential. Then we present inequalities which relate the binding energies of baryons and mesons when one assumes a simple relation between the quark antiquark potential in mesons and the potential between three quarks in baryons.

In Chapter 10, we present some bounds on the short-range correlations inside baryons. This is an important quantity for hyperfine splittings and weak decays. Unfortunately, the existing rigorous results are restricted to the case of equal-mass quarks.

In Chapter 11, we apply the non-relativistic quark model to the phenomenology of the baryon spectrum and present various results on tests of flavour independence, the short-range character of the hyperfine interaction, etc.

1.4 A guide to related references

The present report is by no means a review of the 3-body quantum problem. We restrict ourselves here to a confining and symmetric potential interaction, the symmetry being broken only through the quark masses. Other aspects of the 3-body problem, in particular scattering with finite-range potentials, can be found in textbooks [12] or in the "Few-Body Conference" proceedings [1].

Since in this report we are dealing mostly with the technical aspects of the underlying 3-body problem, we shall be rather brief on the derivation of the quark interaction from QCD. Lattice simulations, bag models, or string pictures, for instance, provide some support for the "Coulomb-plus-linear" potential or its power-law approximation $A + Br^{\beta}$ which we shall use for numerical illustrations or phenomenological applications. The question of possible 3-body forces, which deserves some attention, will be raised in Chapter 9, where we discuss the links between mesons and baryons.

Throughout this review, we shall very often disregard spin-dependent forces, especially when their complexity goes beyond a simple spin spin potential (usually considered as short-range and treated perturbatively). The Lorentz nature of confinement is, of course, a key issue in quark dynamics [13]. Our goal here is to provide a solid framework for handling the 3-body problem with central forces. Extensions to include

spin orbit or tensor forces are straightforward, though they involve some complicated algebra.

There are, of course, other approaches to hadron spectroscopy. Bag models [14], QCD sum rules [15], and lattice simulations [16] have been discussed extensively. The differences with respect to the Non-Relativistic Quark Model (NRQM) are obvious. More interesting, perhaps, are the convergences: some static limits of bags or of lattice calculations provide us with the effective interquark potential for $Q\overline{Q}$ or QQQ systems, to be compared with the empirical potentials used in NRQM. There are links between various non-perturbative quantities such as: vacuum expectation values in sum rules, string constant, slope of the linear potential, bag pressure, and energy gaps in phase transitions, which are tentatively computed on lattices.

The NRQM clearly suffers from weaknesses: non-relativistic dynamics, absence of explicit quark antiquark pairs, instantaneous interaction, etc. It is easy to list in advance good reasons why it should never work. It seems more challenging to understand within QCD studies why the NRQM actually describes the hadron world so well.

Chapter 2

THE TWO-BODY PROBLEM

2.1 Introduction

In this chapter, we present a brief review of the 2-body problem, as it enters into the non-relativistic quark model of mesons. Experts can easily skip this chapter and read instead more advanced reviews on quarkonium [17, 18, 19, 20]. Note, however, that we present some mathematical results on the level ordering, level spacing, and mass dependence of the energy, which will be useful for the generalization to the 3-body case.

Important concepts will be introduced for non-experts: Jacobi variables, scaling laws, numerical solutions, i.e. the basic tools for few-body calculations.

2.2 Basic equations

The simplest model of mesons describes them as quark–antiquark bound states of the non-relativistic Hamiltonian

$$H = \frac{\vec{p}_1^{\,2}}{2m_1} + \frac{\vec{p}_2^{\,2}}{2m_2} + V(r_{12}). \tag{2.2.1}$$

V, the central part of the quark–antiquark potential, is flavour independent. It may be supplemented by spin–spin, spin–orbit, or tensor components to describe the fine or hyperfine structure of the multiplets, but we shall disregard these corrections here.

The centre-of-mass motion is removed by introducing the Jacobi variables

$$\vec{R} = \frac{m_1\vec{r}_1 + m_2\vec{r}_2}{m_1 + m_2} \tag{2.2.2}$$

and

$$\vec{r} = \vec{r}_2 - \vec{r}_1 \tag{2.2.3}$$

as well as $\vec{P}$ and $\vec{p}$, chosen as conjugates of $\vec{R}$ and $\vec{r}$, respectively. Thus

$$H = \frac{\vec{P}^{\,2}}{2(m_1+m_2)} + \widetilde{H} = \frac{\vec{P}^{\,2}}{2(m_1+m_2)} + \frac{\vec{p}^{\,2}}{\mu} + V(r), \tag{2.2.4}$$

where $\mu = 2m_1m_2/(m_1+m_2)$. Solving the eigenvalue equation $\widetilde{H}\Psi = E\Psi$ is most often achieved in spherical coordinates $\vec{r} = (r, \theta, \varphi)$. Owing the rotational invariance of the potential, bound states can be chosen with a well-defined angular momentum l. As explained in any standard textbook [21], introducing

$$\Psi(\vec{r}) = \frac{u(r)}{r} Y_l^m(\theta, \varphi) \tag{2.2.5}$$

leads to the radial equation

$$u''(r) - \frac{l(l+1)}{r^2}u(r) + \mu[E - V(r)]u(r) = 0. \tag{2.2.6}$$

Note that we use $\hbar = c = 1$ very often in this review. States have the following indices: l for the angular momentum, m for the magnetic number (eigenvalue of l_z), and n for the number of nodes of $u(r)$ in $]0, +\infty[$. Note that E and $u(r)$ do not depend on m. The standard scheme for indices consists thus of: $\Psi_{n,l,m}(\vec{r})$, $u_{n,l}(r)$, and $E_{n,l}$. Some indices are omitted whenever possible.

2.3 Properties of the wave functions

If $V(r)$ is not too singular near the origin

$$r \to 0 \implies u(r) \propto r^{l+1}, \tag{2.3.1}$$

For large r, $u(r)$ decreases exponentially. If $V(r) = Br^\beta$, with $\beta > 0$, then

$$r \to \infty \implies u(r) \propto \text{polynomial} \times \exp\left(-\frac{2}{\beta+2}\sqrt{\mu B}r^{1+\beta/2}\right). \tag{2.3.2}$$

The radial function of the $(n+1)^{\text{th}}$ state of given l, $u_{n,l}(r)$, has n nodes $r_i^{(n)}$, $(i = 1, n)$ and according to the Sturm–Liouville theorem [22]

$$0 < r_1^{(n+1)} < r_1^{(n)} < r_2^{(n+1)} \cdots < r_n^{(n)} < r_{n+1}^{(n+1)}. \tag{2.3.3}$$

The $u_{n,l}$ satisfy the orthonormality condition

$$\int_0^\infty u_{n,l}u_{n',l}\mathrm{d}r = \delta_{n,n'}. \tag{2.3.4}$$

Note that the u's can be chosen as real if V is real. For computing the leptonic width or the hyperfine splitting of S-states, one often needs the probability of finding the quark and the antiquark at the same place, i.e.

$$\delta_n = |\Psi_{n,0,0}(0)|^2 = \frac{u'^2_{n,0}}{4\pi}. \tag{2.3.5}$$

The following identity, attributed to Schwinger [17]

$$\delta_n = \frac{\mu}{4\pi}\int_0^\infty V'(r)u_{n,0}^2(r)\mathrm{d}r \tag{2.3.6}$$

turns out to be quite useful. While a rough variational or numerical solution often gives very bad estimates of $\Psi_{n,0,0}(0)$, it becomes suprisingly accurate when δ_n is computed through the above integral.

2.4 Scaling laws

Power-law potentials exhibit simple scaling properties [17, 23]. If

$$V(r) = B\epsilon(\beta)r^\beta \tag{2.4.1}$$

is an attractive potential (B is positive and ϵ is the sign function) and $E_{n,l}(\mu, B)$ the energy of a level of given n and l, then

$$E_{n,l}(\mu, B) = E_{n,l}(1,1)\mu^{-\beta/(\beta+2)}B^{2/(\beta+2)} \tag{2.4.2}$$

and the corresponding wave function scales as

$$u(r;\mu,B) = r_0^{-1/2}u(r/r_0;1,1), \tag{2.4.3}$$

where the distance

$$r_0 = (\mu B)^{-1/(\beta+2)} \tag{2.4.4}$$

plays the role of a kind of "Bohr radius" for the potential (2.4.1).

In a logarithmic potential, $V = B\ln r$, the size of the wave function is governed by (2.4.3) with $r_0 = (\mu B)^{-1/2}$, whereas the levels experience an overall shift when changing μ, since

$$E_{n,l}(\mu, B) = BE_{n,l}(1,1) - \frac{B}{2}\ln\mu - \frac{B}{2}\ln B. \tag{2.4.5}$$

For fixed B, the levels spacings are independent of the reduced mass μ.

Scaling properties exist, in fact, for many potentials. For instance, to study the differents cases of the popular "Coulomb-plus-linear" potential

$$V(r) = -\frac{a}{r} + br \tag{2.4.6}$$

with various masses, it is sufficient to study the one-parameter family corresponding to $a = \mu = 1$ and various values of b.

2.5 Numerical solutions

There are hundreds of possible methods for solving the radial equation (2.2.6) for confining potentials, and many new suggestions can be found by reading journals of mathematical physics or computational physics as well as the American Journal of Physics and similar publications [24]. Let us describe briefly two methods: the Numerov method and the Multhopp method.

In the simplest of the direct numerical solutions of the radial equation (2.2.6), one separates the numerical integration in r at a given energy E, and the search for the eigenvalues. Hartree [25], for instance, gave an efficient method based on the Numerov algorithm, which nowadays can easily be implemented on computers or even on programmable calculators. Let us rewrite Eq. (2.2.6) as

$$u''(r) = f(r)u(r) \tag{2.5.1}$$

and search for an outgoing $u_{\mathrm{out}}(r)$ solution starting from $u_{\mathrm{out}}(r) \propto r^{l+1}$ near the origin and an ingoing solution $u_{\mathrm{in}}(r)$ starting from $u_{\mathrm{in}}(r) \propto \exp(-\int\sqrt{f}\mathrm{d}r)$ at large r. Using the Taylor expansion and the above differential equation, one easily shows that the values u_n of u_{out} (or of u_{in}) at equally spaced points $r = nh$ fulfil

$$u_{n+1}\left(1 - \frac{h^2}{12}f_{n+1}\right) + u_{n-1}\left(1 - \frac{h^2}{12}f_{n-1}\right) = 2u_n\left(1 + \frac{5h^2}{12}f_n\right) + \mathrm{O}(h^6), \tag{2.5.2}$$

leading to a very accurate (and stable) iterative algorithm for computing the u_n's.

Now the $(n+1)^{\mathrm{th}}$ energy E_n is determined as follows. A trial energy E is above E_n if the corresponding outgoing solution has at least $(n+1)$ nodes in $]0, r_c[$, where r_c is the classical turning point, for which $E = V(r_c)$. One ends quickly with an interval $a_n < E_n < b_n$ in which E_n is the only possible eigenvalue. In this interval, E_n is the only value for which one can match the incoming and the outgoing solutions as well as their first derivative. One can always impose

$$u_{\mathrm{in}}(r_0) = u_{\mathrm{out}}(r_0) \quad \text{and} \quad \int_0^{r_0} u_{\mathrm{out}}^2(r)\mathrm{d}r + \int_{r_0}^\infty u_{\mathrm{in}}^2(r)\mathrm{d}r = 1. \tag{2.5.3}$$

If $u'_{\mathrm{in}}(r_0) \neq u'_{\mathrm{out}}(r_0)$ for some trial energy $\tilde{E}$, then a better estimate of E_n is given by

$$\tilde{E} \longrightarrow \tilde{E} + \mathrm{d}\tilde{E} = \tilde{E} - \frac{u(r_0)}{\mu}[u'_{\mathrm{in}}(r_0) - u'_{\mathrm{out}}(r_0)] \tag{2.5.4}$$

Iterative applications of this recipe converge very rapidly towards E_n. Equation (2.5.4) may be derived from the Wronskian theorem, whose many uses in quantum mechanics are well described in Ref. [21]. Alternatively, one may consider that the mismatching solution $\{u(r) = u_{\mathrm{out}}$ for $0 < r < r_o$ and $u(r) = u_{\mathrm{in}}(r)$ for $r_o < r < \infty\}$ corresponds exactly to the eigenvalue $\tilde{E}$ for the modified potential

$$\tilde{V}(r) = V(r) + A\delta(r - r_0) \tag{2.5.5}$$

with

$$\mu A u(r_0) = u'_{\rm in}(r_0) - u'_{\rm out}(r_0). \tag{2.5.6}$$

When first-order perturbation theory is applied to V starting from the solution of $\tilde{V}$, one gets exactly the prescription (2.5.4).

The application of matrix methods to quarkonium calculations was proposed independently by Basdevant et al.[26] and Olsson et al.[27] (and, probably, many others!). One of the many possible variants is the following. The transformation

$$x = \frac{r}{r + r_0}, \quad r = r_0 \frac{x}{1 - x} \tag{2.5.7}$$

leads to the new equation

$$-\frac{1}{\mu}\frac{(1-x)^4}{r_0^2} v''(x) + V[r(x)]v(x) = Ev(x), \tag{2.5.8}$$

where

$$v(x) = (1 - x)u[r(x)]\sqrt{r_0} \tag{2.5.9}$$

is submitted to $v(0) = v(1) = 0$. The value of r_0 should be chosen to be of the order of the typical radius of the wave function. One now computes v from its Fourier expansion

$$v(x) = \sum_{i=1}^{N} a_i \sin(i\pi x). \tag{2.5.10}$$

For finite N, all information is contained in the a_i's and thus in the values v_j of $v(x)$ at the points $x_j = j/(N + 1)$, since

$$a_i = \frac{2}{N+1} \sum_{j=1}^{N} v_j \sin \frac{ij\pi}{N+1}. \tag{2.5.11}$$

One ends with the matrix eigenvalue equation

$$\sum_i A_{ij} v_j = E v_i, \tag{2.5.12}$$

where

$$A_{ij} = \frac{(1-x_i)^4}{\mu r_0^2} \frac{2\pi^2}{N+1} \left(\sum_{k=1}^{N} k^2 \sin k\pi x_i \sin k\pi x_j \right) + \delta_{ij} V[r(x_i)], \tag{2.5.13}$$

which is a matrix with "hidden" symmetry. Indeed, the simple change of function

$$w(x) = \frac{v(x)}{(1-x)^2} = \frac{u[r(x)]}{1-x}\sqrt{r_0}, \tag{2.5.14}$$

which, not surprisingly, corresponds to the simple normalization

$$\int_0^1 w^2(x) \mathrm{d}x = 1, \tag{2.5.15}$$

leads to the new matrix equation $\sum B_{ij} w_j = E w_i$ where, again, $w_j = w(j/(N + 1))$, and the matrix

$$B_{ij} = \frac{(1-x_i)^2(1-x_j)^2}{\mu r_0^2} \frac{2\pi^2}{N+1} \left(\sum_{k=1}^{N} k^2 \sin k\pi x_i \sin k\pi x_j \right) + \delta_{ij} V[r(x_i)] \tag{2.5.16}$$

is now symmetric. The diagonalization provides an approximation of the N first levels. A level of given radial number n is well described as soon as $N \gg n$, and the convergence as $N \to \infty$ is reasonably achieved, provided the parameter r_0 has been chosen to be of the right order of magnitude. The wave functions are mutually orthogonal, to the extent that the scalar product is replaced by its discretized approximation

$$\int_0^\infty u_n(r) u_{n'}(r) \mathrm{d}r = \sum_i w_n(x_i) w_{n'}(x_i). \tag{2.5.17}$$

The tail of the wave function as $r \to \infty$ is, however, not too well reproduced, since the exponential vanishing of $u(r)$ is replaced by a zero of finite order for $w(x)$ at $x = 1$. The main advantage of this method, for our purpose, is its immediate generalization to coupled equations. This will be very useful for Faddeev, hyperspherical, or Born-Oppenheimer approaches to the 3-body problem.

For illustration, we display in Table 2.1 the lowest eigenvalues of the linear potential $V(r) = r$ in the case $\mu = 1$, as a function of the dimension N of the matrix (2.5.16). The exact eigenvalues are given by the negative of the zeros of the Airy function [28]. The parameter r_0 is chosen as being $\alpha_0^{-1/2}$ where $\exp(-\alpha_0 r^2/2)$ is the best variational approximation of Gaussian type to the ground state.

2.6 Semi-classical approximation

For high radial number n or orbital momentum l, the Wentzel–Kramers–Brilloin (WKB) method is known to provide an excellent approximation. In fact, the WKB approximation works already surprisingly well for small values of n or l. We refer here to the review of Quigg and Rosner [17], who present a detailed study of the WKB approximation for confining potentials. Let us simply recall here some basic results.

In the WKB approximation, the eigenenergies $E_{n,0}$ of S-waves are given by

$$\int_0^{r_c} \sqrt{\mu[E - V(r)]} \mathrm{d}r = \left(n + \frac{3}{4}\right)\pi, \tag{2.6.1}$$

Table 2.1: Eigenvalues of the linear potential computed with an increasing number of points in the discretization procedure described in Section 2.5. Note that the parameter r_0 is optimized for the $n = 0$ state of any given l. Another choice could improve the convergence for radial excitations.

(n,l)	$N=8$	$N=16$	$N=32$	Exact
(0,0)	2.33727	2.33810	2.33811	2.33811
(1,0)	4.10306	4.08848	4.08795	4.08795
(2,0)	5.25794	5.50337	5.52057	5.52056
(0,1)	3.34873	3.36120	3.36125	3.36125
(1,1)	5.03186	4.88522	4.88445	4.88445
(0,2)	4.21405	4.24820	4.24818	4.24818

where r_c is the classical turning point, defined by $V(r_c) = E$. This formula is exact for the harmonic oscillator. There exists a variant, appropriate for potentials which are singular at the origin, and this modified formula is exact in the Coulomb case [17].

For positive power-law potentials Br^β, Eq. (2.6.1) and its generalizations to orbital excitations result in a simple analytic expression ($\mu = B = 1$) [17]

$$E_{n,l}^{\text{WKB}} = \left[\frac{2\beta\sqrt{\pi}\Gamma(\frac{3}{2}+\frac{1}{\beta})}{\Gamma(\frac{1}{\beta})}(n+\frac{3}{4}+\frac{l}{2})\right]^{2\beta/(\beta+2)} . \tag{2.6.2}$$

For the radial excitations with $l = 0$ in a linear potential ($\beta = 1$), one gets the results shown in Table 2.2, where a comparison is made with the exact eigenvalues.

Table 2.3 shows the WKB approximation *vs.*compared with the exact numerical value for the leading Regge trajectory ($n = 0$) of the linear potential. Also shown is the variational approximation obtained from the trial wave function $r^{l+1}\exp(-\frac{1}{2}\alpha r^2)$ borrowed from the harmonic oscillator, with the result

$$E_{0,l}^{\text{var}} = 3\left(\frac{3}{2}+l\right)\left[\frac{\Gamma(2+l)}{\Gamma(\frac{3}{2}+l)}\frac{1}{3+2l}\right]^{3/2} . \tag{2.6.3}$$

The quality of the WKB approximation at large orbital momentum is good, but not impressive.

2.7 Level order

We now present some mathematical properties of 2-body Hamiltonians. In one or two dimensions, any attractive potential supports at least one bound state (some local attraction is sufficient) [29]. In three dimensions, this is not true any more. For

Table 2.2: WKB and exact energies for S-wave energy levels in the potential $V(r) = r$

n	WKB	Exact
0	2.3202	2.3381
1	4.0818	4.0879
2	5.5172	5.5206
3	6.7844	6.7867
4	7.9425	7.9441
5	9.0214	9.0226
6	10.0391	10.0402
7	11.0077	11.0085
8	11.9353	11.9360
9	12.8281	12.8288

instance, a Yukawa potential $V = -B\exp(-\alpha r)/r$, with $\alpha > 0$, does not provide any bound state if B is too small. For $\alpha = 0$, on the other hand, one gets the Coulomb potential, which has an infinite number of bound states, with $E < 0$, as well as a continuum spectrum of positive energies. In simple models of quarkonium, we are dealing with confining potentials, which support an infinite number of bound states.

From the Sturm–Liouville theorem [22] and the positivity of the centrifugal barrier $l(l+1)/r^2$, the ground state always corresponds to $n = 0$ and $l = 0$ (the local character of $V(r)$ is crucial here) and the energy increases with n or with l. The relative position of the radial and orbital excitations depends, however, on the shape of $V(r)$. Figure 2.1 shows the location of the first levels for $V = -1/r$, $V = r$, and $V = r^2$. The ordering and spacing patterns are rather different for these simple examples. For more general potentials, the following results have been obtained:

i) The "Coulomb" theorem

If $V(r) = -r^{-1}$, then $E_{n,l} = E_{n+1,l-1}$. Remember that n denotes the number of nodes, not the principal quantum number of atomic physics, which is $n + l + 1$. The following theorem was proved, first for the lowest levels or for small perturbations around the Coulomb case, and later in a general way [30]

$$\Delta V(r) \gtrsim 0 \quad \Longrightarrow \quad E_{n,l} \lesssim E_{n+1,l-1}. \tag{2.7.1}$$

Note that one hardly elaborates a necessary condition on the potential for such a spectral property, since the binding energies do not uniquely determine the potential.

The Coulomb theorem ensures that the quarkonium potential $V(r) = -a/r + br$ gives the desired ordering $\Psi' > \chi$ in charmonium and $\Upsilon' > \chi_b$ in $b\bar{b}$. The condition $\Delta V > 0$ can be read as the charge seen by the quark increasing when the distance to the antiquark increases, in agreement with the ideas of asymptotic freedom and confinement.

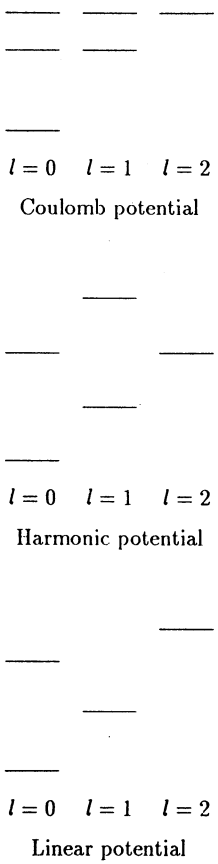

Figure 2.1: First levels of the Coulomb, harmonic, and linear potentials

Table 2.3: WKB, exact and variational energies for the lowest Regge trajectory in the potential $V(r) = r$

l	WKB	Exact	Variat.
0	2.3202	2.3381	2.3448
1	3.2616	3.3612	3.3678
2	4.0818	4.2482	4.2544
3	4.8263	5.0509	5.0569
4	5.5172	5.7944	5.8001
5	6.1671	6.4930	6.4985
6	6.7844	7.1559	7.1612
7	7.3748	7.7894	7.7946
8	7.9425	8.3982	8.4032

The theorem also has applications in atomic physics. If a low-lying muon μ^- starts experiencing the size of a nucleus A, then one expects $E_{1,0} < E_{0,1}$, or $E_{2S} < E_{2P}$ in the usual notations, for the Aμ^- system, as it is observed. On the other hand, for alkali atoms, i.e. for an external electron in the field of a nucleus surronded by close spherical shells of electrons, $E_{1,0} > E_{0,1}$, again in agreement with observation.

ii) The "harmonic-oscillator" theorem

If $V(r) = r^2$, then $E_{n,l} = E_{n+1,l+2}$. This degeneracy is broken in the following way [30]:

$$\frac{\mathrm{d}^2 V}{\mathrm{d}(r^2)^2} \gtrless 0 \quad \Longrightarrow \quad E_{n,l} \lesseqgtr E_{n+1,l+2}. \tag{2.7.2}$$

For instance, if one describes the charmonium spectrum with the Coulomb-plus-linear model, one obtains the right ordering Ψ''(D-state) > Ψ'(S-state). The theorem (2.7.2) will be useful in the 3-body case since the 2-body systems factorize out in the limit of harmonic forces.

iii) Regge trajectory

In the harmonic-oscillator case, $E_{0,l} \propto (3 + 2l)$ grows linearly in l. The following result has been established [31]:

$$Y(r) \equiv \frac{\mathrm{d}}{\mathrm{d}r}\left[\frac{1}{r}\frac{\mathrm{d}V}{\mathrm{d}r}\right] \gtrless 0 \quad \Longrightarrow \quad E(0,l) \text{ concave (or convex) in } l. \tag{2.7.3}$$

iv) Spacing of radial excitations

In the harmonic-oscillator case, at fixed l, the energy $E_{n,l} \propto (3 + 4n + 2l)$ grows linearly in n. This means that $\Delta = 0$, where $\Delta \equiv E_{n+1,l} + E_{n-1,l} - 2E_{n,l}$. If one considers a potential $V(r)$, one can restrict oneself to the $l = 0$ case, and, otherwise, incorporate the centrifugal barrier into V. The following results have been established.

If $V(r) = r^2 + v(r)$ is nearly harmonic, i.e. if $v(r)$ is treated to first order, then [32]

$$Z(r) \equiv \frac{\mathrm{d}}{\mathrm{d}r}\left[\frac{\mathrm{d}}{\mathrm{d}r}\left(\frac{1}{r}\frac{\mathrm{d}v}{\mathrm{d}r}\right)\right] \gtrless 0 \text{ and } \lim_{r\to 0} r^3 v = 0 \implies \Delta \gtrless 0. \tag{2.7.4}$$

Counter examples show that this result does not always hold beyond perturbation theory.

2.8 Mass dependence of the binding energy

Let us once more consider the reduced Hamiltonian $\widetilde{H}$ of Eq. (2.2.4) and denote by $E(\mu)$ one of the eigenenergies and by $\phi(\mu)$ the corresponding wave function. Obviously

$$\frac{\mathrm{d}E}{\mathrm{d}\mu} < 0. \tag{2.8.1}$$

More precisely, from the Feynmann Hellmann theorem [33]

$$\frac{\mathrm{d}E}{\mathrm{d}\mu} = -\frac{1}{\mu^2}\left\langle \phi(\mu) \mid \vec{p}^{\,2} \mid \phi(\mu)\right\rangle \equiv -\frac{1}{\mu}T(\mu). \tag{2.8.2}$$

We also note that $\widetilde{H}$ depends linearly on μ^{-1}. We can thus use the general theorem that if a Hamitonian depends linearly upon a parameter λ, its ground state energy is concave in λ

$$H = A + \lambda B \implies \frac{\mathrm{d}^2 E_0}{\mathrm{d}\lambda^2} \leq 0. \tag{2.8.3}$$

This follows from second-order perturbation theory or from the variational principle [33]. Here, once the constituent masses are added, one gets inequalities between the ground-state masses of any given angular momentum l

$$\mathcal{M}_{0,l}(m_1, m_1) + \mathcal{M}_{0,l}(m_2, m_2) \leq 2\mathcal{M}_{0,l}(m_1, m_2), \tag{2.8.4}$$

or

$$(\mathrm{Q}\overline{\mathrm{Q}})_l + (\mathrm{q}\bar{\mathrm{q}})_l \leq 2(\mathrm{Q}\bar{\mathrm{q}})_l. \tag{2.8.5}$$

For instance, neglecting spin effects,

$$\varphi(\mathrm{s}\bar{\mathrm{s}}) + \mathrm{J}/\Psi(\mathrm{c}\bar{\mathrm{c}}) < 2D_{\mathrm{s}}^{*}(\mathrm{c}\bar{\mathrm{s}}), \tag{2.8.6}$$

in agreement with experiment [5] ($1.02 + 3.10 < 2 \times 2.11\,\mathrm{GeV}$). Similarly, one can derive

$$\mathrm{b}\bar{\mathrm{s}} + \mathrm{c}\bar{\mathrm{d}} < \mathrm{c}\bar{\mathrm{s}} + \mathrm{b}\bar{\mathrm{d}}. \tag{2.8.7}$$

The convexity inequality (2.8.4) cannot be written for radial excitations: one should instead consider the sum of the n first levels.

Chapter 3

THE HARMONIC-OSCILLATOR MODEL

3.1 Introduction

Although the aim of this review is to discuss elaborate methods for solving the 3-body problem, the very simple harmonic-oscillator model deserves some presentation. First, it has played an essential role in the development of the quark model, with, in particular, the pioneering works of Dalitz [34] and Greenberg [4] and the very complete and convincing studies of the baryon spectrum by Dalitz and Horgan [35], Isgur and Karl [36], Gromes et al.[37], Cutkosky and Hendrick [38], Hey et al.[6] and many others [39]. The harmonic-oscillator model may also serve as a basis or a starting point for accurate variational methods. Its understanding is anyhow necessary for getting some insight into the 3-body problem and, in particular, into the difficulties associated with the symmetrization of the wave functions.

3.2 The linear oscillator

The one-dimensional harmonic oscillator is treated in any standard textbook [21]. The Hamiltonian

$$H = \frac{P^2}{2m} + \frac{1}{2}KX^2 \tag{3.2.1}$$

is rewritten as

$$H = \frac{1}{2}\sqrt{\frac{K}{m}}h = \frac{1}{2}\sqrt{\frac{K}{m}}\left[-\frac{\mathrm{d}^2}{\mathrm{d}x^2} + x^2\right] \tag{3.2.2}$$

using the scaling transformation of Section 2.4 which reads here $x = (Km)^{1/4}X$. The reduced Hamiltonian has eigenvalues

$$\epsilon_n = 1 + 2n, \quad n = 0, 1, 2... \tag{3.2.3}$$

and eigenfunctions

$$\begin{aligned}\phi_0(x) &= \pi^{-\frac{1}{4}} e^{-\frac{1}{2}x^2} \\ \phi_n(x) &= (2^n n!)(x - \frac{\mathrm{d}}{\mathrm{d}x})^n \phi_0(x), \\ &= (2^n n!)^{-\frac{1}{2}} H_n(x)\phi_0(x)\end{aligned} \tag{3.2.4}$$

where $H_n(x)$ is the Hermite polynomial

$$H_n(x) = (-1)^n \exp x^2 \left(\frac{\mathrm{d}^n}{\mathrm{d}x^n} e^{-x^2}\right). \tag{3.2.5}$$

3.3 The spatial oscillator

In the chapter on mesons, we already mentioned that the 3-dimensional oscillator is solvable and may serve as a convenient basis for other potentials.

The scale-independent part h_3 of the Hamiltonian

$$H = \frac{\vec{P}^2}{2M} + \frac{1}{2}K\vec{R}^2 = \frac{1}{2}\sqrt{\frac{K}{M}}h_3 = \frac{1}{2}\sqrt{\frac{K}{M}}[-\Delta + \vec{r}^2] \tag{3.3.1}$$

can be written

$$h_3 = h_1(x) + h_1(y) + h_1(z) \tag{3.3.2}$$

resulting in eigenvalues

$$\epsilon_N = 3 + 2N, \quad N = 0, 1... \tag{3.3.3}$$

with eigenspaces of dimension

$$d_N^{(3)} = \frac{(N+1)(N+2)}{2}, \tag{3.3.4}$$

which have a possible basis

$$\Psi_{n_x n_y n_z}(\vec{r}) = \phi_{n_x}(x)\phi_{n_y}(y)\phi_{n_z}(z). \tag{3.3.5}$$

An alternative approach consists of using spherical coordinates, as in Section 2.2. This provides a new labelling of the eigenvalues

$$\epsilon_{n,l} = 3 + 4n + 2l. \tag{3.3.6}$$

Here l is the orbital momentum and n is the number of nodes of the reduced radial wave function $u_{n,l}(r)$, whose expression is

$$u_{n,l}(r) = \sqrt{\frac{2n!}{\Gamma(n + l + \frac{3}{2})}} r^{l+1} \mathcal{L}_n^{l+1/2}(r^2) e^{-\frac{1}{2}r^2}, \tag{3.3.7}$$

where $\mathcal{L}$ is a Laguerre polynomial

$$\mathcal{L}_n^\alpha(x) = \sum_{m=0}^{n} \frac{\Gamma(n + \alpha + 1)}{\Gamma(n - m + 1)\Gamma(\alpha + m + 1)} \frac{(-x)^m}{m!} \tag{3.3.8}$$

whose generating function is

$$(1 - y)^{-\alpha - 1} \exp\left(\frac{xy}{y - 1}\right) = \sum_{n=0}^{\infty} y^n \mathcal{L}_n^\alpha(x). \tag{3.3.9}$$

One may notice the useful relations

$$\begin{aligned}\left[\frac{\mathrm{d}}{\mathrm{d}r} - \frac{l+1}{r} + r\right] u_{n+1,l}(r) &= -\sqrt{4n+4}\, u_{n,l+1}(r) \\ \left[-\frac{\mathrm{d}}{\mathrm{d}r} - \frac{l+1}{r} + r\right] u_{n,l+1}(r) &= -\sqrt{4n+4}\, u_{n+1,l}(r) \\ \left[\frac{\mathrm{d}}{\mathrm{d}r} - \frac{l+1}{r} - r\right] u_{n,l}\ (r) &= -\sqrt{4n+4l+6}\, u_{n,l+1}(r) \\ \left[-\frac{\mathrm{d}}{\mathrm{d}r} - \frac{l+1}{r} - r\right] u_{n,l+1}(r) &= -\sqrt{4n+4l+6}\, u_{n,l+1}(r)\end{aligned} \tag{3.3.10}$$

and the useful integral

$$\int_0^\infty u_{0,l}^2(r) r^\beta \mathrm{d}r = \frac{\Gamma(\frac{3}{2} + l + \frac{\beta}{2})}{\Gamma(\frac{3}{2} + l)}. \tag{3.3.11}$$

We have here a first example where levels are described in two different bases, namely $|\, n_x, n_y, n_z\rangle$ or $|\, n, l, m\rangle$, with the restriction $N = n_x + n_y + n_z = 2n + l$.

3.4 Three-body oscillator with equal masses

We start from the symmetric Hamiltonian

$$H = \frac{\vec{p}_1^2}{2m} + \frac{\vec{p}_2^2}{2m} + \frac{\vec{p}_3^2}{2m} + \frac{1}{2}K(\vec{r}_{12}^2 + \vec{r}_{23}^2 + \vec{r}_{31}^2), \tag{3.4.1}$$

where $\vec{r}_{ij} \equiv \vec{r}_j - \vec{r}_i$, and introduce the Jacobi coordinates

$$\begin{aligned}\vec{\rho} &= \vec{r}_2 - \vec{r}_1 \\ \vec{\lambda} &= (2\vec{r}_3 - \vec{r}_1 - \vec{r}_2)/\sqrt{3} \\ \vec{R} &= (\vec{r}_1 + \vec{r}_2 + \vec{r}_3)/3\end{aligned} \tag{3.4.2}$$

as well as their conjugate momenta $\vec{p}_\rho$, $\vec{p}_\lambda$, and $\vec{P}$. This results in

$$H = \frac{\vec{P}^2}{6m} + \frac{\vec{p}_\rho^2}{m} + \frac{\vec{p}_\lambda^2}{m} + \frac{3}{4}K(\vec{\rho}^2 + \vec{\lambda}^2). \tag{3.4.3}$$

We now disregard the centre-of-mass kinetic energy which vanishes in the rest frame of the baryon. The Hamiltonian appears as the sum of two 3-dimensional harmonic oscillators. We thus find the eigenvalues

$$E_N = \sqrt{\frac{3K}{4m}}(6+2N), \tag{3.4.4}$$

where

$$N = 2n_\rho + l_\rho + 2n_\lambda + l_\lambda. \tag{3.4.5}$$

Using, again, the scaling laws of Section 2.4, which are immediately generalized to more than two bodies, one can assume that $3/4K = m = 1$.

The associated degeneracy is

$$d_N^{(6)} = \frac{(N+1)(N+2)(N+3)(N+4)(N+5)}{120} = \frac{(N+1)_5}{5!} \tag{3.4.6}$$

The index (6) reminds us that H can be viewed as a 6-dimensional oscillator. One can easily check the generalization $d_N^{(q+1)} = (N+1)_q/q!$

A basis for the eigenspaces is provided by states of the type

$$|\, n_\rho, l_\rho, m_\rho; n_\lambda, l_\lambda, m_\lambda\rangle = |\, n_\rho, l_\rho, m_\rho\rangle \otimes |\, n_\lambda, l_\lambda, m_\lambda\rangle, \tag{3.4.7}$$

which can be arranged by Clebsch–Gordan coupling into states of given total angular momentum $\vec{l} = \vec{l}_\rho + \vec{l}_\lambda$ with the notations

$$\begin{aligned} |\, n_\rho, l_\rho; n_\lambda, l_\lambda; l, m\rangle &= (|\, n_\rho, l_\rho\rangle \otimes |\, n_\lambda, l_\lambda\rangle)_{l,m} \\ &= \sum \mathrm{CG}\; |\, n_\rho, l_\rho, m_\rho; n_\lambda, l_\lambda, m_\lambda\rangle \end{aligned} \tag{3.4.8}$$

For $N > 1$, these states, however, do not exhibit simple permutation properties. To impose the restrictions of the Pauli principle, one should recombine the states (3.4.8) having the same N, l, and m into states of well-defined permutation symmetry. This will be done shortly, after some basic reminders about the permutation group S_3.

3.5 Permutation of three quarks

The $3! = 6$ permutations of the quarks $(1,2,3)$ are generated by the two operators

$$P_\rightharpoonup(1,2,3) = (2,3,1) \qquad P_{12}(1,2,3) = (2,1,3). \tag{3.5.1}$$

There are three basic behaviours or, in other words, three types of irreducible representations of the group S_3:

i) a symmetric behaviour (sometimes called "fully symmetric"), for instance

$$\vec{\rho}^{\,2} + \vec{\lambda}^{\,2} = \frac{2}{3}(r_{12}^2 + r_{23}^2 + r_{31}^2), \quad (\vec{\lambda}^{\,2} - \vec{\rho}^{\,2})^2 + 4(\vec{\lambda}\cdot\vec{\rho})^2. \tag{3.5.2}$$

ii) an antisymmetric behaviour (sometimes called "fully antisymmetric")

$$P_\rightharpoonup f = f = -P_{12} f. \tag{3.5.3}$$

Examples are

$$\epsilon_{ijk}, \quad \vec{\rho}\times\vec{\lambda}. \tag{3.5.4}$$

iii) a behaviour of mixed symmetry, whose prototype are the Jacobi coordinates $\vec{\rho}$ and $\vec{\lambda}$ themselves. In Eq. (3.4.2), the third particle obviously plays a particular role, so let us redefine (we forget the vector character, which is not essential here)

$$\rho^{(3)} = \rho \qquad \text{and} \qquad \lambda^{(3)} = \lambda, \tag{3.5.5}$$

and, similarly,

$$\begin{aligned} \rho^{(1)} &= r_3 - r_2, \qquad \lambda^{(1)} = \frac{2r_1 - r_3 - r_2}{\sqrt{3}}, \\ \rho^{(2)} &= r_1 - r_3, \qquad \lambda^{(2)} = \frac{2r_2 - r_1 - r_3}{\sqrt{3}} \end{aligned} \tag{3.5.6}$$

Then, if the index $i+1$ is computed modulo 3,

$$\begin{pmatrix} \lambda^{(i+1)} \\ \rho^{(i+1)} \end{pmatrix} = \begin{pmatrix} -1/2 & -\sqrt{3/2} \\ \sqrt{3/2} & -1/2 \end{pmatrix} \begin{pmatrix} \lambda^{(i)} \\ \rho^{(i)} \end{pmatrix} \tag{3.5.7}$$

where, as expected, a rotation of angle $2\pi/3$ occurs.

A pair of mixed symmetry behaves like the real and the imaginary part of

$$z = \lambda + i\rho \tag{3.5.8}$$

on which the basic permutation operators act as follows:

$$P_\rightharpoonup z = jz, \quad P_\leftharpoondown z = P_\rightharpoonup^{-1} z = j^2 z, \quad P_{12} z = z^* \tag{3.5.9}$$

where $j = \exp(2i\pi/3)$, as usual. The usefulness of this complex notation was often underlined [40]. It manifests itself when one analyses the permutation properties of a product of two irreducible representations. If one denotes the symmetric, antisymmetric, and mixed symmetry types of behaviour by S, A, and $MS = MS_\lambda + iMS_\rho$, respectively, one easily gets the following rules

$$\begin{aligned} S \otimes [S, A, MS] &= S, A, MS \\ A \otimes [S, A, MS] &= [A, S, -iMS] \\ MS \otimes MS' &= MS'' \\ MS \otimes MS'^* &= S + iA. \end{aligned} \tag{3.5.10}$$

Any function of the three quarks can be separated into a sum of functions with basic behaviour, using the projector identities

$$1 = \frac{1+P_{12}}{2} + \frac{1-P_{12}}{2} \tag{3.5.11}$$

and

$$1 = \frac{1+P_{\rightarrow}+P_{\rightarrow}^2}{3} + \frac{1+jP_{\rightarrow}+j^2P_{\rightarrow}^2}{3} + \frac{1+j^2P_{\rightarrow}+jP_{\rightarrow}^2}{3}. \tag{3.5.12}$$

Consider, for instance, $f = x_1y_3$. Using (3.5.11) and (3.5.12), one gets

$$\begin{aligned} f = \ & 1/6[\ x_1y_3 + \ x_2y_3 + x_2y_1 + x_3y_1 + x_3y_2 + x_1y_2] \\ & +1/6[\ x_1y_3 - \ x_2y_3 + x_2y_1 - x_3y_1 + x_3y_2 - x_1y_2] \\ & +1/6[2x_1y_3 + 2x_2y_3 - x_2y_1 - x_3y_1 - x_3y_2 - x_1y_2] \\ & +1/6[2x_1y_3 - 2x_2y_3 - x_2y_1 + x_3y_1 - x_3y_2 + x_1y_2] \end{aligned} \tag{3.5.13}$$

or, in short,

$$f(1,2,3) = f_S + f_A + f_\lambda + f'_\rho, \tag{3.5.14}$$

where the "prime" emphasizes that the third and fourth terms are not partners of the same mixed symmetry doublet. There exists f_ρ and f'_λ, which occur in other permutations of f. For instance,

$$f(2,3,1) = f_S + f_A - \frac{1}{2}f_\lambda - \sqrt{\frac{3}{2}}f_\rho + \sqrt{\frac{3}{2}}f'_\lambda - \frac{1}{2}f'_\rho. \tag{3.5.15}$$

3.6 Colour, spin, and isospin wave functions

In quantum chromodynamics, the colour group is $SU(3)_c$, where the indice is written to avoid confusion with the SU(3) group of flavour. In a baryon, the colour coupling of the three quarks to form a singlet, schematically

$$\Phi_c = \epsilon_{ijk}\phi_c^i\phi_c^j\phi_c^k \tag{3.6.1}$$

is antisymmetric under the exchange of the three quarks. This property is, in fact, one of the reasons for inventing colour [41].

Out of the spins of the two first quarks, one can build spin $S = 0$ and $S = 1$ states, which are respectively odd and even under P_{12}, the exchange of these quarks. When supplemented by the third spin, they lead to one spin $S = 3/2$ multiplet, which is symmetric, and two spin $S = 1/2$ doublets, which are partners of mixed symmetry. These spin wave functions are

$$\begin{aligned} |\,3/2,3/2\rangle &= |\uparrow\uparrow\uparrow\rangle \\ |\,3/2,1/2\rangle &= \frac{1}{\sqrt{3}}[|\downarrow\uparrow\uparrow\rangle + |\uparrow\downarrow\uparrow\rangle + |\uparrow\uparrow\downarrow\rangle] \\ |\,3/2,-1/2\rangle &= \frac{1}{\sqrt{3}}[|\uparrow\downarrow\downarrow\rangle + |\downarrow\uparrow\downarrow\rangle + |\downarrow\downarrow\uparrow\rangle] \\ |\,3/2,-3/2\rangle &= |\downarrow\downarrow\downarrow\rangle \end{aligned} \tag{3.6.2}$$

and

$$\begin{aligned} |\,1/2^+_\lambda\rangle &= \frac{1}{\sqrt{6}}[2\,|\uparrow\uparrow\downarrow\rangle - |\downarrow\uparrow\uparrow\rangle - |\uparrow\downarrow\uparrow\rangle] \\ |\,1/2^+_\rho\rangle &= \frac{1}{\sqrt{2}}[|\uparrow\downarrow\uparrow\rangle - |\downarrow\uparrow\downarrow\rangle] \end{aligned} \tag{3.6.3}$$

$$\begin{aligned} |\,1/2^-_\lambda\rangle &= \frac{1}{\sqrt{6}}[-2\,|\downarrow\downarrow\uparrow\rangle + |\downarrow\uparrow\downarrow\rangle + |\uparrow\downarrow\downarrow\rangle] \\ |\,1/2^-_\rho\rangle &= \frac{1}{\sqrt{2}}[|\uparrow\downarrow\downarrow\rangle - |\downarrow\uparrow\downarrow\rangle]. \end{aligned} \tag{3.6.4}$$

The formal analogy between the $|\,1/2_\lambda\rangle$, $|\,1/2_\rho\rangle$ pairs, and the Jacobi coordinates $\vec{\lambda}$, $\vec{\rho}$ given in (3.4.2) makes it clear that they have the same behaviour under permutations.

Isospin wave functions are built in exactly the same way, with $\uparrow$ replaced by u and $\downarrow$ replaced by d.

States with three identical quarks such as those of the Ω^- family (sss) have a simple structure: either the spin wave function corresponds to spin $S = \frac{3}{2}$ and the space wave function has to be symmetric, or the total spin is $S = \frac{1}{2}$ and one should combine the corresponding spin wave functions with a pair of mixed-symmetry space wave functions, as in Eq. (3.5.10), to form an overall spin-space wave function which is symmetric.

The above combinations are also found in qqq baryons made of ordinary quarks (q = u or d), when isospin is $I = 3/2$. This is the Δ family. When isospin is $I = 1/2$, i.e. for the nucleon family, new arrangements exist. First, isopsin $I = 1/2$ and spin $S = 1/2$ can be combined to form a symmetric spin-isospin wave function. This is what occurs for the nucleon itself and some of its excitations. The spin-isospin wave function can also be of mixed symmetry and is associated with a mixed-symmetry spatial wave function. Finally, there is the possibility of an antisymmetric spin-isospin wave function which allows for the use of an antisymmetric spatial wave function such as $\vec{\rho}\times\vec{\lambda}\exp[-\alpha(\vec{\rho}^2+\vec{\lambda}^2)]$.

3.7 Spatial wave functions of given permutation symmetry

Let us come back to the reduced and rescaled Hamiltonian

$$h = \vec{p}_\rho^{\,2} + \vec{\rho}^{\,2} + \vec{p}_\lambda^{\,2} + \vec{\lambda}^2. \tag{3.7.1}$$

The wave functions are often labelled with N, the number of quanta, with l^P, the total angular momentum and parity, and with the dimension of the SU(6) representation. The Hamiltonian (3.7.1) has, indeed, a symmetry of structure $U(6) \equiv SU(6) \times U(1)$, where U(1) is associated with the number of quanta N [6]. In fact, SU(6) also denotes another symmetry combining spin and flavour. It becomes exact when one neglects hyperfine effects and takes the limit of equal quark masses $m_u = m_d = m_s$. We refer to the specialized literature [6] for these group theoretical aspects of the harmonic

oscillator. For our purpose, it is sufficient to know the following correspondence between SU(6) representations and permutation properties:

$$\begin{aligned}[56] &= \textit{symmetric}\\ [20] &= \textit{antisymmetric}\\ [70] &= \textit{mixed symmetry}.\end{aligned} \tag{3.7.2}$$

By superposition of the factorized states (3.4.8), one can form:

$N = 0$

$$|\,56,0^+\rangle = |\,0,0\rangle\otimes|\,0,0\rangle \tag{3.7.3}$$

$N = 1$

$$\begin{aligned}|\,70_\lambda,1^-\rangle &= |\,0,0\rangle\otimes|\,0,1\rangle\\ |\,70_\rho,1^-\rangle &= |\,0,1\rangle\otimes|\,0,0\rangle,\end{aligned} \tag{3.7.4}$$

$N = 2$

$$\begin{aligned}|\,20,1^+\rangle &= (|\,0,1\rangle\otimes|\,0,1\rangle)_1\\ |\,70_\lambda,2^+\rangle &= \frac{1}{\sqrt{2}}(|\,0,2\rangle\otimes|\,0,0\rangle - |\,0,0\rangle\otimes|\,0,2\rangle)\\ |\,70_\rho,2^+\rangle &= (|\,0,1\rangle\otimes|\,0,1\rangle)_2\\ |\,56,2^+\rangle &= \frac{1}{\sqrt{2}}(|\,0,2\rangle\otimes|\,0,0\rangle + |\,0,0\rangle\otimes|\,0,2\rangle)\\ |\,70_\lambda,0^+\rangle &= \frac{1}{\sqrt{2}}(|\,1,0\rangle\otimes|\,0,0\rangle - |\,0,0\rangle\otimes|\,1,0\rangle)\\ |\,70_\rho,0^+\rangle &= (|\,0,1\rangle\otimes|\,0,1\rangle)_0\\ |\,56,0^+\rangle &= \frac{1}{\sqrt{2}}(|\,1,0\rangle\otimes|\,0,0\rangle + |\,0,0\rangle\otimes|\,1,0\rangle),\end{aligned} \tag{3.7.5}$$

$N = 3, \quad l^P = 3^-$

$$\begin{aligned}|\,56,3^-\rangle &= \frac{1}{2}[|\,0,0\rangle\otimes|\,0,3\rangle - \sqrt{3}(|\,0,2\rangle\otimes|\,0,1\rangle)_3]\\ |\,20,3^-\rangle &= \frac{1}{2}[\sqrt{3}(|\,0,1\rangle\otimes|\,0,2\rangle)_3 - |\,0,3\rangle\otimes|\,0,0\rangle]\\ |\,70_\lambda,3^-\rangle &= \frac{1}{2}[\sqrt{3}\,|\,0,0\rangle\otimes|\,0,3\rangle + (|\,0,2\rangle\otimes|\,0,1\rangle)_3]\\ |\,70_\rho,3^-\rangle &= \frac{1}{2}[(|\,0,1\rangle\otimes|\,0,2\rangle)_3 + \sqrt{3}\,|\,0,3\rangle\otimes|\,0,0\rangle]\end{aligned} \tag{3.7.6}$$

$N = 3, \quad l^P = 2^-$

$$\begin{aligned}|\,70_\lambda,2^-\rangle &= (|\,0,2\rangle\otimes|\,0,1\rangle)_2\\ |\,70_\rho,2^-\rangle &= (|\,0,1\rangle\otimes|\,0,2\rangle)_2,\end{aligned} \tag{3.7.7}$$

$N = 3, \quad l^P = 1^-$

$$\begin{aligned}|\,56,1^-\rangle &= \frac{1}{\sqrt{12}}[-\sqrt{3}\,|\,0,0\rangle\otimes|\,1,1\rangle + \sqrt{5}\,|\,1,0\rangle\otimes|\,0,1\rangle + 2(|\,0,2\rangle\otimes|\,0,1\rangle)_1]\\ |\,20,1^-\rangle &= \frac{1}{\sqrt{12}}[-\sqrt{3}\,|\,1,1\rangle\otimes|\,0,0\rangle + \sqrt{5}\,|\,0,1\rangle\otimes|\,1,0\rangle + 2(|\,0,1\rangle\otimes|\,0,2\rangle)_1]\\ |\,70_\lambda,1^-\rangle' &= \frac{1}{2\sqrt{2}}[\sqrt{5}\,|\,0,0\rangle\otimes|\,1,1\rangle + \sqrt{3}\,|\,0,1\rangle\otimes|\,1,0\rangle]\\ |\,70_\rho,1^-\rangle' &= \frac{1}{2\sqrt{2}}[\sqrt{5}\,|\,1,1\rangle\otimes|\,0,0\rangle + \sqrt{3}\,|\,0,1\rangle\otimes|\,1,0\rangle]\\ |\,70_\lambda,1^-\rangle'' &= \frac{1}{\sqrt{24}}[\sqrt{3}\,|\,1,1\rangle\otimes|\,0,0\rangle - \sqrt{5}\,|\,1,0\rangle\otimes|\,0,1\rangle + 4(|\,0,2\rangle\otimes|\,0,1\rangle)_1]\\ |\,70_\rho,1^-\rangle'' &= \frac{1}{\sqrt{24}}[\sqrt{3}\,|\,1,1\rangle\otimes|\,0,0\rangle - \sqrt{5}\,|\,0,1\rangle\otimes|\,1,0\rangle + 4(|\,0,1\rangle\otimes|\,0,2\rangle)_1].\end{aligned} \tag{3.7.8}$$

Up to $N = 2$ or even $N = 3$, one can obtain these combinations of the factorized states $|\,n_\rho,l_\rho\rangle\otimes|\,n_\lambda,l_\lambda\rangle$ by empirical methods. For instance, dealing with a scalar ($l = 0$) polynomial of degree 2, one easily identify $\vec{\rho}^{\,2} + \vec{\lambda}^{\,2}$ as being symmetric, whereas $\vec{\lambda}^{\,2} - \vec{\rho}^{\,2}$ and $-2\vec{\lambda}\cdot\vec{\rho}$ form a pair of mixed symmetry.

For larger N, however, one hardly avoids the use of more systematic methods. In each eigenspace labelled by N, with energy $6+2N$, one can consider the subspaces (N, l) of given total angular momentum and in each subspace diagonalize the permutation operator $P_{\rightarrow}$ (P_{12} is already diagonalized by the even or odd character of l_ρ). The relevant matrix elements

$$
\begin{aligned}
&{}_l\langle n'_\lambda, l'_\lambda \mid \otimes \langle n'_\rho, l'_\rho \mid P_{\rightarrow} \mid n_\rho, l_\rho \rangle \otimes \mid n_\lambda, l_\lambda \rangle_l = \\
&\int \mathrm{d}^3\vec{\rho}\mathrm{d}^3\vec{\lambda}\phi^*_{n'_\lambda,l'_\lambda}(\vec{\lambda})\phi^*_{n'_\rho,l'_\rho}(\vec{\rho})\phi_{n_\rho,l_\rho}\left(-\frac{1}{2}\vec{\rho}+\frac{\sqrt{3}}{2}\vec{\lambda}\right)\phi_{n_\lambda,l_\lambda}\left(-\frac{1}{2}\vec{\lambda}-\frac{\sqrt{3}}{2}\vec{\rho}\right)
\end{aligned}
\tag{3.7.9}
$$

(the Clebsch–Gordan summations are omitted for better reading in the integral) are called the "Brody–Moshinsky" coefficients [42]. They can be computed by astute recursion relations [43, 44], or (still exactly) by brute force computer algebra. Other methods have been proposed, for instance by Horgan [45], to construct the harmonic-oscillator wave functions of given angular momentum, parity and permutation properties.

3.8 Harmonic oscillator with unequal masses

For unequal masses, one may choose the Jacobi coordinates as

$$
\vec{\rho} = \vec{r}_2 - \vec{r}_1 \quad \text{and} \quad \vec{\lambda} = \left[\vec{r}_3 - \frac{m_1\vec{r}_1 + m_2\vec{r}_2}{m_1+m_2}\right]\sqrt{\frac{m_3(m_1+m_2)^2}{m_1m_2(m_1+m_2+m_3)}}, \tag{3.8.1}
$$

so that a single reduced mass $2m_1m_2/(m_1+m_2)$ enters into the kinetic energy. We now restrict ourselves to the case of two different masses

$$
m_1 = m_2 = m \quad \text{and} \quad m_3 = m', \tag{3.8.2}
$$

for which the harmonic oscillator is still exactly solvable. The Jacobi coordinates read

$$
\vec{\rho} = \vec{r}_2 - \vec{r}_1 \quad \text{and} \quad \vec{\lambda} = [2\vec{r}_3 - (\vec{r}_1 + \vec{r}_2)]\sqrt{\frac{m'}{2m+m'}}\,. \tag{3.8.3}
$$

The reduced part of the Hamiltonian

$$
H = \sum \frac{\vec{p}_i^{\,2}}{2m_i} + \frac{1}{2}K\sum r_{ij}^2 \tag{3.8.4}
$$

is

$$
\widetilde{H} = \frac{\vec{p}_\rho^{\,2}}{m} + \frac{3}{4}K\vec{\rho}^{\,2} + \frac{\vec{p}_\lambda^{\,2}}{m} + \frac{3}{4}K\frac{m}{\mu}\vec{\lambda}^{\,2}, \tag{3.8.5}
$$

with

$$
\frac{1}{\mu} = \frac{1}{3m} + \frac{2}{3m'}. \tag{3.8.6}
$$

Factorization still works, so the energies are

$$
E(n_\rho, l_\rho, n_\lambda, l_\lambda) = \sqrt{\frac{3K}{4m}}(3 + 4n_\rho + 2l_\rho) + \sqrt{\frac{3K}{4\mu}}(3 + 4n_\lambda + 2l_\lambda) \tag{3.8.7}
$$

and the corresponding wave functions are

$$
\Psi(n_\rho, l_\rho, n_\lambda, l_\lambda; \vec{\rho}, \vec{\lambda}) = (\alpha_\rho\alpha_\lambda)^{3/4}\left[\Phi_{n_\rho,l_\rho,m_\rho}(\alpha_\rho\vec{\rho})\Phi_{n_\lambda,l_\lambda,m_\lambda}(\alpha_\lambda\vec{\lambda})\right]_{l,m}, \tag{3.8.8}
$$

where $\alpha_\rho = \sqrt{3Km/4}$ and $\alpha_\lambda = \sqrt{3Km^2/(4\mu)}$. One should notice that if $m' > m$, as in Λ, Λ_c, or Λ_b, then $\mu > m$ and the excitations of λ-type are lower than their analogues of ρ-type. The reverse is true if $m' < m$.

Chapter 4

VARIATIONAL METHODS

4.1 Introduction

Variational calculations of few-body bound states have been designed and performed since the beginning of quantum mechanics. More and more elaborate methods have been used [46], in particular for atomic and molecular physics, where a high accuracy is often needed.

Since baryons present themselves as rather compact objects, with quarks tightly bound together, we do not need the ultimate refinements of variational techniques for computing their energy and wave functions. We shall thus restrict ourselves in this chapter to a simple introduction to elementary variational calculations.

In fact, if one likes challenging few-body calculations, one should consider multi-quark spectroscopy. A state such as $qq\bar{q}\bar{q}$ "hesitates" between a compact configuration, with all quarks close together, and a separation into $q\bar{q} + q\bar{q}$. A good variational wave function should incorporate these two components and this results in lengthy calculations [47].

Coming back to baryons, we shall consider a Hamiltonian

$$H = \sum_i \frac{\vec{p}_i^{\,2}}{2m_i} + \sum_{i<j} V(r_{ij}) = \frac{\vec{P}^{\,2}}{2(m_1+m_2+m_3)} + \widetilde{H}. \tag{4.1.1}$$

The extension to include spin–spin forces, or a flavour-dependent potential $V_{ij}(r_{ij})$, or 3-body forces, does not lead to essentially new difficulties.

For the ground state, variational calculations are based on the Rayleigh–Ritz principle

$$E_0 \equiv \left\langle \Psi_0 \mid \widetilde{H} \mid \Psi_0 \right\rangle = \min_{\varphi} \left\langle \varphi \mid \widetilde{H} \mid \varphi \right\rangle \tag{4.1.2}$$

and its consequence that if $\varphi_0 = \Psi_0 + \delta\Psi_0$ is an approximation of the true wave function Ψ_0, the approximate energy $\tilde{E}_0 = \left\langle \varphi_0 \mid \widetilde{H} \mid \varphi_0 \right\rangle$ departs from E_0 to second order only. In other words, the binding energy is always better approximated than the wave function, a property that one should keep in mind for the applications.

The same minimization procedure can be applied to every ground state in a sector of some definite parity, angular momentum or permutation properties. Its energy can be approximated from above by using trial wave functions carrying appropriate quantum numbers.

The serious difficulties occur for radial excitations. One may ignore orthogonality problems and search for a stationary value of the functional

$$E[\varphi] = \left\langle \varphi \mid \widetilde{H} \mid \varphi \right\rangle \tag{4.1.3}$$

for each level independently, but without any guarantee of success. A more systematic search consists of introducing a set of n orthogonal wave functions $f_i(\alpha; \vec{\rho}, \vec{\lambda})$, spanning a sub-space $\mathcal{H}_n(\alpha)$, where α denotes all the parameters. For any given α, one diagonalizes the restriction of the Hamiltonian $\widetilde{H}$ to $\mathcal{H}_n(\alpha)$, resulting in eigenvalues $\epsilon_0(\alpha), \epsilon_1(\alpha) \ldots \epsilon_{n-1}(\alpha)$. The best approximation to the j^{th} state consists of minimizing $\epsilon_{j-1}(\alpha)$ with respect to α. In general, this leads to a different set of parameters α for each level, and orthogonality is lost. To restore orthogonality, one should adopt a compromise by fixing α at once for all levels of interest.

4.2 General properties of variational solutions

It is amazing that variational solutions obey the same general theorems as the exact solutions. This was first pointed out in a remarkable article by Fock [48]. Let us give a few examples. We shall assume that the set of trial wave functions is globally invariant under rescaling $\vec{r}_i \to \lambda \vec{r}_i$.

i) Scaling laws. The variational approximation to a power-law interaction $\sum B_{ij} r_{ij}^{\beta}$ behaves like

$$E \propto \mu^{-\beta/(2+\beta)} \gamma^{2/(2+\beta)} \tag{4.2.1}$$

if all quark masses are simultaneously multiplied by μ and strength coefficients B_{ij} by γ.

ii) Virial theorem. If Ψ is a variational approximation to $H = T + V$, T being the kinetic energy operator, then

$$\langle \Psi \mid T \mid \Psi \rangle = \tfrac{1}{2} \left\langle \Psi \mid \sum_i \vec{r}_i \cdot \frac{\partial V}{\partial \vec{r}_i} \mid \Psi \right\rangle. \tag{4.2.2}$$

iii) Convexity. Consider mesons for simplicity, bound by a flavour-independent potential. Then

$$E^{\text{var}}(Q\overline{Q}) + E^{\text{var}}(q\bar{q}) \leq 2E^{\text{var}}(Q\bar{q}) \tag{4.2.3}$$

as for the true energies (see Section 2.8).

iv) Inequalities between mesons and baryons. If the trial wave function of baryons $\Psi(\vec{r}_1, \vec{r}_2, \vec{r}_3)$ belongs to the set of trial wave functions of mesons for any given $\vec{r}_3$, then

$$E^{\text{var}}(qqq) \geq \tfrac{3}{2} E^{\text{var}}(q\bar{q}), \tag{4.2.4}$$

provided one adopts the "$\frac{1}{2}$ rule" $V_{qq} = \frac{1}{2} V_{q\bar{q}}$, which will be discussed in more detail in Chapter 9.

4.3 Harmonic-oscillator expansion (equal masses)

The method, which can also be used for mesons, is the following. One expands the eigenstates of

$$\widetilde{H} = \frac{\vec{p}_\rho^{\,2}}{m} + \frac{\vec{p}_\lambda^{\,2}}{m} + \sum_{i<j} V(r_{ij}) \tag{4.3.1}$$

into the eigenstates of

$$H_0 = \frac{\vec{p}_\rho^{\,2}}{m} + \frac{\vec{p}_\lambda^{\,2}}{m} + K(\vec{\rho}^{\,2} + \vec{\lambda}^{\,2}), \tag{4.3.2}$$

i.e.

$$\Phi_{l,m} = \sum_{n_\rho,l_\rho,n_\lambda,l_\lambda} c_{n_\rho,l_\rho,n_\lambda,l_\lambda}(\mid n_\rho,l_\rho\rangle\otimes\mid n_\lambda,l_\lambda\rangle)_{l,m}, \tag{4.3.3}$$

and studies the convergence as a function of the value of the maximal number of quanta allowed in the expansion, $N = 2n_\rho + l_\rho + 2n_\lambda + l_\lambda$. In principle, one could optimize the variational parameter K for each N. For high N, this results into expensive calculations and numerical instabilities. So, in practice, one optimizes K for a small number of quanta N' and then pushes the expansion up to larger N.

For given N and K, the harmonic-oscillator (h.o.) expansion results in the diagonalization of a symmetric matrix, which is the restriction of $\widetilde{H}$ to the sub-space spanned by the first levels of H_0.

As an illustration, let us compute the two first levels having angular momentum and parity $l^P = 0^+$, corresponding to quark masses $m_i = 1$ and a linear confinement. The h.o. basis is made of these states with the label $[56, 0^+]$ in Section 3.7. We rename them as

$$\begin{array}{l} \mid 1\rangle\ (N=0), \qquad \mid 2\rangle\ (N=2), \qquad \mid 3\rangle, \mid 4\rangle\ (N=4) \\ \mid 5\rangle, \mid 6\rangle, \mid 7\rangle\ (N=6), \qquad \mid 8\rangle, \mid 9\rangle, \mid 10\rangle, \mid 11\rangle\ (N=8) \end{array} \tag{4.3.4}$$

The results shown in Table 4.1 correspond to different prescriptions for the variational parameter K, namely different levels of expansion N' at which it is adjusted. As pointed out by Moshinsky [49], minimizing the ground state at the $N' = 2$ order does not provide any improvement with respect to $N' = 0$. Otherwise, the value of the harmonic oscillator parameter K depends rather sensitively on which level and to which order the minimization is performed. However, the accuracy of the eventual energies depends less on the prescription adopted for K than on the number of quanta N introduced in the expansion.

Another output of such a calculation is the set of coefficients c which describe the wave function. For instance, in the case where K is optimized at the $N' = 4$ order and the expansion pushed up to $N = 8$, one obtains, for the wave function $\Psi = \sum c_i \mid i\rangle$ of the ground state and its first radial excitation the coefficients given in Table 4.2.

Note that the convergence is rather clear for the ground state, which is dominated by the $N = 0$ component $c_1 \mid 1\rangle$. There is more mixing of configurations for the excited states, as is usual in variational calculations.

Table 4.1: Symmetric and scalar states ([56,0^+]) for quark masses $m_i = 1$ and linear confinement $V = \frac{1}{2}\sum r_{ij}$ using a harmonic-oscillator expansion up to N quanta. The oscillator parameter K is adjusted by minimizing either the first or second level with an expansion limited to N' quanta (the minimized energy is underlined). The exact values are very close to: $E_{0,0} = 3.8631$, $E_{1,0} = 5.3207$, and $E_{2,0} = 6.5953$.

N	N'	$\alpha = K^{1/2}$	$E_{0,0}$	$E_{1,0}$	$E_{2,0}$
0			<u>3.8711</u>		
2			3.8711	5.3766	
4	0	0.4301	3.8640	5.3468	6.8082
6			3.8635	5.3214	6.6831
8			3.8632	5.3215	6.6008
4			<u>3.8636</u>	5.3695	7.0149
6	4	0.4782	3.8634	5.3259	6.7671
8			3.8632	5.3224	6.6364
2			3.8732	<u>5.3445</u>	
4	2	0.3811	3.8651	5.3388	6.6729
6			3.8639	5.3223	6.6367
8			3.8634	5.3217	6.5975

Table 4.2: Coefficients of the harmonic-oscillator expansion for the ground state and first excitation with $l^P = 0^+$. It includes up to $N = 8$ quanta, but the oscillator strength is determined by minimizing the ground state energy when the expansion is truncated at the $N' = 4$ level. Quark masses are $m_i = 1$, and the interquark potential $\frac{1}{2}\sum r_{ij}$.

State	c_1 ($N=0$)	c_2 ($N=2$)	c_3, c_4 ($N=4$)	$c_5 - c_7$ ($N=6$)	$c_8 - c_{11}$ ($N=8$)
$n=0$	0.99431	-0.08993	-0.01953 0.05287	-0.00494 -0.00232 -0.00223	0.00115 -0.00178 -0.00304 0.00554
$n=1$	0.10169	0.94301	0.05479 -0.27911	0.01608 -0.02957 0.13209	-0.00454 0.00486 0.00577 -0.02859

4.4 Harmonic oscillator expansion (unequal masses)

We consider here baryons qqQ with single flavour or QQq with double flavour. The quark masses are $m_1 = m_2 = m$ and $m_3 = m'$. The generalization to $m_1 \neq m_2$ is obvious. We use the Jacobi coordinates of Eq. (3.8.55) to deal with a unique reduced mass m. The reduced Hamiltonian

$$\widetilde{H} = \frac{\vec{p}_\rho^{\,2}}{m} + \frac{\vec{p}_\lambda^{\,2}}{m} + \sum_{i<j} V(r_{ij}) \tag{4.4.12}$$

looks formally the same as previously, but it is not symmetric under all permutations and it contains some mass dependence hidden in λ. We still expand the solution of $\widetilde{H}$ into the eigenstates of the symmetric h.o. The expansion mixes symmetric and mixed-symmetry states of the h.o. basis. In the $I^P = 0^+$ sector, for instance, one should include 22 states if the h.o. expansion is pushed up to $N = 8$: the 11 symmetric states listed in Eq. (4.3.4) and 11 mixed-symmetry states which are even in $\vec{\rho}$, i.e. even under P_{12}, the permutation of the two first quarks.

For the numerical illustration, let us consider again a linear potential $\frac{1}{2}\sum r_{ij}$ and the sets of constituent masses (1, 1, 5) and (1, 1, 0.2) which are relevant for qqc and ccq charmed baryons, respectively. We display in Table 4.3 the behaviour of the ground state energy as a function of the maximal number of quanta, N, introduced in the expansion. Also shown is the order N' to which the oscillator parameter K has been optimized. Some remarks are in order:

i) For small N, the convergence is slower than in the symmetric case. However, as soon as some basic mixed-symmetry components are included in the wave function, i.e. for $N > 2$, the convergence becomes much better.

ii) One may wonder why one chooses to expand an asymmetric system such as qqQ or QQq in terms of the symmetric h.o. hamiltonian H_0. This does not favour the convergence and, as we shall see in the next section, alternative parametrizations of the trial wave function can be more efficient if the mass ratio m'/m is very large or very small. The main advantage of the h.o. expansion is to allow for systematic computations of all matrix elements of interest. Those of $V(r_{12})$ are simply

$$\left\langle n'_\rho, l'_\rho; n'_\lambda, l'_\lambda \mid V(r_{12}) \mid n_\rho, l_\rho; n_\lambda, l_\lambda \right\rangle = \delta_{n_\lambda n'_\lambda} \delta_{l_\lambda l'_\lambda} \left\langle n'_\rho, l'_\rho \mid V(\rho) \mid n_\rho, l_\rho \right\rangle \tag{4.4.13}$$

For computing the matrix elements of $V(r_{13})$, one has to perform the rotation

$$\begin{pmatrix} \cos\theta_1 & \sin\theta_1 \\ -\sin\theta_1 & \cos\theta_1 \end{pmatrix} \begin{pmatrix} \vec{\lambda} \\ \vec{\rho} \end{pmatrix} = \begin{pmatrix} \vec{y} \\ \vec{x} \end{pmatrix} \tag{4.4.14}$$

such that

$$\vec{x} = A_1 \vec{r}_{31} = A_1(\vec{r}_1 - \vec{r}_3). \tag{4.4.15}$$

The matrix elements of $V(r_{ij})$ are immediate in the rotated basis $\mid n_x, l_x; n_y, l_y\rangle$. To rewrite them in the original basis, one simply needs the Brody–Moshinsky matrix

$$\langle n_\rho, l_\rho; n_\lambda, l_\lambda \mid n_x, l_x; n_y, l_y \rangle, \tag{4.4.16}$$

for which powerful recursion relations exist and computer codes are available [42, 43, 44].

Table 4.3: Ground state bound by $V = \frac{1}{2}\sum r_{ij}$, using an harmonic-oscillator expansion up to N quanta, with the oscillator parameter adjusted at the N' level. The quark masses are (1, 1, 5) for qqQ, and (1, 1, 0.2) for QQq.

state	N	N'	E_0
qqQ	0	0	3.4729
	2	0	3.4472
	4	4	3.4390
	6	4	3.4383
	8	4	3.4380
QQq	0	0	5.0456
	2	0	4.9634
	4	4	4.9428
	6	4	4.9403
	8	4	4.9395

4.5 Empirical variational methods

As already acknowledged, the h.o. expansion (as well as the hyperspherical expansion of Chapter 5) suffers from being a little heavy, especially in the case of unequal masses. Its main advantage is that convergence can eventually be reached, provided one pushes the calculation far enough.

Now, there exist many alternative parametrizations of the trial wave function which immediately provide a dramatic accuracy, though they are a little empirical in nature. We shall present below the example of the parametrization of the wave function in terms of Gaussian functions. This method is copiously used in theoretical molecular physics.

Let us introduce the method in the simple 2-body case. The radial wave function is written

$$R_{n,l} = \frac{u_{n,l}(r)}{r} = \sum_{i=1}^{q} c_i \left[\frac{\Gamma(\frac{3}{2})}{\Gamma(\frac{3}{2}+l)}\right]^{\frac{1}{2}} (\sqrt{\alpha_i} r)^l \left(\frac{\alpha_i}{\pi}\right)^{\frac{3}{4}} \exp -\tfrac{1}{2}\alpha_i r^2 \tag{4.5.17}$$

and the α_i's and the c_i's are optimized, the latter being subject to a normalization constraint. For given α_i's, the c_i's are obtained by a simple matrix diagonalization. The α_i's are determined by standard minimization algorithms. The choice of the above

parametrization leads to easy calculation of the matrix elements, most often in terms of elementary functions.

With only the $q = 1$ term, the method coincides with the $N = 0$ order of the h.o. expansion. The comparison for increasing q and N is shown in Table 4.4, for angular momentum $l = 0$, reduced mass $\mu = 1$, and potential $V(r) = r$. The Gaussian

Table 4.4: Comparison of the harmonic oscillator expansion and Gaussian expansion for the 2-body linear potential. The exact values given by the first zero of the Airy function is 2.33811...

Number of terms	Harmonic oscillator		Gaussian	
1	$N = 0$	2.34478	$q = 1$	2.34478
2	$N = 2$	2.34478[1]	$q = 2$	2.33825
3	$N = 4$	2.33841	$q = 3$	2.33811

[1]The Moshinsky theorem [49] strikes again.

expansion is clearly more efficient here.

Consider now the case of symmetric baryons (qqq). The starting point coincides with the $N = 0$ order of the h.o. expansion

$$\Psi = \varphi^S_\alpha = \left(\frac{\alpha}{\pi}\right)^{3/2} \exp\left[-\tfrac{1}{2}\alpha(\vec{\rho}^2 + \vec{\lambda}^2)\right] \tag{4.5.18}$$

We name it "1S" for "1 Gaussian with $l_\rho = l_\lambda = 0$". We similarly define "2S", "3S",...parametrizations by superposing $q = 2, 3...$ of these Gaussians.

$$\Psi = \sum_{i=1}^{q} c_i \varphi^S_{\alpha_i} \tag{4.5.19}$$

Incursions into the $l_\rho = l_\lambda > 0$ sectors provide configurations "qP", "qD" which can be added to the "qS" ones. This makes use of

$$\begin{aligned} \varphi^P_\alpha(\vec{\rho}, \vec{\lambda}) &= \frac{2}{\sqrt{3}}\alpha\vec{\rho}\cdot\vec{\lambda}\,\varphi^S_\alpha(\vec{\rho}, \vec{\lambda}) \\ \varphi^D_\alpha(\vec{\rho}, \vec{\lambda}) &= \frac{2}{3\sqrt{5}}\alpha^2\left[3(\vec{\rho}\cdot\vec{\lambda})^2 - \rho^2\lambda^2\right]\varphi^S_\alpha(\vec{\rho}, \vec{\lambda}), \quad \text{etc.} \end{aligned} \tag{4.5.20}$$

For the qqq ground state with quarks of mass $m = 1$ bound by $V = \frac{1}{2}\sum r_{ij}$, one obtains the results of Table 4.5.

This is comparable to a harmonic-oscillator expansion pushed up to $N = 6$.

Consider now the cases of qqQ and QQq baryons, with constituent masses (1, 1, 5) and (1, 1, 0.2), respectively, and the same $V = \frac{1}{2}\sum r_{ij}$. The terms of the variational

wave function can now have different Gaussian parameters for the ρ and λ parts. For instance

$$\varphi^S_{\alpha\beta} = \left(\frac{\alpha}{\pi}\right)^{3/4}\left(\frac{\beta}{\pi}\right)^{3/4} \exp -\tfrac{1}{2}(\alpha\vec{\rho}^2 + \beta\vec{\lambda}^2). \tag{4.5.21}$$

The results are shown in Table 4.5. With only one term, one already obtains a good approximation because the trial wave function can adjust itself to the asymmetry of the system. Note that, for QQq, internal orbital excitations play a less important role than the detailed description of the S-wave sector.

Table 4.5: Empirical variational calculation of the binding energy of the ground state of the potential $V = \frac{1}{2}\sum r_{ij}$ for the quark masses $m_i = 1$ (qqq), $m_i = 1, 1, 5$ (qqQ), and $m_i = 1, 1, 0.2$ (QQq). The exact values are 3.8631, 3.4379, and 4.9392.

Parametrization	qqq	qqQ	QQq
1S	3.8711	3.4451	4.9498
2S	3.8648	3.4394	4.9414
3S	3.8647	3.4391	4.9400
1S+1D	3.8698	3.4441	4.9422
2S+1D	3.8634	3.4383	4.9408

4.6 Short-range correlations

In a variational calculation, it is much more difficult to reproduce short-range behaviour of the wave function than the binding energy. Let us compare the zero-range correlations

$$\delta_{ij} = \left\langle \Psi \mid \delta^{(3)}(r_{ij}) \mid \Psi \right\rangle \tag{4.6.22}$$

which is used in the perturbative treatment of hyperfine splittings (see Chapter 8). We consider again $V = \frac{1}{2}\sum r_{ij}$ and *i)* qqq ($m_i = 1$), *ii)* qqQ ($m_i = 1, 1, 5$), and *iii)* QQq ($m_i = 1, 1, 0.2$), in Table 4.6. We remark that when we try to optimize the oscillator parameter in the h.o. expansion (large N') too much, we do not gain significantly on the binding energy (see Table 4.1), but we get very poor results for short-range correlations. On the other hand, one obtains decent values by fixing the parameter at the lowest approximation ($N' = 0$) and then pushing the expansion further.

These are rather general properties of variational calculations [50]. The optimization of the energy forces the approximate wave function to match the exact one at intermediate distances. If the asymptotic behaviour is poorly reproduced, one has to compensate at short distances to preserve the normalization.

Table 4.6: Short-range correlation coefficients δ_{12} and δ_{13} for the ground state bound by a linear potential $V = \frac{1}{2}\sum r_{ij}$, using either the h.o. expansion or the empirical Gaussian expansion. We consider the symmetric case $m_i = 1$ and the set of constituent masses (1, 1, 5) and (1, 1, 0.2).

Case	Harmonic oscillator	δ_{12}	δ_{13}	Gaussian	δ_{12}	δ_{13}
qqq	$N=0$ $(N'=0)$	0.0507	0.0507	1S	0.0507	0.0507
	$N=2$ $(N'=0)$	0.0507	0.0507	2S	0.0547	0.0547
	$N=4$ $(N'=4)$	0.0471	0.0471	3S	0.0550	0.0550
	$N=6$ $(N'=4)$	0.0473	0.0473	1S+1D	0.0516	0.0516
	$N=8$ $(N'=4)$	0.0478	0.0478	2S+1D	0.0556	0.0556
qqQ	$N=0$ $(N'=0)$	0.0430	0.0926	1S	0.0534	0.0843
	$N=2$ $(N'=0)$	0.0517	0.0851	2S	0.0582	0.0906
	$N=4$ $(N'=4)$	0.0507	0.0829	3S	0.0595	0.0905
	$N=6$ $(N'=4)$	0.0519	0.0830	1S+1D	0.0533	0.0870
	$N=8$ $(N'=4)$	0.0526	0.0839	2S+1D	0.0581	0.0932
QQq	$N=0$ $(N'=0)$	0.0754	0.0145	1S	0.0462	0.0184
	$N=2$ $(N'=0)$	0.0469	0.0176	2S	0.0487	0.0201
	$N=4$ $(N'=4)$	0.0505	0.0183	3S	0.0515	0.0201
	$N=6$ $(N'=4)$	0.0484	0.0188	1S+1D	0.0461	0.0186
	$N=8$ $(N'=4)$	0.0494	0.0191	2S+1D	0.0486	0.0203

4.7 Improved variational methods

So far, we have presented variational calculations with straightforward optimization by explicitly varying the parameters and increasing the basis. One may now try to elaborate a little on the convergence pattern. For instance, one may study the variational energy $E(N)$ as a function of the maximum number of states introduced into the h.o. expansion, and try to guess what $E(\infty)$ should be. To this end, $E(N)$ can be written as a rational function

$$E(N) = \frac{a + b\,N^{\alpha} + c\,N^{2\alpha} + \cdots}{1 + b'N^{\alpha} + c'N^{2\alpha} + \cdots} \tag{4.7.23}$$

The trouble is, however, that the Padé coefficients $a, b, \ldots$ are determined with numerical errors, so one should not amplify the noise in the extrapolation.

We now turn to really "professional" variational calculations [46]. They are generally based on Monte Carlo methods for determining the variation parameters and for computing the integrals that are needed. Papanicolaou and Spathis [51], for instance, expand the wave function on generalized coherent states and diagonalize the Hamiltonian on this basis. Some of their results are shown in Table 4.7. They correspond to quark masses $m_i = 1$ and confining potential $V = \frac{1}{2}\sum r_{ij}^{0.1}$. They can be compared

very favourably with the results shown in Table 5.1, obtained from the hyperspherical expansion applied to the same potential.

Table 4.7: Some energies and short-range correlations of a baryon with quark masses $m_i = 1$, bound by $V = \frac{1}{2}\sum r_{ij}^{0.1}$, obtained by expansion into generalized coherent states and elaborate minimization

State	E_0	$10^3\delta_{12}$
$[56, 0^+]$	1.88017	1.25
$[70, 1^-]$	1.9362	
$[56, 0^+]'$	1.96231	0.93
$[70, 0^+]$	1.97256	0.98
$[20, 1^+]$	1.9885	
$[70, 1^-]'$	1.9964	
$[56, 1^-]$	1.9982	
$[70, 1^-]''$	2.0145	

Chapter 5

THE HYPERSPHERICAL FORMALISM

5.1 Introduction

Hyperspherical coordinates were introduced by Delves [52] and the formalism of hyperspherical expansion was further developed by many authors [40, 53, 54] for 3-body or more complicated bound states. The usefulness of this method for baryon spectroscopy was shown by several groups [55].

The basic idea is rather simple: the two relative coordinates are merged into a single 6-dimensional vector. The 3-body problem in ordinary space becomes equivalent to a 2-body problem in 6 dimensions, with a non-central potential. A generalized partial wave expansion leads to an infinite set of coupled radial equations. In practice, however, a very good convergence is achieved with a few partial waves only.

5.2 Basic formalism

Let us start with the equal mass case, i.e. the reduced Hamiltonian

$$H = \frac{\vec{p}_\rho^{\,2}}{m} + \frac{\vec{p}_\lambda^{\,2}}{m} + V(\vec{\rho}, \vec{\lambda}). \tag{5.2.1}$$

The 2-body character of V is not crucial, but it greatly simplifies some of the computations, as we shall see.

The 6-dimensional vector $\tilde{r} = (\vec{\rho}, \vec{\lambda})$ is written in spherical coordinates

$$\tilde{r} = (\vec{\rho}, \vec{\lambda}) = (\xi; \Omega_5) = (\xi; \hat{\omega}_\rho, \hat{\omega}_\lambda, \varphi), \tag{5.2.2}$$

where $\xi = (\vec{\rho}^{\,2} + \vec{\lambda}^{\,2})^{1/2}$ and $\varphi = \tan^{-1}(\rho/\lambda)$.

We now introduce a complete set of 6-dimensional spherical harmonics $\mathcal{P}_{[L]}(\Omega_5)$, where $[L]$ denotes the grand orbital momentum $L = 0, 1, 2 \ldots$ and its associated magnetic numbers, i.e. the generalization of the familiar spherical harmonics Y_l^m. One may

define L more precisely by saying that $\xi^L \mathcal{P}_{[L]}(\Omega_5)$ is a harmonic polynomial of degree L in 6 dimensions [56]

$$\Delta_6 \left(\xi^L \mathcal{P}_{[L]}(\Omega_5)\right) \equiv (\Delta_\rho + \Delta_\lambda) \left(\xi^L \mathcal{P}_{[L]}(\Omega_5)\right) = 0. \tag{5.2.3}$$

In spherical coordinates, this leads to the equation

$$\begin{aligned} \mathcal{L}^2 \mathcal{P}_{[L]}(\Omega_5) &= \left[\vec{l}_\rho^{\,2} + \vec{l}_\lambda^{\,2} - \frac{\partial^2}{\partial\varphi^2} - 4\cot 2\varphi \frac{\partial}{\partial\varphi}\right] \mathcal{P}_{[L]}(\Omega_5) \\ &= L(L+4)\mathcal{P}_{[L]}(\Omega_5) \end{aligned} \tag{5.2.4}$$

associated with the normalization condition

$$\int \mathcal{P}^*_{[L]}(\Omega_5)\mathcal{P}_{[L]'}(\Omega_5)\mathrm{d}\Omega_5 = \delta_{[L],[L]'} \tag{5.2.5}$$

One expands the baryon wave function into hyperspherical harmonics (HH)

$$\Psi(\vec{\rho}, \vec{\lambda}) = \sum_{[L]} \frac{u_{[L]}(\xi)}{\xi^{5/2}} \mathcal{P}_{[L]}(\Omega_5) \tag{5.2.6}$$

so that the Schrödinger equation $H\Psi = E\Psi$, whose expression in spherical coordinates reads

$$\left[\frac{1}{m\xi^{5/2}} \frac{\mathrm{d}^2}{\mathrm{d}\xi^2} \xi^{5/2} - \frac{1}{m} \frac{\mathcal{L}^2 + 15/4}{\xi^2} + E - V(\xi, \Omega_5)\right] \Psi = 0, \tag{5.2.7}$$

becomes equivalent to the infinite set of coupled radial equations

$$\begin{aligned} \frac{1}{m} u''_{[L]}(\xi) - \frac{(L+3/2)(L+5/2)}{m\xi^2} u_{[L]}(\xi) + \left[E - V_{[L],[L]}(\xi)\right] u_{[L]}(\xi) \\ = \sum_{[L]\neq[L]'} V_{[L],[L]'}(\xi) u_{[L]'}(\xi) \end{aligned} \tag{5.2.8}$$

where

$$V_{[L],[L]'}(\xi) = \int \mathrm{d}\Omega_5 \mathcal{P}^*_{[L]}(\Omega_5) V(\xi, \Omega_5) \mathcal{P}_{[L]'}(\Omega_5). \tag{5.2.9}$$

Clearly, solving the 3-body problem that way implies overcoming the following difficulties: listing the appropriate HH, computing the angular projections (5.2.9) and solving the above coupled equations.

5.3 The hyperspherical harmonics

While there is only one HH with $L = 0$, namely $\mathcal{P}_0 = \pi^{-3/2}$, as L increases, the number of HH grows quite fast. There are $N(L) = (L+1)_5/5!$ independent homogeneous polynomials of degree L with 6 variables, and $N(L) - N(L-2)$ independent linear combinations of these are harmonic. So, if one operates without care, one would end

up with a very large number of HH, even if the cut-off $L_{\max}$ in the expansion (5.2.6) is small.

A complete set of HH is provided by the following functions which are eigenstates of the individual orbital momenta l_ρ and l_λ

$$\mathcal{P}_{[L]} = N(\sin\varphi)^{l_\rho}(\cos\varphi)^{l_\lambda} P_n^{l_\rho+1/2,l_\lambda+1/2}(\omega_\rho) Y_{l_\rho}^{m_\rho}(\omega_\rho) Y_{l_\lambda}^{m_\lambda}(\omega_\lambda), \tag{5.3.1}$$

where one has introduced the Jacobi polynomials $P_n^{\alpha,\beta}$ [28] and the normalization coefficient

$$N = \left\{ \frac{2(2n+l_\rho+l_\lambda+2)n!(n+l_\rho+l_\lambda+1)!}{\pi\,[2(n+l_\rho)+1]!!\,[2(n+l_\lambda)+1]!!} \right\}^{1/2} \tag{5.3.2}$$

The integer n, which corresponds to the degree of the Jacobi polynomial, is submitted to the constraint

$$L = l_\rho + l_\lambda + 2n, \tag{5.3.3}$$

Harmonics of given total (ordinary) angular momentum $\vec{l} = \vec{l}_\rho + \vec{l}_\lambda$ (not to be confused with the grand orbital momentum L) are constructed by Clebsch–Gordan coupling of the HH (5.3.1). One should further restrict the expansion (5.2.6) to these HH having the desired permutation properties.

There are several ways of constructing HH of given angular momentum, parity and permutation symmetry. One method consists of using harmonic-oscillator wave functions and removing the Gaussian factor $\exp(-\vec{\lambda}^2 - \vec{\rho}^2)$. More details will be provided in Section 8.3 where we come back to the link between the harmonic oscillator and the HH expansion.

A direct construction of symmetrized HH has been given by Simonov [40], who made great use of the complex vectors $\lambda + i\rho$ and $\lambda - i\rho$ to solve the Laplace equation (5.2.3). For the case of scalar harmonics ($l^P = 0^+$), he arrived at the compact expressions:

$$\begin{aligned} \mathcal{V}_L^\nu &= N_\nu \sqrt{\frac{L+2}{\pi^3}} \cos\alpha\nu\, A^\nu P_n^{\nu,0}(1-2A^2) \\ \mathcal{W}_L^\nu &= \sqrt{\frac{L+2}{\pi^3}} \sin\alpha\nu\, A^\nu P_n^{\nu,0}(1-2A^2) \end{aligned}, \tag{5.3.4}$$

where the scalar variables A and α are introduced

$$A e^{i\alpha} = \frac{\vec{\lambda}^2 - \vec{\rho}^2 + 2i\vec{\lambda}\cdot\vec{\rho}}{\vec{\lambda}^2 + \vec{\rho}^2}. \tag{5.3.5}$$

The integer ν runs from $L/2$ to 0, in steps of 2, so that the degree of the Jacobi polynomial

$$n = \frac{1}{2}\left(\frac{L}{2} - \nu\right) \tag{5.3.6}$$

remains acceptable, i.e. $n \geq 0$. The normalization factor is $N_\nu = 1$ if $\nu \neq 0$ and $N_\nu = 2^{-1/2}$ if $\nu = 0$. All permutation properties of the above harmonics are contained

in the $\cos\alpha\nu$ or $\sin\alpha\nu$ factors: if $\nu = 3\nu'$ (ν' integer) then $\mathcal{V}_L^\nu$ is symmetric and $\mathcal{W}_L^\nu$, if non-vanishing, antisymmetric; otherwise, $\mathcal{V}_L^\nu$ and $\mathcal{W}_L^\nu$ form a pair of mixed symmetry.

In principle, one can write down the HH of any given angular momentum l and projection $l_z = M$, parity P and permutation properties. Barma and Mandelzweig [54], using earlier work [57] on the permutation group, propose

$$\mathcal{P}_{[L]} \propto \exp i\alpha\nu \sum_{m=-l}^{l} D_{Mm}^l(\alpha_1,\alpha_2,\alpha_3) F_m(A), \tag{5.3.7}$$

where α_1, α_2 and α_3 are the Euler angles defining the position of the particle plane $(\vec{\rho}, \vec{\lambda})$ with respect to fixed axes and are thus expressable in terms of $\hat{\omega}_\rho$ and $\hat{\omega}_\lambda$; D_{Mm}^l are the Wigner rotation functions; $F_m(A)$ are given by a differential equation that is deduced from the original equation (5.2.3) or (5.2.4). However, no concise expression as simple as (5.3.4) can be exhibited for general l.

5.4 The radial potentials

The potentials which enter into the coupled equations are given by Eq. (5.2.9). For simple 2-body potentials inserted between the scalar harmonics of Simonov, the corresponding integral can be carried out analytically [53, 54]. Otherwise, the computation is more painful.

A possible strategy consists of expanding the potential itself into HH, say

$$V(\xi,\Omega_5) = \sum_{[L]} v_{[L]}(\xi)\mathcal{Q}_{[L]}(\Omega_5), \tag{5.4.1}$$

where the summation is restricted to HH that are scalar and fully symmetric, i.e. of the type $\mathcal{Q}_{[L]} = \mathcal{V}_L^{3\nu'}$. Then

$$V_{[L],[L]'}(\xi) = \sum_{[L]''} v_{[L]''}(\xi)\,\langle [L]' \mid [L]'' \mid [L]\rangle\,. \tag{5.4.2}$$

The so-called "3H" coefficients which enter into the above expression are independent of the potential and thus can be stored once aand for all. They are given by

$$\langle [L]' \mid [L]'' \mid [L]\rangle = \int \mathrm{d}\Omega_5 \mathcal{P}_{[L]}^*(\Omega_5)\mathcal{Q}_{[L]''}(\Omega_5)\mathcal{P}_{[L]'}(\Omega_5), \tag{5.4.3}$$

and are submitted to the selection rule $|L - L'| \leq L'' \leq L + L'$.

5.5 The coupled equations

The coupled equations (5.2.8) can be solved by several numerical means. For instance, one can use the discretization algorithm described in Section 2.5 for mesons, which is easily generalized to coupled equations.

Although present computers allow one to diagonalize very large matrices, it seems desirable to optimize the efficiency of the method. The main question deals with the HH one has to actually include in the hyperspherical expansion (5.2.6). A simple strategy consists of taking all HH of appropriate quantum numbers up to a value $L_{\max}$ of the grand orbital momentum and studying the convergence as $L_{\max}$ increases. In fact, for a given L, only a few HH contribute significantly. This leads to the improved strategy of "potential harmonics" [53]. Consider for instance the ground state, whose wave function is scalar and symmetric. Then the lowest and dominant harmonics is $\mathcal{P}_0 = \pi^{-3/2}$. For each L, one constructs the potential harmonic as being the linear combination which is maximally coupled to $\mathcal{P}_0$. It is

$$\mathcal{R}_L = \frac{\sum V_{0,[L]} \mathcal{P}_{[L]}}{\left(\sum V_{0,[L]}^2\right)^{1/2}}, \tag{5.5.1}$$

where the summation runs over the magnetic numbers associated with L. It is coupled to $\mathcal{P}_0$ through the transition potential

$$\langle 0 \,|\, V \,|\, \mathcal{R}_L \rangle = \left(\sum V_{0,[L]}^2\right)^{1/2} \tag{5.5.2}$$

The word "potential" comes from $\mathcal{R}_L$ containing the harmonics that are present in the expansion of the potential itself.

For power-law potentials, $\mathcal{R}_L$ is independent of ξ. For general potentials, $\mathcal{R}_L$ depends on ξ, but the method remains applicable [53].

In practice, one can first compute the bound state in the approximation of potential harmonics, with a fairly large $L_{\max}$. Then the effect of non-potential harmonics of low L, say $\mathcal{S}_{[L]}$, can be estimated by solving Sternheimer-type equations. If

$$\Psi(\vec{\rho}, \vec{\lambda}) = \sum_L \frac{v_L(\xi)}{\xi^{5/2}} \mathcal{R}_L(\Omega_5) + \sum_{[L]} \frac{w_{[L]}(\xi)}{\xi^{5/2}} \mathcal{S}_{[L]}(\Omega_5) \tag{5.5.3}$$

at first order

$$\begin{aligned} \frac{1}{m} w''_{[L]}(\xi) - \frac{(L+3/2)(L+5/2)}{m\xi^2} w_{[L]}(\xi) + \left[E_0 - V_{[L],[L]}(\xi)\right] w_{[L]}(\xi) \\ = \sum_{L'} V_{[L],L'}(\xi) v_{L'}(\xi) + \sum_{[L] \neq [L]'} V_{[L],[L]'}(\xi) w_{[L]'}(\xi) \end{aligned}, \tag{5.5.4}$$

where E_0 is frozen to its value at the approximation of potential harmonics. The second-order correction to the energy is

$$\Delta E = E - E_0 = \sum_{L',[L]} \int_0^\infty w_{[L]}(\xi) V_{[L],L'}(\xi) u_{L'}(\xi) d\xi \tag{5.5.5}$$

In practice, one often neglects the last term in Eq. (5.5.3), which only contributes to higher orders: then the corrections can be computed separately for each non-potential harmonic.

5.6 Results

The convergence of the hyperspherical expansion for baryons was studied in some detail in Ref. [58]. Table 5.1 shows the result of a calculation with equal masses $m_i = 1$ and the simple power-law potential $V = \frac{1}{2}\sum r_{ij}^{0.1}$, for the ground-state energy and the correlation coefficient $\delta^{(3)}(r_{12})$. In Table 5.2, we use instead a linear potential $V = \frac{1}{2}\sum r_{ij}$. The convergence is spectacular for the binding energy and slightly slower for the correlation coefficient. Similar conclusions were reached by other authors [55].

For excited states, the convergence pattern is less impressive and, in practice, one has to include more harmonics in the calculation.

Table 5.1: Ground-state energy E_0 and correlation coefficient $\delta^{(3)}(r_{12})$ in the potential $V = \frac{1}{2}\sum r_{ij}^{0.1}$ with unit quark masses, as a function of the maximal grand orbital. N is the number of coupled equations.

$L_{\max}$	N	E_0	$10^3\delta^{(3)}(r_{12})$
0	1	1.88075	1.128
4	2	1.88032	1.186
6	3	1.88020	1.221
8	4	1.88019	1.232
10	5	1.88018	1.239
12	7	1.88018	1.245
14	8	1.88017	1.248
16	10	1.88017	1.249

Table 5.2: Energy and correlation coefficient for the ground state ($n = 0$) and its hyper-radial excitation ($n = 1$) for a linear potential $V = \frac{1}{2}\sum r_{ij}$ and masses $m_i = 1$

$L_{\max}$	$E_{n=0}$	$\delta^{(3)}(r_{12})_{n=0}$	$E_{n=1}$	$\delta^{(3)}(r_{12})_{n=1}$
0	3.8647	0.05504	5.3280	0.05505
4	3.8633	0.05628	5.3217	0.05597
6	3.8631	0.05680	5.3208	0.05652
8	3.8631	0.05689	5.3207	0.05664

5.7 Extension to unequal masses

Let us consider now a baryon made of different quarks. We use the Jacobi coordinates of Eq. (3.8.1) and the corresponding reduced mass $\mu = 2m_1m_2/(m_1 + m_2)$. If two quarks are identical, as in Λ, Σ or Ξ type of baryons, or almost identical, as s and u in Ξ_c^+, they are assigned to labels 1 or 2. This helps to enforce the exact or approximate symmetry constraints. The hyperspherical treatment of

$$H = \frac{1}{\mu}(\vec{p}_\rho^{\,2} + \vec{p}_\lambda^{\,2}) + V(\vec{\rho}, \vec{\lambda}) \tag{5.7.1}$$

is then performed as for identical quarks. There are, however, more harmonics into the expansion, since some (if $m_1 = m_2 \neq m_3$) or all (if $m_1 \neq m_2 \neq m_3$) symmetry constrains are relaxed. This makes the use of potential harmonics more desirable.

In Ref. [58] is studied the case of harmonic forces, for which an exact solution is available. The results of the linear model $V = \frac{1}{2}\sum r_{ij}^{\beta}$ with $\beta = 1$, $m_1 = m_2 = 1$, and $m_3 = m'$ are shown in Table 5.3. Another example, more suited to double-charm baryons [7] is given in Table 5.3. The hyperscalar approximation is obviously rather poor for the wave function. However, the convergence remains satisfactory as $L_{\max}$ increases.

Table 5.3: Convergence of the hyperspherical expansion for a power-law potential $V = \frac{1}{2}\sum r_{ij}^{\beta}$ with quark masses $m_1 = m_2 = 1$ and $m_3 = m'$ (for $\beta = 0.1$, the correlation coefficients are multiplied by 10^3)

β	m'	$L_{\max}$	E_0	$\delta^{(3)}(r_{12})$	$\delta^{(3)}(r_{13})$
		0	3.4671	0.0468	0.1006
		2	3.4405	0.0569	0.0924
1	5	4	3.4381	0.0587	0.0944
		6	3.4380	0.0595	0.0945
		8	3.4379	0.0598	0.0949
		0	5.0372	0.0819	0.0158
		2	4.9523	0.0503	0.0193
1	0.2	4	4.9303	0.0530	0.0203
		6	4.9393	0.0522	0.0205
		8	4.9392	0.0523	0.0206
		0	1.9481	1.1891	0.2289
		2	1.9463	0.8866	0.2706
0.1	0.2	4	1.9453	0.9972	0.2932
		6	1.9452	0.9853	0.2980
		8	1.9452	0.9983	0.3018

Chapter 6

FADDEEV EQUATIONS

6.1 Introduction

The Faddeev equations [59] were first written to handle scattering problems in momentum space with short-range potentials. We shall show below that they can be adapted to describe, in configuration space, bound states produced by confining potentials.

In nuclear physics, one is dealing with rather delicate potentials, with sharp variations and strong spin dependence. The difficulty in computing the 3-nucleon properties very accurately has led to (friendly but) animated controversies between the school of Faddeev equations and the school of hyperspherical expansion and other variational methods. With the simple potentials used in baryon spectroscopy, both approaches lead to very accurate results, so that the choice between them is mostly a matter of taste [60]. The method of Faddeev equations was applied to baryon spectroscopy for instance in Ref. [61].

6.2 Basic equations

We follow here the approach of Noyes [62], Merkuriev [63] and the Grenoble group [64]. Let us consider the symmetric Hamiltonian

$$H = H_0 + V_1 + V_2 + V_3, \tag{6.2.1}$$

where H_0 is the relative kinetic energy of the three identical quarks (thus free of centre-of-mass motion), and $V_1 = V(r_{23})$ and so on. We use the Jacobi variables of Eq. (3.4.2) $\vec{\rho} = \vec{\rho}^{(3)}$ and $\vec{\lambda} = \vec{\lambda}^{(3)}$ as well as the other variables $\vec{\rho}^{(i)}$, $\vec{\lambda}^{(i)}$ deduced by the circular permutation (3.5.7).

Let us search for a symmetric eigenstate $\Psi(\vec{\rho}, \vec{\lambda})$, which could be, for instance, the ground state with spin $S = 3/2$, in the form

$$\Psi(\vec{\rho}, \vec{\lambda}) = \Psi_1(\vec{\rho}, \vec{\lambda}) + \Psi_2(\vec{\rho}, \vec{\lambda}) + \Psi_3(\vec{\rho}, \vec{\lambda}), \tag{6.2.2}$$

where

i) Ψ_3 is even in $\vec{\rho}$

ii) Ψ_3 has the same short-range and long-range behaviour as the total wave function $\Psi(\vec{\rho},\vec{\lambda})$

iii) the other components Ψ_i are deduced by circular permutation, namely

$$\Psi_i(\vec{\rho},\vec{\lambda}) = \Psi_3(\vec{\rho}^{(i)},\vec{\lambda}^{(i)}). \tag{6.2.3}$$

Clearly, the set of equations

$$(E - H_0)\Psi_i = V_i(\Psi_1 + \Psi_2 + \Psi_3), \quad i = 1,2,3 \tag{6.2.4}$$

implies the desired Schrödinger equation $H\Psi = E\Psi$ for the total wave function Ψ. The uniqueness of the Faddeev decomposition does not raise much problem in this bound-state problem, unlike in scattering situations with three or more particles, for which this delicate question is discussed, *e.g.* by Merkuriev [63] or Omnes [65].

For identical particles, one has simply to solve the equation

$$(E - H_0)\Psi_3(\vec{\rho},\vec{\lambda}) = V_3(1 + P_{\rightharpoonup} + P_{\leftharpoondown})\Psi_3(\vec{\rho},\vec{\lambda}) \tag{6.2.5}$$

For an antisymmetric state, one imposes Ψ_3 to be odd in $\vec{\rho}$. For a state of mixed symmetry, the parenthesis is replaced by $(1 + jP_{\rightharpoonup} + j^2P_{\leftharpoondown})$.

6.3 Solving the Faddeev equation

Since there are several ways of building a state of given total angular momentum J by combining the angular momenta $l_\rho(\equiv a)$ and $l_\lambda(\equiv b)$, let us introduce the normalized harmonics

$$\mathcal{Y}^M_{a,b,J}(\hat{\rho},\hat{\lambda}) = \sum_{a',b'} \langle a,a';b,b' \mid J,M\rangle Y^{a'}_a(\hat{\rho})Y^{b'}_b(\hat{\lambda}), \tag{6.3.1}$$

and the partial-wave expansion

$$\Psi_3(\vec{\rho},\vec{\lambda}) = \sum_{a,b} \frac{\phi_{ab}(\rho,\lambda)}{\rho\lambda}\mathcal{Y}^M_{a,b,J}(\hat{\rho},\hat{\lambda}). \tag{6.3.2}$$

The projection of the Noyes–Faddeev equation (6.2.5) gives

$$\begin{aligned} &E + \frac{1}{m}\left[\frac{\partial^2}{\partial\rho^2} + \frac{\partial^2}{\partial\lambda^2} - \frac{a(a+1)}{\rho^2} - \frac{b(b+1)}{\lambda^2} - V(\rho)\right]\phi_{ab}(\rho,\lambda) \\ &\quad = V(\rho)\sum_{a',b'}\int_{-1}^{+1} h^J_{a,b;a',b'}(\rho,\lambda,u)\phi_{a'b'}(\rho^{(1)},\lambda^{(1)})\mathrm{d}u. \end{aligned} \tag{6.3.3}$$

Here we notice that the $P_{\rightharpoonup}$ and $P_{\leftharpoondown}$ terms give the same contribution. For computing the kernel h, we introduce the rotated coordinates $\vec{\rho}^{(1)}$, $\vec{\lambda}^{(1)}$ and the angular variables u and $u^{(1)}$ given by

$$\vec{\lambda}^{(1)} + i\vec{\rho}^{(1)} = j(\vec{\lambda} + i\vec{\rho}), \quad \vec{\lambda}\cdot\vec{\rho} = \lambda\rho u, \quad \vec{\lambda}^{(1)}\cdot\vec{\rho}^{(1)} = \lambda^{(1)}\rho^{(1)}u^{(1)}, \tag{6.3.4}$$

so that

$$\int \mathrm{d}^2\hat{\rho}^2\mathrm{d}^2\hat{\lambda}\left[\mathcal{Y}^M_{a,b,J}(\hat{\rho},\hat{\lambda})\right]^* \mathcal{Y}^M_{a',b',J}(\hat{\rho}^{(1)},\hat{\lambda}^{(1)}) = \int_{-1}^{+1}\frac{\rho^{(1)}\lambda^{(1)}}{\rho\lambda}h^J_{a,b;a',b'}(\rho,\lambda,u)\mathrm{d}u. \tag{6.3.5}$$

Explicit expressions for h exist in the literature [64]. For the $J = 0$ case, h is simply given by

$$h^0_{a,b;a',b'} = \frac{\rho\lambda}{\rho^{(1)}\lambda^{(1)}}\sqrt{2a+1}\sqrt{2b+1}\delta_{ab}\delta_{a'b'}P_a(u)P_{a'}(u^{(1)}), \tag{6.3.6}$$

where P_n is a Legendre polynomial.

6.4 Numerical solution of the Faddeev equations

The set of coupled equations (6.3.3) can be solved numerically almost as it stands. For instance one can use the mapping and discretization procedure proposed in Section 2.5 for mesons. If r_0 is a plausible scale of the interquark distances, we introduce

$$x(\rho) = \frac{\rho}{\rho + r_0}, \quad y(\lambda) = \frac{\lambda}{\lambda + r_0} \tag{6.4.1}$$

and

$$\phi_{ab}(\rho,\lambda) = \frac{1}{r_0(1-x)(1-y)}v_{ab}(x,y), \tag{6.4.2}$$

where

$$v_{ab}(x,y) = \sum_{i,j} v_{abij}\sum_{m,n=1}^{N}\sin\frac{i\pi n}{N+1}\sin n\pi x\sin\frac{j\pi m}{N+1}\sin n\pi y. \tag{6.4.3}$$

The v_{abij}, the unknowns of our problem, are the values of $v_{abij}(x,y)$ at selected points $[x_i,y_j] = [i/(N+1), j/(N+1)]$. They are given, together with the energies E, by the matrix equation

$$\sum_{a'b'i'j'} A_{abij,a'b'i'j'}v_{a'b'i'j'} = Ev_{abij} \tag{6.4.4}$$

with

$$\begin{aligned} A_{abij,a'b'i'j'} &= \delta_{aa'}\delta_{bb'}\frac{\hbar^2}{mr_0^2}\left\{t(x_i,x_{i'})\delta_{jj'} + \delta_{ii'}t(y_j,y_{j'})\right\} \\ &\quad + \delta_{aa'}\delta_{bb'}\frac{\hbar^2}{mr_0^2}\delta_{ii'}\delta_{jj'}\left[a(a+1)\frac{(1-x_i)^2}{x_i^2} + b(b+1)\frac{(1-y_j)^2}{y_j^2}\right], \\ &\quad + V[\rho(x_i)]\left[\delta_{aa'}\delta_{bb'}\delta_{ii'}\delta_{jj'} + (1-x_i)(1-y_j)B_{abij,a'b'i'j'}\right] \end{aligned} \tag{6.4.5}$$

where the matrix elements of the radial kinetic energy have been already given in Section 2.5.

$$t(x_i,x_{i'}) = (1-x_i)^4\frac{2\pi^2}{N+1}\sum_k k^2\sin k\pi x_i\sin k\pi x_{i'}. \tag{6.4.6}$$

The most delicate (and time-consuming) part comes from the permutation operators. It reads

$$B_{abij,a'b'i'j'} = \int_{-1}^{+1} \mathrm{d}u\, h^J_{ab;a'b'}(\rho_i, \lambda_j, u) \left(\sum_{k=1}^{N} \frac{2}{N+1} \sin k\pi x_{i'} \sin k\pi \tilde{x}_{ij} \right) \times \left(\sum_{q=1}^{N} \frac{2}{N+1} \sin q\pi x_{i'} \sin q\pi \tilde{y}_{ij} \right), \tag{6.4.7}$$

where

$$\begin{aligned} \rho_i &= \rho(x_i) \\ \lambda_j &= \lambda(y_j) \\ \rho'_{ij} &= \frac{1}{2}(\rho_i^2 + 3\lambda_j^2 - 2\rho_i\lambda_j u)^{1/2} \\ \lambda'_{ij} &= \frac{1}{2}(3\rho_i^2 + \lambda_j^2 + 2\rho_i\lambda_j u)^{1/2} \\ \tilde{x}_{ij} &= x(\rho'_{ij}) \\ \tilde{y}_{ij} &= y(\lambda'_{ij}). \end{aligned} \tag{6.4.8}$$

Among the many possible variants, one consists of using polar coordinates

$$\rho = r \sin\theta, \quad \lambda = r\cos\theta, \tag{6.4.9}$$

which are similar to the hyperspherical coordinates of Section 5.2. One can then perform the Fourier expansion in the rescaled variables $x = r/(r + r_0)$ and $y = 2\theta/\pi$. The advantage is that the kernel h conserves the hyper-radius r, thus reducing the number of times it has to be computed. If, however, the potential $V(\rho)$ varies rapidly, one has to introduce many points in the discretization of the θ dependence, at least for large r.

6.5 Results

We present below some results concerning the symmetric $J = 0$ case, i.e. the $[56, 0^+]$ states in our previous notation. We first notice that, for the harmonic oscillator, the partial-wave expansion is exactly restricted to angular momenta $a = b = 0$. It is thus useful to test the algorithms by solving Eq. (6.3.3) with $V(\rho) = \rho^2$.

Let us now consider the linear potential $V(r) = \frac{1}{2}\sum r_{ij}$ and analyse the results as a function of the maximal orbital momentum $a_{\max}$ introduced in the partial-wave expansion (6.3.2). A well-known trick consists of shifting the potential, to optimize the dominance of the $a = 0$ partial wave and ensure a nice asymptotic decrease of the Faddeev component Ψ_3 [66]. More precisely, one performs the computation with $V = \sum[\frac{1}{2}r_{ij} - v_0]$ and eventually adds $3v_0$ to the eigenvalues. The results shown in Table 6.1 have been obtained with $v_0 = 2$. Preliminary investigations have confirmed that the results look much better for such large values of v_0.

The accuracy is not impressive for the eigenenergies, at least when they are computed as eigenvalues of the coupled integro-differential equations (6.3.8). This could probably be improved by recomputing the energy as $\langle \Psi \,|\, H \,|\, \Psi \rangle$ [66]. On the other hand, one should stress the impressive quality of the Faddeev wave function. With only the lowest partial wave $a = b = 0$, the correlation coefficient δ_{12} is obtained almost exactly. We have seen in the previous chapters that it was very painful to achieve a decent convergence for δ_{12} with variational methods.

Table 6.1: Binding energy and short-range correlation coefficient of the two first $J^P = 0^+$ levels in the linear potential $V = \frac{1}{2}\sum r_{ij}$, with quark masses $m_i = 1$, obtained by solving the Faddeev equations. The substraction constant is $v_0 = 2$ and $a_{\max}$ denotes the maximal orbital momentum in the Faddeev amplitude.

$a_{\max}$	$E_{0,0}$	$\delta_{12}^{n=0}$	$E_{1,0}$	$\delta_{12}^{n=1}$
0	3.863	0.0566	5.318	0.0565
2	3.862	0.0570	5.317	0.0568

Chapter 7

QUARK–DIQUARK AND BORN–OPPENHEIMER APPROXIMATIONS

7.1 Introduction

Though the 3-body problem for baryons is not too complicated when appropriate methods are used, some simplifications are welcome, especially if in addition to the technical aspects, they shed some light on the quark dynamics.

In this respect, one should acknowledge that the hyperscalar approximation does not have any simple and obvious physical interpretation. One may simply say that, out of the many degrees of freedom, one can extract one collective distance which governs the main features of the wave function.

In contrast, the quark–diquark approximation and the Born–Oppenheimer approximation, when they are valid, immediately tell us that the dynamics lies essentially in one single interquark separation, and that we are dealing with an effective 2-body problem.

7.2 The diquark–quark approximation

Diquarks are almost as old as quarks. The possibility that quarks might cluster pairwise in baryons, leading to a simple 2-body structure, has been suggested by many authors since the early days of the quark model. There are currently many speculations on the use of diquarks to analyse baryon production in e^+e^- experiments, in hadronization of jets, or in the decay of heavy particles [11]. We shall restrict ourselves here to the domain of baryon spectroscopy.

The first consequence of the extreme version of the quark–diquark picture would be a dramatic simplification of the spectrum. States like the $[20, 1^+]$ level of the $N = 2$ band of the harmonic oscillator, where both "ρ" and "λ" degrees of freedom are excited,

should be absent in the diquark model. These states are, however, hardly formed in the usual meson–nucleon or photon–nucleon entrance channels, where spectator diagrams are favoured. Therefore, the distinction between the conventional 3-quark model and the diquark–quark model requires high-statistics production experiments. This could be one of the goals of a future high-intensity hadron factory [67].

Another striking consequence of the extreme quark–diquark model would be the appearence of new types of hadrons. If diquarks are taken seriously as elementary constituents, then, besides ordinary hadrons which are mesons (quark–antiquark) and baryons (quark–diquark), one should find "diquonia" (diquark–antidiquark) and, perhaps, "dibaryons". It is sufficient to say here that there is no firm experimental evidence for such states.

In a weaker version of the diquark model, one simply assumes that a diquark clustering occurs in baryons, leading to a simplified phenomenological picture in terms of a quark surrounding a diquark. This was, for instance, the point of view adopted by Lichtenberg et al.[68], who described ordinary mesons and baryons with a unique potential, the diquark mass being an adjustable parameter.

This suggests analysing rigorously to what extent diquark clustering actually results from the quark dynamics. For instance, it was claimed for many years that orbitally-excited baryons *should* consist of a quark and a diquark at both ends of a rotating string, with a colour $(3 - \bar{3})$ structure, since the experimental Regge slope α' (defined as $M^2 = \alpha' J$) is the same as for mesons. Martin [11, 69] has shown that this clustering, in fact, results from the ordinary 3-quark dynamics. He considered the Hamiltonian

$$H = \sum_i \frac{\vec{p}_i^{\,2}}{2m} + b \sum_{i<j} r_{ij} \tag{7.2.1}$$

and looked for the lowest classical configuration of given angular momentum l. For low l, the minimum corresponds to the symmetric configuration of an equilateral triangle. As l becomes larger, the minimum is obtained (modulo permutations) for $r_{12} = 0$ and $r_{31} = r_{32} = r$. Since the quantum states of high l are sharply localized in a pocket of attraction between an external and an internal centrifugal barrier, the classical configuration is likely to provide a very good approximation of the quantum states. Martin [69] also analysed the case of a collective potential [70]

$$V = b \min(d_1 + d_2 + d_3), \tag{7.2.2}$$

where the sum of the distances linking the quarks to a junction is minimized with respect to the location of the junction. This corresponds to a generalization of the linear potential for mesons, where the chromoelectric flux has the minimal length from the quark to the antiquark. Relativistic kinematics was also considered in Ref. [69]. In each case, the same conclusion was reached: high l baryons seem to be of the quark–diquark type, in the semi-classical approximation.

A full quantum, but numerical, study was carried out in Ref. [71], with restriction to the non-relativistic case with pairwise interaction. Various flavour configurations of different angular momentum l were analysed.

A first means of investigation consists of comparing the $(q_1q_2q_3)$ 3-body mass spectrum to the $[(q_1q_2)-q_3]$ approximation, where one first computes the mass of the (q_1q_2) diquark out of the quark–quark potential $v(r_{12})$ and then the mass of the baryon as a diquark–quark state bound by the 2-body potential $V = 2v(r_{31} = r_{32} = r)$. This comparison of masses is a little disappointing. The agreement between the approximate and the exact masses is often accidental and does not imply a genuine diquark clustering inside the baryon.

Some 3-body wave functions were also analysed in Ref. [71], for various flavour combinations and various angular momenta. In general, there is no diquark clustering in the wave function, with some noticeable exceptions:

– Ground-state baryons with two heavy quarks, QQq, look like a localized colour source QQ surrounded by a light quark q. The effect is, however, less and less pronounced for excited states, suggesting instead the use of the Born–Oppenheimer approximation, as discussed in the next section.

– At high angular momenta, baryons exhibit a clear quark–diquark structure (of course, in the case of identical quarks, several pair-clusterings are present to comply with the desired permutation symmetry, but they do interfere with each other). Again, this clustering results from the dynamics and does not require the help of mysterious short-range forces to keep the quarks together. For double-charm baryons, the asymptotic clustering is of the (Qq)–Q type, i.e. differs from the structure experienced by the ground state.

7.3 The Born–Oppenheimer approximation

The Born–Oppenheimer method is very often used in molecular physics and other few-body problems and always turns out to be very efficient and to actually work better than expected. This method seems particularly suited for baryons bearing two units of heavy flavour, since the heavy quarks move much more slowly than the light quark.

Let us consider a $(1,2,3) = (QQq)$ baryon, with quark masses m, m and m'. The generalization to $m_1 \neq m_2$ is obvious. With the Jacobi coordinates of Eq. (3.8.55), the Hamiltonian reads

$$H = \frac{\vec{p}_\rho^{\,2}}{m} + \frac{\vec{p}_\lambda^{\,2}}{m} + \sum_{i<j} v(r_{ij}) \equiv \frac{\vec{p}_\rho^{\,2}}{m} + v(\rho) + h(\vec{\rho},\vec{\lambda}). \tag{7.3.3}$$

By including the recoil of the charmed core, we greatly improve the accuracy of the calculation, at no expense.

For any fixed $\vec{\rho}$, one can compute the eigenstates corresponding to the stationary states of the light quark, i.e.

$$h(\vec{\rho},\vec{\lambda}) f(\vec{\rho},\vec{\lambda}) = \epsilon(\rho) f(\vec{\rho},\vec{\lambda}). \tag{7.3.4}$$

This corresponds to a one-particle problem in a non-central potential. Astute calculations could make use of elliptic or bi-polar coordinates. In fact, one may simply use an

ordinary expansion into partial waves

$$f(\vec{\rho},\vec{\lambda}) = \sum_l \frac{u_l(\rho,\lambda)}{\lambda} Y_l^0(\theta), \tag{7.3.5}$$

resulting in coupled equations for the u_l's.

Consider first the ground state. If one adds the light-quark energy $\epsilon(\rho)$ to the direct interaction between the heavy quarks, one gets the simplest (and well-known) form of the Born–Oppenheimer approximation, sometimes referred to as the "extreme adiabatic" [72]

$$\left[-\frac{\Delta_\rho}{m} + v_{12}(\rho) + \epsilon(\rho)\right] \phi_0(\vec{\rho}) = E^{\rm EA} \phi_0(\vec{\rho}), \tag{7.3.6}$$

which overestimates the binding, i.e. is antivariational. Indeed, $E^{\rm EA} \leq E^{\rm exact}$ results from the operator inequality [33]

$$h(\vec{\rho},\vec{\lambda}) > \epsilon(\rho) \quad \forall \vec{\rho}. \tag{7.3.7}$$

The method is in fact more systematic. The exact wave function $\Psi(\vec{\rho},\vec{\lambda})$ of the (QQq) system can be expanded as

$$\Psi(\vec{\rho},\vec{\lambda}) = \sum_n \phi_n(\vec{\lambda}) f_n(\vec{\rho},\vec{\lambda}), \tag{7.3.8}$$

reducing the 3-body problem to an infinite set of coupled equations for the $\phi_n(\vec{\lambda})$

Keeping only the first term in the above expansion corresponds to a variational approximation, with a trial wave function $\phi_0 f_0$. This is sometimes called [72] the "uncoupled adiabatic" or "variational adiabatic" approximation

$$\left[-\frac{\Delta_\rho}{m} + v_{12}(\rho) + \epsilon(\rho) - \left\langle f_0 \,|\, \frac{\Delta_\rho}{m} \,|\, f_0 \right\rangle\right] \phi_0(\vec{\rho}) = E^{\rm UA} \phi_0(\vec{\rho}). \tag{7.3.9}$$

For improved calculations, one has to keep more terms in Eq. (7.3.8). An optimal choice consists of grouping together the $f_n(\vec{\rho},\vec{\lambda})$ in a combination which provides the maximal correction. This is reminiscent of the potential harmonics in hyperspherical expansions, as studied in Section 5.5. Here, we remark that $f_0(\vec{\rho},\vec{\lambda})$ is coupled to the higher adiabatics through the kinetic energy. So, we use a normalized $\nabla_{\hat{\rho}} f_0(\vec{\rho},\vec{\lambda})$ to supplement $f_0(\vec{\rho},\vec{\lambda})$, namely

$$\Psi(\vec{\rho},\vec{\lambda}) = \phi_0(\vec{\lambda}) f_0(\vec{\rho},\vec{\lambda}) + \phi_b(\vec{\lambda}) f_b(\vec{\rho},\vec{\lambda}) \tag{7.3.10}$$

with

$$f_b(\vec{\rho},\vec{\lambda}) = \frac{\hat{\rho}\, \nabla_{\hat{\rho}} f_0(\vec{\rho},\vec{\lambda})}{\sqrt{\int |\, \hat{\rho}\, \nabla_{\hat{\rho}} f_0(\vec{\rho},\vec{\lambda})\,|^2\, {\rm d}^3\rho}} \tag{7.3.11}$$

Solving the two coupled equations in f_0 and f_b gives the so-called "coupled adiabatic" approximation [72], which is always extremely close to (above) the exact result.

Detailed numerical studies of the Born–Oppenheimer approximation have been performed in the context of studies of baryons with double charm [7, 73]. The method works quite well for ccq configurations, as expected, but also for the ssq or even qqq cases. In Table 7.1, we display a comparison of the extreme and uncoupled adiabatic approximations with exact results for the mmm' system with masses $m = 1$ and $m' = 0.2$, 0.5 and 1, bound by the smooth $1/2\sum r_{ij}^{0.1}$ potential. The quality of the approximation is impressive for both the energy of the first levels and the short-range correlation.

What about the excited states in the Born–Oppenheimer approximation? We consider here the optimal case $m' \gg m$. This implies that it is much more economical to excite the relative motion of the heavy quarks than the motion of the light quark around them. For instance, in the harmonic oscillator model, there is a ratio exactly $[2m/(2m'+m)]^{1/2}$ between the corresponding excitation energies. Then, for the first excited states, the light-quark wave function remains in the lowest adiabatic $f_0(\vec{\rho},\vec{\lambda})$: the binding energy and the qq distribution is obtained from the low-lying excited states of Eq. (7.3.9) or (7.3.6).

Higher states may also consist of an excitation of the light quark, corresponding to a dominant $\tilde{\phi}_0 f_n$ component. In general, one hardly avoids mixing between such a configuration and the previous ones, so that accurate estimates require solving coupled equations. Still, the Born–Oppenheimer method provides one of the most efficient accesses to these states.

Table 7.1: Lowest levels and short-range qq correlations for qqq′ in the potential $V = \frac{1}{2}\sum r_{ij}^{0.1}$, calculated either exactly or with two versions of the Born–Oppenheimer method, the extreme and the variational adiabatic approximations

m	m'	Method	$E_{0,0}$	$10^3\delta_{12}^{n=0}$	$E_{1,0}$	$10^3\delta_{12}^{n=1}$	$E_{0,1}$
		extr.	1.9450	1.001	2.0157	0.714	1.9922
1	0.2	exact	1.9452	0.998	2.0160	0.715	1.9925
		var.	1.9453	1.002	2.0163	0.715	1.9926
		extr.	1.9037	1.128	1.9823	0.816	1.9557
1	0.5	exact	1.9042	1.124	1.9815	0.819	1.9565
		var.	1.9045	1.131	1.9838	0.818	1.9570
		extr.	1.8794	1.233	1.9636	0.887	1.9350
1	1	exact	1.8802	1.249	1.9590	0.905	1.9362
		var.	1.8810	1.237	1.9664	0.892	1.9374

Chapter 8

LEVEL ORDER

8.1 Introduction

Shortly after the discovery of charmonium, in November 1974, several $c\bar{c}$ potentials were proposed, with an astonishing descriptive and predictive power. It was quickly realized that many different potentials $V(r)$ can describe the main features of the data, namely the level ordering of the various radial and orbital excitations. This led Martin and others to search systematically sufficient conditions to be fulfilled by the potential in order to ensure a certain level ordering or a certain pattern of the level spacing.

With the discovery of the upsilon family, the game (anticipated in fact by Eichten and Gottfried [74]) became even more challenging. One has to find classes of potentials describing different quarkonium families simultaneously, a tribute paid to the universality of the quark–antiquark potential. Many works have been published on the mass dependence of the binding energies and related tests of flavour independence.

The accumulation of new mathematical results on the confined 2-body problem during the last 15 years is actually impressive. This encouraged some colleagues and myself to also investigate the 3-body case. We checked our conjecture that the difficulty is far more severe than in the 2-body case but we discovered, from the many papers on the quark model of baryons, that there are already a lot of partial results, just waiting to be collected together and generalized. This is why we are able to present here and in the next chapter a fair quantity of results on the 3-body binding energies.

8.2 Nearly harmonic potentials

We first consider the case where the harmonic-oscillator Hamiltonian (3.7.44) is perturbed by a small additional potential

$$V = \vec{\rho}^2 + \vec{\lambda}^2 + \delta V = \vec{\rho}^2 + \vec{\lambda}^2 + v(r_{12}) + v(r_{23}) + v(r_{31}). \tag{8.2.1}$$

We note $\delta(n,l)$ the 2-body matrix elements

$$\delta(n,l) = \langle n,l \mid v \mid n,l\rangle = \int v(\vec{\rho})|\varphi_{n,l}(\vec{\rho})|^2 \mathrm{d}^3\vec{\rho} \tag{8.2.2}$$

and notice that, thanks to the polynomial (times a Gaussian) structure of the h.o. wave functions, one can express all matrix elements in terms of the $\delta(0,l)$'s which occur for nodeless states. For instance

$$\begin{aligned}
\delta(1,0) &= \frac{3}{2}\delta(0,0) - 3\delta(0,1) + \frac{5}{2}\delta(0,2) \\
\delta(1,1) &= \frac{5}{2}\delta(0,1) - 5\delta(0,2) + \frac{7}{2}\delta(0,3) \\
\delta(1,2) &= \frac{7}{2}\delta(0,2) - 7\delta(0,3) + \frac{9}{2}\delta(0,4) \\
\delta(2,0) &= \frac{15}{8}\delta(0,0) - \frac{15}{2}\delta(0,1) + \frac{65}{4}\delta(0,2) - \frac{35}{2}\delta(0,2) + \frac{63}{8}\delta(0,4).
\end{aligned} \tag{8.2.3}$$

It is easy to compute the energy shifts due to δV in terms of these 2-body matrix elements $\delta(n,l)$ and, in turn, to express the results with the $\delta(0,l)$ only. Of course, one has to make use of the permutation properties of the wave functions. One gets:

$N = 0$

$$\epsilon(56,0^+) = 3\delta(0,0), \tag{8.2.4}$$

$N = 1$

$$\epsilon(70,1^-) = \frac{3}{2}[\delta(0,0) + \delta(0,1)] \tag{8.2.5}$$

(the mixed symmetry partners remain degenerate to all orders),

$N = 2$

$$\begin{aligned}
\epsilon(20,1^+) &= 3\delta(0,1) \\
\epsilon(70,2^+) &= \frac{3}{4}\delta(0,0) + \frac{3}{2}\delta(0,1) + \frac{3}{4}\delta(0,2) \\
\epsilon(56,2^+) &= \frac{3}{2}\delta(0,0) + \frac{3}{2}\delta(0,2) \\
\epsilon(70,0^+) &= \frac{15}{8}\delta(0,0) - \frac{3}{4}\delta(0,1) + \frac{15}{8}\delta(0,2) \\
\epsilon(56,0^+)' &= \frac{15}{4}\delta(0,0) - \frac{9}{2}\delta(0,1) + \frac{15}{4}\delta(0,2),
\end{aligned} \tag{8.2.6}$$

$N = 3, \quad l = 3$

$$\begin{aligned}
\epsilon(56,3^-) &= \frac{3}{4}\delta(0,0) + \frac{9}{4}\delta(0,2) \\
\epsilon(20,3^-) &= \frac{9}{4}\delta(0,1) + \frac{3}{4}\delta(0,3) \\
\epsilon(70,3^-) &= \frac{9}{8}\delta(0,0) + \frac{3}{8}\delta(0,1) + \frac{3}{8}\delta(0,2) + \frac{9}{8}\delta(0,3),
\end{aligned} \tag{8.2.7}$$

$N = 3, \quad l = 2$

$$\epsilon(70,2^-) = \frac{3}{2}\delta(0,2) + \frac{3}{2}\delta(0,1), \tag{8.2.8}$$

and

$N = 3, \quad l = 1$

$$\begin{aligned}
\epsilon(56,1^-) &= \frac{21}{8}\delta(0,0) - \frac{15}{4}\delta(0,1) + \frac{33}{8}\delta(0,2) \\
\epsilon(20,1^-) &= \frac{33}{8}\delta(0,1) - \frac{15}{4}\delta(0,2) + \frac{21}{8}\delta(0,3),
\end{aligned} \tag{8.2.9}$$

The perturbation mixes the $\mid 70,1^-\rangle'$ and $\mid 70,1^-\rangle''$ states. One has to diagonalize the matrix

$$E(70,1^-) = \begin{pmatrix} \epsilon' & t \\ t & \epsilon'' \end{pmatrix} \tag{8.2.10}$$

with

$$\begin{aligned}
\epsilon' &= \frac{3}{32}[16\delta(0,0) + 13\delta(0,1) - 35\delta(0,2) + 35\delta(0,3)] \\
\epsilon'' &= \frac{1}{32}[21\delta(0,0) + 27\delta(0,1) + 27\delta(0,2) + 21\delta(0,3)] \\
t &= \frac{3\sqrt{5}}{32}[-\delta(0,0) + 9\delta(0,1) - 15\delta(0,2) + 7\delta(0,3)].
\end{aligned} \tag{8.2.11}$$

As a check, one can compute the trace of v in each (N,l) subspace using either the symmetrized basis $\mid 56,l^P\rangle, \mid 20,l^P\rangle$, etc. or the original basis $\mid n_\rho,l_\rho\rangle\otimes\mid n_\lambda,l_\lambda\rangle$. For instance, in the $(N=3,\ l^P=1^-)$ case, one has to satisfy

$$\begin{aligned}
\epsilon(56,1^-) + \epsilon(20,1^-) + 2\epsilon' + 2\epsilon'' &= \sum_b \langle b \mid \delta V \mid b\rangle \\
&= \frac{5}{2}\delta(0,0) + \frac{3}{2}\delta(0,1) - \frac{3}{2}\delta(0,2) + \frac{7}{2}\delta(0,3),
\end{aligned} \tag{8.2.12}$$

where

$$b = |\,0,0\rangle\otimes|\,1,1\rangle, \quad |\,1,0\rangle\otimes|\,0,1\rangle, \quad (|\,0,2\rangle\otimes|\,0,1\rangle)_1,$$
$$|\,1,1\rangle\otimes|\,1,0\rangle, \quad |\,0,1\rangle\otimes|\,1,0\rangle, \quad \text{and} \quad (|\,0,1\rangle\otimes|\,0,2\rangle)_1.$$

This allows one to detect a misprint for $\epsilon(56,1^-)$ in the review by Hey *et al* [6], and to check that their original expression [75] is correct, with the correspondence $a = 3\delta(0,0)$, $b = \frac{9}{2}\delta(0,1)$, $c = \frac{45}{2}\delta(0,2)$, $d = \frac{315}{8}\delta(0,3)$.

The pattern of Eq. (8.2.6) for the $N = 2$ level has been analysed by several authors [76, 77, 78, 79]. One can set

$$\begin{aligned} \bar{\epsilon}_{N=2} &= \frac{15}{16}\delta(0,0) + \frac{9}{8}\delta(0,1) + \frac{15}{16}\delta(0,2) \\ \Delta &= \frac{15}{4}[2\delta(0,1) - \delta(0,0) - \delta(0,2)]. \end{aligned} \tag{8.2.13}$$

While the notation $\Delta = \epsilon(20,1^+) - \epsilon(56,0^+)'$, corresponding to the overall spread of the $N = 2$ multiplet, has been adopted by all authors, the choice of $\bar{\epsilon}_{N=2}$ seems rather arbitrary. The above prescription, as we shall see in Section 8.3, corresponds to the hyperscalar contribution of the perturbation δV. With (8.2.13), one can rewrite the $N = 2$ shifts (8.2.6) as

$$\begin{aligned} \epsilon(20,1^+) &= \bar{\epsilon}_{N=2} + \frac{1}{4}\Delta \\ \epsilon(70,2^+) &= \bar{\epsilon}_{N=2} + \frac{1}{20}\Delta \\ \epsilon(56,2^+) &= \bar{\epsilon}_{N=2} - \frac{3}{20}\Delta \\ \epsilon(70,0^+) &= \bar{\epsilon}_{N=2} - \frac{1}{4}\Delta \\ \epsilon(56,0^+)' &= \bar{\epsilon}_{N=2} - \frac{3}{4}\Delta, \end{aligned} \tag{8.2.14}$$

corresponding to the famous splitting pattern of Fig. 8.1.

It has been noticed [37] that Δ is positive for any attractive power-law potential $\epsilon(\alpha)r^\alpha$, where ϵ is the sign function. In particular, if the popular "Coulomb-plus-linear" potential is split into its best harmonic approximation (for $N = 2$) and a correction to it, say

$$V = -\frac{a}{r} + br = a' + b'r^2 + v, \tag{8.2.15}$$

then one gets $\Delta > 0$. In fact, the splitting parameter Δ measures the concavity of the leading Regge trajectory, for a nearly harmonic 2-body potential. Thus from the perturbative version of the theorem (2.7.41), we obtain [80, 79]

$$Y \equiv \frac{\mathrm{d}}{\mathrm{d}r}\left[\frac{1}{r}\frac{\mathrm{d}v}{\mathrm{d}r}\right] \lesseqgtr 0 \quad \Longrightarrow \quad \Delta \gtreqless 0 \tag{8.2.16}$$

The appearance of this differential operator is not surprising, since Δ has to vanish if $v(r)$ is constant or harmonic.

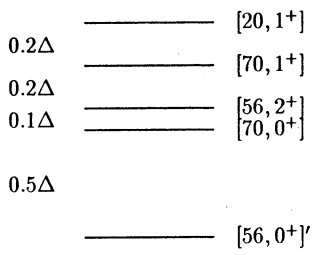

Figure 8.1: Splitting pattern of the N=2 multiplet for 2-body perturbations of the harmonic oscillator

There are generalizations, where one has to give the collective radial excitation $[56,0^+]'$ a special treatment, whereas the separation between the four states $[20,1^+]$, $[70,1^+]$, $[56,2^+]$ and $[70,0^+]$ remains in the simple ratio 2:2:1, as illustrated in Fig. 8.2. This occurs for a 3-body perturbation of the harmonic oscillator [81], or as explained in the next Section, for nearly hyperscalar potentials.

The structure of the $N = 3$ multiplet was analysed by A.J.G. Hey et al.[6, 75] in terms of the rather powerful but abstract $SP(12,C)$ group symmetry, and also by Cutkosky and Hendrick [38] and by Taxil et al.[79], who used more modest tools. If one defines

$$\begin{aligned} \bar{\epsilon}_{N=3} &= \frac{3}{32}[7\delta(0,0) + 9\delta(0,1) + 9\delta(0,2) + 7\delta(0,3)] \\ \eta &= \frac{3}{8}\{[2\delta(0,1) - \delta(0,0) - \delta(0,2)] + [2\delta(0,2) - \delta(0,1) - \delta(0,3)]\} \\ \gamma &= -\frac{3}{4}\{[2\delta(0,1) - \delta(0,0) - \delta(0,2)] + [2\delta(0,2) - \delta(0,1) - \delta(0,3)]\}, \end{aligned} \tag{8.2.17}$$

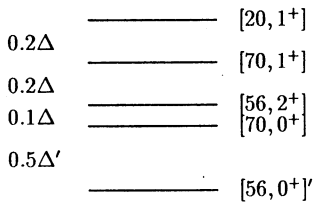

Figure 8.2: Generalized splitting pattern of the N=2 multiplet for 3-body perturbations of the harmonic oscillator or for a nearly hyperscalar potential

one gets

$$\begin{aligned}
\epsilon(56,3^-) &= \bar{\epsilon}_{N=3} + \frac{3}{4}\eta + \frac{1}{2}\gamma \\
\epsilon(20,3^-) &= \bar{\epsilon}_{N=3} + \frac{3}{4}\eta - \frac{1}{2}\gamma \\
\epsilon(70,3^-) &= \bar{\epsilon}_{N=3} - \frac{5}{4}\eta \\
\epsilon(70,2^-) &= \bar{\epsilon}_{N=3} + \frac{7}{4}\eta \\
\epsilon(56,1^-) &= \bar{\epsilon}_{N=3} - \frac{7}{4}\eta + \frac{7}{4}\gamma \\
\epsilon(20,1^-) &= \bar{\epsilon}_{N=3} - \frac{7}{4}\eta - \frac{7}{4}\gamma \\
\epsilon' &= \bar{\epsilon}_{N=3} - 5\eta - \gamma \\
\epsilon'' &= \bar{\epsilon}_{N=3} \\
t &= -\frac{\sqrt{5}}{4}(3\eta + 2\gamma).
\end{aligned} \tag{8.2.18}$$

There is an overall shift $\bar{\epsilon}_{N=3}$ of the levels and then all spacings are governed by the two quantities η and γ. This is illustrated in Fig. 8.3, for a linear perturbation to the harmonic oscillator.

One may rewrite the quantities η and γ as

$$\begin{aligned}
\eta &= \frac{3}{8}\left[f(1) + f(2)\right] \\
\gamma &= \frac{3}{4}\left[f(2) - f(1)\right],
\end{aligned} \tag{8.2.19}$$

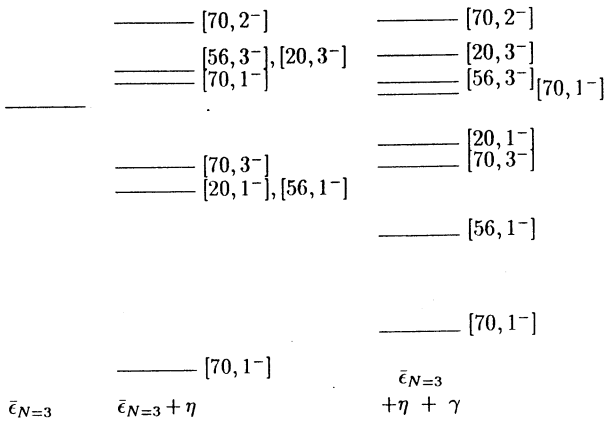

Figure 8.3: Splitting pattern of the $N = 3$ multiplet for a harmonic oscillator perturbed by a linear 2-body potential. In the first column, the whole $N = 3$ multiplet is shifted by $\bar{\epsilon}_{N=3}$ from its unperturbed value (not shown). The effect of η induces a splitting which is further modified by the term γ, defined in Eq. (8.2.19).

where again $f(l) = 2\delta(0,l) - \delta(0,l-1) - \delta(0,l+1)$ measures the concavity of the lowest Regge trajectory and is thus governed by the sign of Y

$$Y \lesseqgtr 0 \quad \Longrightarrow \quad \eta \gtrless 0. \tag{8.2.20}$$

The quantity γ is a kind of discretized third derivative in l. It was shown in Ref. [79] that

$$W \equiv \frac{\mathrm{d}}{\mathrm{d}r}\left[\frac{1}{r}\frac{\mathrm{d}}{\mathrm{d}r}\left(\frac{1}{r}\frac{\mathrm{d}v}{\mathrm{d}r}\right)\right] \gtrless 0 \quad \Longrightarrow \quad \gamma \lesseqgtr 0, \tag{8.2.21}$$

provided that $\lim_{r\to 0} r^3 v = 0$. One can hardly guess the form of the differential operator W without some preliminary study. In fact, if one introduces a perturbation $v = Br^\beta$, one gets by straightforward calculation that $\gamma \propto B\beta(\beta-2)(\beta-4)$. It vanishes for $\beta = 0$ and $\beta = 2$, as expected, and also for $\beta = 4$, leading to the expression of $W\left[v(r)\right]$. The proof of (8.2.21) can be sketched as follows. One starts from

$$\gamma = \frac{3}{4}\int_0^\infty v(r)dr\left[(2u_{0,2}^2 - u_{0,1}^2 - u_{0,3}^2) - (2u_{0,1}^2 - u_{0,2}^2 - u_{0,0}^2)\right] \tag{8.2.22}$$

and performs a sequence of integrations by parts which transform the integral into

$$\gamma = \frac{3}{4}\int_0^\infty W\left[v(r)\right]K(r)dr \tag{8.2.23}$$

From the explicit expression of the harmonic-oscillator radial functions $u^2_{n,l}(r)$, one gets $K(r) \propto -r^7 \exp(-r^2)$, which always remains negative. More details can be found in Ref. [79].

8.3 Nearly hyperscalar potentials

The potential in Eq. (8.2.1) is a special case of a more general class of "nearly hyperscalar" potentials

$$V(\vec{r}_1, \vec{r}_2, \vec{r}_3) = V_0(\xi) + \sum_{i<j} v(r_{ij}), \tag{8.3.24}$$

or, if one gives up the 2-body character,

$$V(\vec{r}_1, \vec{r}_2, \vec{r}_3) = V_0(\xi) + \delta V(\vec{r}_1, \vec{r}_2, \vec{r}_3), \tag{8.3.25}$$

or equivalently, in the more abstract terms of the hyperspherical expansion of the potential

$$V(\vec{r}_1, \vec{r}_2, \vec{r}_3) = \pi^{3/2} \left[V_0(\xi)\mathcal{Q}_0(\Omega) + V_4(\xi)\mathcal{Q}_4(\Omega) + V_6(\xi)\mathcal{Q}_6(\Omega) + \ldots \right], \tag{8.3.26}$$

where $\mathcal{Q}_0(\Omega) = \pi^{-3/2}$, $\mathcal{Q}_4(\Omega)$, etc. are the lowest scalar and fully symmetric hyperspherical harmonics, given in Section 5.3, and where the $L > 0$ components V_4, V_6,... are small.

For simplicity, we use the same notations $\alpha = [56, 0^+]$, $[70, 1^-]$, $[20, 1^+]$... as for the harmonic-oscillator states to stress their angular momentum and permutation properties.

If the potential V is nearly hyperscalar, one may approximate the wave function of each state by its lowest hyperspherical component, say

$$\Psi_{L,\alpha}(\vec{\rho}, \vec{\lambda}) = \frac{u_{L,\alpha}}{\xi^{5/2}} \mathcal{P}_{L,\alpha}(\Omega), \tag{8.3.27}$$

where $u_{L,\alpha}$ and the binding energy are given by the single radial equation ($m = \hbar = 1$).

$$u''_{L,\alpha} - \frac{(L+3/2)(L+5/2)}{\xi^2} u_{L,\alpha} + [E - U_{L,\alpha}]\, u_{L,\alpha} = 0, \tag{8.3.28}$$

where

$$U_{L,\alpha} = \int \mathcal{P}^*_{L,\alpha}(\Omega) V(\vec{r}_1, \vec{r}_2, \vec{r}_3) \mathcal{P}_{L,\alpha}(\Omega) d\Omega. \tag{8.3.29}$$

Inserting the expansion (8.3.26) results in the following expressions for the $U_{L,\alpha}(\xi)$:

($L = 0$)

$$[56, 0^+] \qquad V_0(\xi), \tag{8.3.30}$$

($L = 1$)

$$[70, 1^-] \qquad V_0(\xi), \tag{8.3.31}$$

($L = 2$)

$$\begin{aligned}
&[20, 1^+] \quad V_0(\xi) + 5\frac{\sqrt{3}}{15} V_4(\xi) \\
&[70, 2^+] \quad V_0(\xi) + \frac{\sqrt{3}}{15} V_4(\xi) \\
&[56, 2^+] \quad V_0(\xi) - 3\frac{\sqrt{3}}{15} V_4(\xi) \\
&[70, 0^+] \quad V_0(\xi) - 5\frac{\sqrt{3}}{15} V_4(\xi),
\end{aligned} \tag{8.3.32}$$

($L = 3$)

$$\begin{aligned}
&[56, 3^-] \quad V_0(\xi) + \frac{\sqrt{3}}{7} V_4(\xi) + \frac{\sqrt{2}}{7} V_6(\xi) \\
&[20, 3^-] \quad V_0(\xi) + \frac{\sqrt{3}}{7} V_4(\xi) - \frac{\sqrt{2}}{7} V_6(\xi) \\
&[70, 3^-] \quad V_0(\xi) - \frac{5\sqrt{3}}{21} V_4(\xi) \\
&[70, 2^-] \quad V_0(\xi) + \frac{\sqrt{3}}{3} V_4(\xi) \\
&[56, 1^-] \quad V_0(\xi) - \frac{\sqrt{3}}{3} V_4(\xi) + \frac{\sqrt{2}}{2} V_6(\xi) \\
&[20, 1^-] \quad V_0(\xi) - \frac{\sqrt{3}}{3} V_4(\xi) - \frac{\sqrt{2}}{2} V_6(\xi) \\
&[70, 1^-] \quad V_0(\xi).
\end{aligned} \tag{8.3.33}$$

These expressions can be obtained either by direct angular integration of Eq. (8.3.29), or by considering the special case $V_0(\xi) = \xi^2$, and using the formula of Section 8.2 for the potentials $v(r_{ij}) = r^n_{ij}$, with $n = 0, 4$ or 6. This enables us to switch on one after the other the $L = 0$, $L = 4$ and $L = 6$ multipoles of the potential. This is one more illustration of the many links between the hyperspherical formalism and the harmonic oscillator [43].

If one compares the Eqs. (8.3.32) with the $N = 2$ sequence in the harmonic oscillator as appearing in Eqs. (8.2.6) and (8.2.14), one notices the absence of the $[56, 0^+]$. This state is a hyper-radial excitation of the $L = 0$ ground state. Similarly, the $[70, 1^-]$ state

of the $N = 3$ band is a hyper-radial excitation of the $L = 1$ level.

Now, if the radial equation (8.3.28) is first solved with $V_0(\xi)$ alone and if the terms in $V_4(\xi)$ and $V_6(\xi)$ are treated at first order, one gets very simple relations between the energies.

In the positive-parity sector, one gets the splitting pattern of Fig. 8.2.

The negative-parity states are shown in Fig. 8.4. For illustration we have chosen a linear potential $V = \Sigma\, r_{ij}$, treated to first order around its hyperscalar approximation, but the ratios between the various splittings in each column are model-independent.

8.4 Lowest excitation

So far, we have studied separately the ordering and splitting of positive-parity excitations and the corresponding pattern of the negative-parity states. We now address the following question: which is the lowest excitation? the positive-parity radial excitation $\mid 1\rangle \equiv [56, 0^+]'$ or the negative-parity orbital excitation $\mid 2\rangle \equiv [70, 1^-]$? This question is motivated by the anomalously low location of the Roper resonance in the excitation spectrum of N and Δ.

In the case of harmonic confinement, the radial excitation energy E_1 is twice as high as the orbital excitation E_2, say $R = 1/2$, where

$$R \equiv \frac{E_2 - E_0}{E_1 - E_0}. \tag{8.4.34}$$

For a hyperscalar Coulombic potential $V = -(r_{12}^2 + r_{23}^2 + r_{31}^2)^{-1/2}$, one gets the degeneracy $R = 1$.

For a general potential $V(\vec{r}_1, \vec{r}_2, \vec{r}_3)$, invariant under rotations and translations, and symmetric, but *not necessarily pairwise*, one remarks that the same projection governs the radial equations of $\mid 1\rangle$ and $\mid 2\rangle$. As seen in Eqs. (8.3.30) and (8.3.31), this is $V_0(\xi)$, the hyperscalar projection of the potential. At this approximation (hereafter denoted $E_i^{\rm hs}$), one has to compare the eigenvalue equations ($i = 1, 2$).

$$u_i''(\xi) - \frac{l_i(l_i+1)}{\xi^2} u_i(\xi) + \left[E_i^{\rm hs} - V_0(\xi)\right] u_i(\xi) = 0 \tag{8.4.35}$$

with $l_1 = 3/2$, $n_1 = 1$ and $l_2 = 5/2$, $n_2 = 0$, n_i being the usual radial (Liouville) index. One can now use the Coulomb theorem (2.7.39), which is immediately applicable to half-integer values of l and one obtains

$$\Delta V_0(\xi) \gtrless 0 \quad \Longrightarrow \quad E_1^{\rm hs} \gtrless E_2^{\rm hs} \tag{8.4.36}$$

One can elaborate a little on the above condition, in the simple case of a 2-body interaction, for which [53]

$$V_0(\xi) = 3\, \frac{\int_0^{\pi/2} \sin^2\varphi \cos^2\varphi\, v(\xi \sin\varphi)\, d\varphi}{\int_0^{\pi/2} \sin^2\varphi \cos^2\varphi d\varphi}, \tag{8.4.37}$$

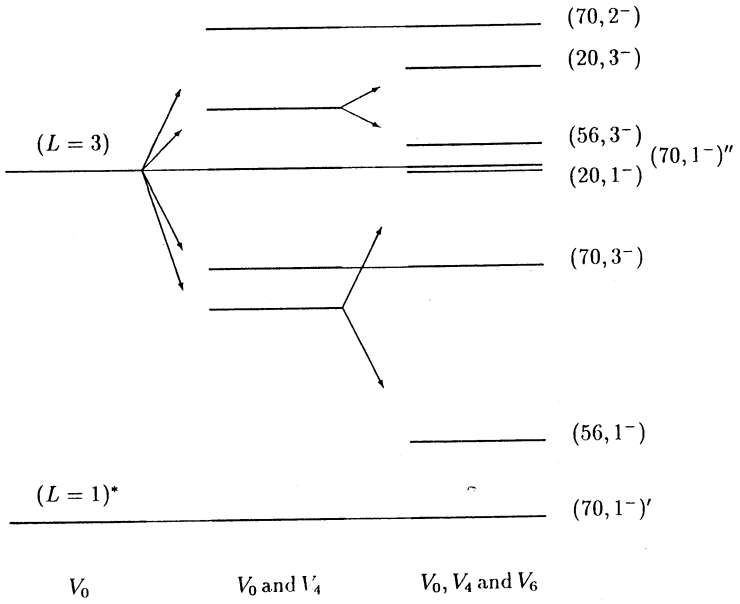

Figure 8.4: Splitting pattern of the negative-parity states for a linear potential treated at first order around its hyperscalar approximation. The bottom line $(70, 1^-)'$ corresponds to the hyper-radial excitation of the $L = 1$ state. The other states belong to the $L = 3$ multiplet. The figure exhibits the splitting pattern one gets when switching on the corrections V_4 and V_6 to the hyperscalar potential V_0.

Obviously, if $v(r)$ is concave (convex) in r^{-1}, $V_0(\xi)$ will be concave (convex) in ξ^{-1} and the theorem (8.4.36) will be applicable. Thus, with any plausible interquark potential, we obtain

$$E_1^{\rm hs} > E_2^{\rm hs}, \qquad \text{i.e. } R < 1 \tag{8.4.38}$$

at the lowest order in the hyperspherical expansion [82]. The effect is rather pronounced, since $R \simeq 0.7$ for a linear potential. For such smooth and symmetric potentials, the corrections $E_i - E_i^{\rm hs}$ due to higher hyperspherical harmonics are extremely small and cannot change the level order. This is confirmed by numerical calculations.

More challenging is the case of a gravitational interaction

$$V = -(\frac{1}{r_{12}} + \frac{1}{r_{23}} + \frac{1}{r_{31}}) \tag{8.4.39}$$

which, at first approximation, gives rise to the hyperscalar potential proportional to $-(r_{12}^2 + r_{23}^2 + r_{31}^2)^{-1/2}$. At this approximation, $E_1 = E_2$. The breaking of the $E_1 = E_2$ degeneracy has been studied numerically by S. Fleck [73], whose work updates that of Ref. [82]. She computed the successive approximations $\tilde{E}_1(L_{\rm max})$ and $\tilde{E}_2(L_{\rm max})$ as a function of the maximal "grand" orbital momentum $L_{\rm max}$ introduced in the wave function. It appears clearly that $E_2 > E_1$ when one approaches convergence.

Chapter 9

MASS INEQUALITIES

9.1 Introduction

In this chapter, we first discuss the mass dependence of the 3-body binding energy and derive inequalities linking baryons of different flavour content. Then we present inequalities relating the binding energies of baryons to those of simpler 2-body systems, which can, to some extent, be identified as mesons. The rough inequalities by Ader et al.and Nussinov [83, 84] have been significantly improved recently [85, 86], so that the lower bounds now become rather accurate approximations of the 3-body binding energies in terms of 2-body binding energies.

9.2 Mass dependence of the three-body binding energy

The Hamiltonian

$$H = \sum_i \frac{\vec{p}_i^{\,2}}{2m_i} + V(\vec{r}_1, \vec{r}_2, \vec{r}_3) \tag{9.2.1}$$

depends linearly on the inverse of each constituent mass, so $E_0(m_1, m_2, m_3)$, the lowest energy, is a concave function of each m_i^{-1}. This is an important consequence of the flavour independence of the central potential V.

As a first application [87], one may compare $\Lambda_{\rm b}$(bud), $\Lambda_{\rm c}$(cud), and Λ(sud) and get

$$E(\Lambda_{\rm b}) \leq \frac{m_{\rm b}^{-1} - m_{\rm c}^{-1}}{m_{\rm s}^{-1} - m_{\rm c}^{-1}} E(\Lambda) + \frac{m_{\rm b}^{-1} - m_{\rm s}^{-1}}{m_{\rm c}^{-1} - m_{\rm s}^{-1}} E(\Lambda_{\rm c}). \tag{9.2.2}$$

If the Hamiltonian is supplemented by spin–spin forces of the type

$$H_{\rm HF} = \sum_{i<j} V_{\rm SS}(r) \frac{\vec{\sigma}_i \cdot \vec{\sigma}_i}{m_i m_j}, \tag{9.2.3}$$

where $V_{\rm SS}(r)$ is a flavour-independent short-range function, one keeps the linearity of the Hamiltonian in m_1^{-1}, and the inequality still holds.

Another example is provided by the baryons with double flavour: $\Xi_{bb}(bbq)$, $\Xi_{cc}(ccq)$, and $\Xi(ssq)$. If one uses the central Hamiltonian (9.2.1), one gets

$$E(\Xi_{bb}) \leq \frac{m_b^{-1} - m_c^{-1}}{m_s^{-1} - m_c^{-1}} E(\Xi) + \frac{m_b^{-1} - m_s^{-1}}{m_c^{-1} - m_s^{-1}} E(\Xi_{cc}). \tag{9.2.4}$$

Hyperfine corrections (9.2.3) introduce terms in $(m_Q m_q)^{-1}$ still linear in m_Q^{-1} and a term $V_{SS}(r_{12}) m_Q^{-2}$, which unfortunately has the wrong concavity in m_Q^{-1}, since $V_{SS}(r) > 0$ in most models.

To regain contact with the real world, consider the following sequence: $\Xi^*(ssq)$, $\Omega^-(sss)$, and $\Omega_c^*(ssc)$, all with spin 3/2. The Hamiltonian, including the hyperfine term, is linear in m_3^{-1}, so that

$$E(\Omega_c^*) \leq \frac{m_c^{-1} - m_q^{-1}}{m_s^{-1} - m_q^{-1}} E(\Omega) + \frac{m_c^{-1} - m_s^{-1}}{m_q^{-1} - m_s^{-1}} E(\Xi^*). \tag{9.2.5}$$

The upper limits (9.2.2), (9.2.4) and (9.2.5) depend, however, on the quark masses, so that the comparison with experimental results is not immediate. It would be much more appealing to write down inequalities where the quark masses disappear and a direct comparison with experimental baryon masses is feasible. If one considers, for instance, the simple 2-body result (2.8.47), $Q\bar{q} + q\bar{q} < 2Q\bar{q}$, one is tempted to write down the following generalization to the 3-body case

$$\mathcal{M}(MMm') + \mathcal{M}(mmm') \leq 2\mathcal{M}(Mmm'). \tag{9.2.6}$$

For $m' = m$, this inequality is related to possible departures from the Gell-Mann–Okubo mass formula and, for $m' = M$ to the equal-spacing rule of the decuplet as we shall see in Chapter 11.

Since the inequality (9.2.6) is satisfied in all numerical calculations based on reasonable potentials, it was believed for some time to be a general property of flavour-independent potentials. The situation was clarified by E. Lieb and further investigated by Martin et al.[88]. There are, in fact, counter-examples to (9.2.6), involving large mass ratios, for instance $m' = m \gg M$ and very sharp potentials such as infinite square-wells. For smooth potentials suited for baryon spectroscopy, the inequality is satisfied in both $m' = m$ and $m' = M$ cases.

Similarly, one would very much like to compare the symmetric baryons $\Delta(qqq)$, $\Omega(sss)$ and $\Omega_{ccc}(ccc)$ to the recently identified $\Xi_c(csq)$ baryon. The tempting inequality

$$3(csq) > (ccc) + (sss) + (qqq) \tag{9.2.7}$$

cannot be derived on the back of an envelope. Indeed, if one defines

$$\overline{H} = \frac{1}{3}[H(qqq) + H(sss) + H(ccc)], \tag{9.2.8}$$

one immediately gets the result that

$$E_0(\overline{H}) \geq \frac{1}{3}[E_0(qqq) + E_0(sss) + E_0(ccc)]. \tag{9.2.9}$$

The trouble is that the true $H(csq)$ contains not only the symmetric piece $\overline{H}$ but also a mixed symmetry piece, which lowers its energy. With realistic potentials, however, the inequality (9.2.7) is satisfied.

9.3 Relation between the quark–antiquark and the quark–quark potential

In simultaneous descriptions of the meson and baryon spectra, one often adopts the following relation between the quark–quark potential in a baryon and the quark–antiquark potential of quarkonia [89, 90]

$$V_{qq} = \frac{1}{2} V_{q\bar{q}}. \tag{9.3.10}$$

This "1/2 rule" works reasonably well phenomenologically. There are some arguments in favour of this rule, which are summarized below.

In the particular configurations where two quarks coincide, the third quark feels a localized colour $\bar{3}$ source, which behaves exactly as an antiquark and the above rule holds exactly.

If one believes that the potential is pairwise, it can be expanded according to its colour structure in the t-channel: singlet exchange or octet exchange

$$V_{q\bar{q}} = V_1 + V_8, \tag{9.3.11}$$

and from simple $SU(3)_c$ colour algebra

$$V_{qq} = V_1 + \frac{1}{2} V_8 \tag{9.3.12}$$

The singlet-exchange piece cannot dominate or even contribute to confinement, otherwise all colour-singlet hadrons would be confined together. The simplest choice consists of assuming $V_1 = 0$, leading to Eq. (9.3.10). Of course, one cannot eliminate the possibility of a non-confining piece of colour-singlet exchange.

Now, some 3-body forces might well be present, making illusory the comparison of V_{qq} and $V_{q\bar{q}}$. Fortunately, the situation is rather encouraging when one considers the most plausible model for interquark forces. The potential

$$V = -\frac{a}{r} + br \tag{9.3.13}$$

is often interpreted as the superposition of one-gluon exchange, for which the "1/2 rule" holds exactly, and a linear confinement corresponding to the shortest length of

a chromoelectric flux-tube linking the quark to the antiquark. This is supported by lattice calculations, string models, flux-tube models, adiabatic bag models, etc. The most plausible generalization of br to baryons, with regard to gauge invariance, consists of the so-called "Y-shape" potential [70] (already introduced in Chapter 7)

$$V = b \min_J (d_1 + d_2 + d_3) \tag{9.3.14}$$

It consists of the sum of the distances between the quarks and a "junction" J, whose location should minimize the potential.

One is back to a well-known "travelling salesman" or "road design" problem, where the connection between given points should be accomplished at minimum cost. When the triangle $q_1q_2q_3$ has ordinary angles $\hat{q}_i < 120°$, the flux lines d_i make 120° with respect to each other. If, say, $\hat{q}_1 > 120°$, then the junction coincides with q_1. One easily proves [70]

$$\frac{1}{2}\sum r_{ij} \leq \min(d_1 + d_2 + d_3) \leq \frac{1}{\sqrt{3}}\sum r_{ij} \tag{9.3.15}$$

so that the 1/2 rule is almost exactly satisfied and the departure goes in the right direction for the purpose of the inequalities we shall present in the rest of the chapter.

9.4 Simple lower bound on baryon energies

Let $E_3(m; \frac{1}{2}V)$ be the lowest energy of a system of three identical quarks governed by the Hamiltonian

$$H_3(m; \tfrac{1}{2}V) = \sum_i \frac{\vec{p}_i^{\,2}}{2m} + \sum_{i<j} \frac{1}{2}V(r_{ij}), \tag{9.4.16}$$

where the 1/2 factor is introduced for convenience, even if one does not believe in the colour rule (9.3.10). Ader et al. [83] and, independently, Nussinov [84] have noticed that

$$H_3(m; \tfrac{1}{2}V) = \frac{1}{2}\sum_{i<j}\left[\frac{\vec{p}_i^{\,2}}{2m} + \frac{\vec{p}_j^{\,2}}{2m} + V(r_{ij})\right] \equiv \frac{1}{2}\sum_{i<j} H_2(m; V). \tag{9.4.17}$$

In each bracket, the operator is bounded by its lowest eigenvalue $E_2(m; V)$ and hence

$$E_3(m; \tfrac{1}{2}V) \geq \frac{3}{2}E_2(m; V). \tag{9.4.18}$$

In fact, this inequality is nothing but a slightly modified version of an old result derived in studies of self-interacting N-boson systems. The literature can be traced back from Refs. [85, 86]. One can, indeed, rewrite and generalize (9.4.18) as

$$E_N(m; V) \geq \frac{N(N-1)}{2}E_2\left[m(N-1); V\right], \tag{9.4.19}$$

so that, if $V = -a/r$

$$E_N(m, g^2) \geq -\frac{mN(N-1)^2}{8}a^2. \tag{9.4.20}$$

Coming back to the hadron sector, we obtain for the ground states of mesons and baryons the amazingly simple inequality

$$\mathrm{QQQ} \geq \frac{3}{2}\mathrm{Q\overline{Q}}, \tag{9.4.21}$$

meaning that a quark "weighs" more in baryons than in mesons. A first generalization concerns unequal masses. One easily derives [84, 91]

$$\mathrm{Q_1Q_2Q_3} \geq \frac{1}{2}\left(\mathrm{Q_1\overline{Q}_2 + Q_2\overline{Q}_3 + Q_3\overline{Q}_1}\right) \tag{9.4.22}$$

provided that $V_{\mathrm{Q_iQ_j}} = \frac{1}{2}V_{\mathrm{Q_i\overline{Q}_j}}$ for each pair. Flavour independence is not necessary here.

Note, however, that some other generalizations do not hold. For instance, one may rewrite (9.4.18) as $\mathrm{QQQ} + \mathrm{\overline{QQQ}} \geq 3\mathrm{Q\overline{Q}}$ explaining why quark rearrangement is an allowed mechanism for a symmetric baryon–antibaryon annihilation. Now, if the mass ratio M/m is large enough, one gets the inverted inequality

$$\mathrm{\overline{QQQ}} + \mathrm{qqq} < 3\mathrm{\overline{Q}q}. \tag{9.4.23}$$

An antibaryon with charm $C = -3$ would not annihilate on ordinary matter, and instead would scatter elastically until it decays weakly. In a flavour-independent potential, indeed, the heavy quarks preferentially remain together, to experience more binding. This effect is also responsible for the stability of the "tetraquark" $\mathrm{\overline{Q}Qqq}$ [83, 47].

Some spin effects can be incorporated in these inequalities [92]. Consider, for instance, a potential appropriate for S-waves

$$V_{ij} = V_{\mathrm{C}}(r_{ij}) + \vec{\sigma}_i \cdot \vec{\sigma}_j V_{\mathrm{SS}}(r_{ij}) \tag{9.4.24}$$

with a central and a spin–spin piece, the latter being likely to depend on the quark masses, as per eq. (9.2.3). On can immediately compare spin 3/2 baryons to vector mesons, by using the spin–triplet potential $V_{\mathrm{C}} + V_{\mathrm{SS}}$. Some examples follow (the experimental values [5] are shown for comparison, in units of GeV/c^2).

$$\begin{aligned}
\Omega &> \tfrac{3}{2}\varphi && (1.672 > 1.530)\\
\Delta &> \tfrac{3}{2}\rho && (1.232 > 1.155)\\
\Sigma^* &> \mathrm{K}^* + \tfrac{1}{2}\rho && (1.385 > 1.275)\\
\Xi^* &> \rho + \tfrac{1}{2}\varphi && (1.532 > 1.280)\\
\Omega_{\mathrm{c}} &> \mathrm{D}_{\mathrm{s}}^* + \tfrac{1}{2}\varphi && (2.740 > 2.623).
\end{aligned} \tag{9.4.25}$$

We also have the predictions

$$\begin{aligned}
\Sigma_{\mathrm{b}}^* &> \mathrm{B}^* + \tfrac{1}{2}\rho = 5.710\\
\Omega_{\mathrm{ccc}} &> \tfrac{3}{2}\,\mathrm{J/\Psi} \quad = 4.545.
\end{aligned} \tag{9.4.26}$$

In the spin $\frac{1}{2}$ sector, one finds pairs with spin 1, i.e. $\sigma_{ij} \equiv \langle \vec{\sigma}_i \cdot \vec{\sigma}_j \rangle = 1$, like ss in Ξ, pairs with spin 0, i.e. $\sigma_{ij} = -3$, like ud in Λ, and pairs in a mixture of spin 0 and spin 1 states. In a baryon such as Λ, $\sigma_{su} = 0$, whereas in a Σ, $\sigma_{su} = -2$. Since the Hamiltonian depends linearly on these $\vec{\sigma}_i \cdot \vec{\sigma}_j$, we can use the concavity theorem (9.2.4) to constrain the masses of fictitious mesons with $\sigma = 0$ or -2 from pseudoscalars and vectors

$$\begin{aligned} \mathcal{M}(\sigma = -2) &> \tfrac{3}{4}\mathcal{M}(\sigma = -3) + \tfrac{1}{4}\mathcal{M}(\sigma = 1) \\ \mathcal{M}(\sigma = 0) &> \tfrac{1}{4}\mathcal{M}(\sigma = -3) + \tfrac{3}{4}\mathcal{M}(\sigma = 1). \end{aligned} \tag{9.4.27}$$

Hence the inequality on qqQ states of Λ-type or Σ-type reads

$$\begin{aligned} \Lambda_Q &> \tfrac{1}{2}(q\bar{q})_{J=0} + \tfrac{3}{4}(Q\bar{q})_{J=1} + \tfrac{1}{4}(Q\bar{q})_{J=0} \\ \Sigma_Q &> \tfrac{1}{2}(q\bar{q})_{J=1} + \tfrac{1}{4}(q\bar{q})_{J=1} + \tfrac{3}{4}(Q\bar{q})_{J=0} \cdot \end{aligned} \tag{9.4.28}$$

Examples, are, in the Λ sector

$$\begin{aligned} \Lambda &> \tfrac{1}{2}\pi + \tfrac{3}{4}K^* + \tfrac{1}{4}K \qquad (1.116 > 0.863) \\ \Lambda_c &> \tfrac{1}{2}\rho + \tfrac{3}{4}D^* + \tfrac{1}{4}D \qquad (2.282 > 2.042), \end{aligned} \tag{9.4.29}$$

and the prediction

$$\Lambda_b > \tfrac{1}{2}\pi + \tfrac{3}{4}B^* + \tfrac{1}{4}B = 5.379. \tag{9.4.30}$$

In the Σ-sector

$$\begin{aligned} N &> \tfrac{3}{4}\rho + \tfrac{3}{4}\pi \qquad (0.938 > 0.681) \\ \Sigma &> \tfrac{1}{2}\rho + \tfrac{3}{4}K + \tfrac{1}{4}K^* \qquad (1.190 > 0.979) \\ \Xi &> \tfrac{1}{2}\varphi + \tfrac{3}{4}K + \tfrac{1}{4}K^* \qquad (1.319 > 1.104) \\ \Sigma_c &> \tfrac{1}{2}\rho + \tfrac{3}{4}D + \tfrac{1}{4}D^* \qquad (2.450 > 2.288), \end{aligned} \tag{9.4.31}$$

$$\begin{aligned} \Sigma_b &> \tfrac{1}{2}\rho + \tfrac{3}{4}B + \tfrac{1}{4}B^* \;= 5.670 \\ \Xi_{cc} &> \tfrac{1}{2}J/\Psi + \tfrac{3}{4}D + \tfrac{1}{4}D^* = 3.441. \end{aligned} \tag{9.4.32}$$

For the Ξ_c and Ξ_c', with quark content csu, one is tempted to write

$$\Xi_c > \tfrac{1}{2}K + \tfrac{1}{8}D + \tfrac{3}{8}D^* + \tfrac{1}{8}D_s + \tfrac{3}{8}D_s^* \quad (2.460 > 2.272) \tag{9.4.33}$$

$$\Xi_c' > \tfrac{1}{2}K^* + \tfrac{3}{8}D + \tfrac{1}{8}D^* + \tfrac{3}{8}D_s + \tfrac{1}{8}D_s^* = 2.400 \tag{9.4.34}$$

In fact there is a mixing between the Λ-type and the Σ-type configurations. This pushes the Ξ_c' up, so that (9.4.34) is safe. It pushes the Ξ_c down but the effect is very small [93, 94], so that (9.4.33) is also guaranteed.

9.5 Improved lower bounds

The inequality (9.4.18) provides a rather poor lower bound on the 3-body binding energy. For instance, with $m = 1$ and $V = r^{0.1}$, one obtains $E_3 > 1.854$ whereas the exact value is 1.880 ! To appreciate the crudeness of this lower limit, one may compare

it to the upper limit $E_3 < 1.883$ which one obtains by a simple variational calculation using a Gaussian wave function.

The reason for the discrepancy is simple. One starts from the decomposition (9.4.17) $H_3 = \frac{1}{2}\sum H_2(i,j)$ and replaces the energy of the 2-body subsystem (i,j) by the ground state of H_2 at rest. However, the (ij) pair is actually not at rest in the baryon, and the corresponding kinetic energy is responsible for the sizeable departure of E_3 from its lower bound $\frac{3}{2}E_2$.

The remedy consists of rewriting (9.4.17) in terms of reduced Hamiltonians whose eigenvalues are independent of the particular Galilean frame which is used. To this end, we define as in Eq. (2.2.4)

$$H_2(m;V) = \frac{\vec{P}_{12}^2}{4m} + \frac{\vec{p}_{12}^2}{m} + V(r_{12}) \equiv \frac{\vec{P}_{12}^2}{4m} + \widetilde{H}_2(m;V), \tag{9.5.35}$$

and similarly

$$H_3(m;V) \equiv \frac{\vec{P}_{123}^2}{6m} + \widetilde{H}_3(m;V). \tag{9.5.36}$$

Using the identity

$$\sum_{i=1}^{N} \vec{p}_i^{\,2} = \frac{1}{N}\sum_{i<j}(\vec{p}_i - \vec{p}_j) + \left(\sum_i \vec{p}_i\right)^2 \tag{9.5.37}$$

we easily obtain

$$\widetilde{H}_3(m;\tfrac{1}{2}V) = \frac{1}{2}\sum_{i<j}\widetilde{H}_2(\tfrac{3}{4}m;V), \tag{9.5.38}$$

from which one gets the improved lower limit on ground state

$$E_3(m;\tfrac{1}{2}V) \geq \frac{3}{2}E_2(\tfrac{3}{4}m;V). \tag{9.5.39}$$

The translation-invariant decomposition (9.5.38) was first written by Post [95] and was rediscovered independently in Refs. [85, 86]. The result (9.5.39) clearly constitutes an improvement with respect to the previous inequality (9.4.18) because the constituent mass in E_2 is decreased by a factor 3/4, and therefore the energy E_2 is algebraically increased. For an attractive power-law potential $\epsilon(\beta)r^\beta$, this provides a factor $(4/3)^{\beta/\beta+2}$. A numerical comparison is shown in Table 9.1, where are listed the naïve lower limit (9.4.18), the improved lower limit (9.5.39), the exact energy obtained by hyperspherical expansion, and the variational bound derived from a Gaussian trial wave function. It is worth noticing that the new lower limit (9.5.39) becomes exact in the case of the harmonic oscillator. This is true for an arbitrary number N of bosons and the harmonic oscillator is the only potential for which the inequality is saturated. A beautiful proof of this property has been given by T.T. Wu and is written down in Ref. [86].

The inequality also becomes an equality to lowest order in perturbation for potentials

$$v = ar^2 + b + \lambda v(r). \tag{9.5.40}$$

Table 9.1: Three-body ground state energy $E_3(1;\frac{1}{2}r^\beta)$ compared with the naïve lower limit $\frac{3}{2}E_2(1;r^\beta)$, the improved lower limit $\frac{3}{2}E_2(\frac{3}{4};r^\beta)$ and a simple variational limit approximation $\tilde{E}_3$ obtained with a Gaussian wave function

β	$\frac{3}{2}E_2(1)$	$\frac{3}{2}E_2(\frac{3}{4})$	E_3	$\tilde{E}_3$
-1	-0.37500	-0.28125	-0.26675	-0.23873
-0.5	-0.65759	-0.59746	-0.59173	-0.57964
0.1	1.85359	1.87916	1.88019	1.88278
0.5	2.75009	2.91296	2.91654	2.92590
1	3.50716	3.86013	3.86309	3.87114
2	4.5	5.19615	5.19615	5.19615
3	5.17584	6.15098	6.15591	6.17147

As a consequence, the variational approximations $\bar{E}$ for $E_3(m;\frac{1}{2}V)$ and $E_2(\frac{3}{4}m;V)$ with Gaussian trial wave functions satisfy the equality. For instance, for $V=\epsilon(\beta)r^\beta$, one obtains

$$\bar{E}_3(m;\tfrac{1}{2}V)=\frac{3}{2}\bar{E}_2(\tfrac{3}{4}m;V)=\frac{3\alpha_0}{m}(1+\frac{2}{\beta}) \tag{9.5.41}$$

with

$$\alpha_0=\left[\frac{m|\beta|\Gamma(\frac{3}{2}+\frac{\beta}{2})}{4\Gamma(\frac{3}{2})}\right]^{2/(\beta+2)} \tag{9.5.42}$$

9.6 Comparison of the wave functions

Within the above Gaussian approximation, the r.m.s. separation between quarks, $d_{ij}\equiv\left\langle r_{ij}^2\right\rangle^{1/2}$, experiences the same value in the baryon as in the "pseudomeson" with constituent masses $\frac{3}{4}m$. This approximation corresponds to choose the best harmonic approximation ar^2+b to the potential V. When one treats the anharmonicity $\lambda v(r)$ in perturbation, the pseudomesons, in comparison to baryons, receive large contributions from higher states of the harmonic oscillator. This results in larger shifts, hence in the inequality (9.5.39), and also in larger radii. An illustration is given in Table 9.2, where are compared the r.m.s. separation in baryons and pseudomesons, for (again !) simple potentials $\epsilon(\beta)r^\beta$. Except for $\beta=2$, the quarks are more tightly connected in baryons. The rigorous comparison of the d_{ij}'s is studied in a recent paper [96].

The situation is slightly more complicated when one compares the wave functions at a given point. For instance, in Refs. [97, 98], the zero-range correlation in a baryon, $\delta_{12}=\left\langle\delta^{(3)}(r_{12})\right\rangle$ is compared with its value in the pseudomeson. For a power-law confinement $\epsilon(\beta)r^\beta$, δ_{12} is smaller than in the pseudomeson for $\beta<2$, larger for $\beta>2$

Table 9.2: Numerical comparison of the r.m.s. interquark distances d_3, in the baryon with quark masses $m_i=1$ and potential $\frac{1}{2}\epsilon(\beta)\sum r_{ij}^\beta$ and d_2, in the 2-body system with masses $m=3/4$ and potential $\epsilon(\beta)r^\beta$

β	d_2	d_3
-1	4.6188	4.5077
-0.5	5.0905	5.0008
0.1	7.2883	7.2261
0.5	2.8182	2.8051
1	1.8794	1.8761
2	1.3161	1.3161
3	1.1069	1.1059

and equal for the harmonic case $\beta=2$. This result is rigorous for $\beta\leq 2$, and in fact for any potential such that $\mathrm{d}/\mathrm{d}r(V'/r)<0$ [98]. For $\beta>2$, it is very plausible and has been checked by accurate numerical calculations.

9.7 Connection to physical mesons

Here we keep the "1/2 rule" of Eq. (9.3.10), connecting 2-body potentials in baryons and mesons but we try to connect baryon masses to physical meson masses without using a specific potential. For simplicity we shall ignore spin effects. However, a pure spin-spin force could be included in our considerations, since it leaves the orbital momentum l as a good quantum number and does not introduce l dependence beside the centrifugal barrier in the radial equations.

The problem is that the new inequality (9.5.39) involves the unphysical quark mass $3m/4$ instead of the constituent mass m. However, we notice that, by the Feynman-Hellmann theorem [33]

$$\frac{\mathrm{d}E(m,2V)}{\mathrm{d}m}=-\frac{T(m)}{m}, \tag{9.7.43}$$

where T is the expectation value of the kinetic energy in the ground state, and hence

$$E_2(\frac{3m}{4},2V)=E_2(m,2V)+\int_{3m/4}^{m}T(\mu,2V)\frac{\mathrm{d}\mu}{\mu}. \tag{9.7.44}$$

There is an inequality on $T(m)$ by Bertlmann and Martin [99]

$$T(m)\geq\frac{3}{4}[E_2(l=1,m)-E_2(l=0,m)], \tag{9.7.45}$$

where the energies appearing in the right-hand side are those of the ground state for angular momentum $l = 1$ and $l = 0$, respectively, in particular $E_2(m) \equiv E_2(l = 0, m)$.

Furthermore, if we impose the mild restriction that the potential satisfies

$$\frac{\mathrm{d}V}{\mathrm{d}r} > 0 \quad \text{and} \quad \Delta V \geq 0, \tag{9.7.46}$$

which is an expression of asymptotic freedom (the colour charge seen increases with distance) and is valid for all existing models, phenomenological or QCD motivated, one can prove [99]:

$$\frac{\mathrm{d}}{\mathrm{d}m}\frac{T(m)}{m} < 0. \tag{9.7.47}$$

Putting the above inequalities together results in

$$E_3(m, V) > \frac{3}{2}\left\{E_2(m, 2V, l = 0) + \frac{3}{16}\left[E_2(m, 2V, l = 1) - E_2(m, 2V, l = 0)\right]\right\} \tag{9.7.48}$$

This inequality applies to binding energies as well as to hadron masses since one can add to both sides three times the quark constituent mass m.

For applications one cannot ignore spin completely. If the spin–spin potential is regularized, the derivation can be generalized for a spin-triplet state. To eliminate more or less the tensor and spin–orbit effects, one should average over the three spin-triplet P-states. Utilisation of (9.7.47) is more questionable. However, the range of integration in (9.7.44) is only a quarter of the mass, so that the uncertainty on $T(m)/m$ is not very large.

We can try to apply this to the $\rho - \Delta$ comparison. If we follow the prescriptions of the Particle Data Group [5], the $I^G = 1^+$ triplet P-states a_J are:

$$a_0(980\,\mathrm{MeV}),\ a_1(1270\,\mathrm{MeV}),\ a_2(1320\,\mathrm{MeV}). \tag{9.7.49}$$

This gives an average mass of 1265 MeV and leads, with $m_\rho = 770$ MeV, to

$$M_\Delta > 1294\ \mathrm{MeV}. \tag{9.7.50}$$

We overshoot a little bit since $M_\Delta = 1238$ MeV [5], but this was expected because of the crude treatment of spin effects, the neglect of the coupling to decay channels, etc.

If we consider the centres of gravity of the hyperfine multiplets and incorporate the $b(1233)(1^{+-})$ and the $\rho - \pi$ (assuming that the hyperfine splittings are in the ratio $1 : -3$), we obtain

$$\frac{M_\Delta + M_N}{2}(= +1087) \geq 1096 \tag{9.7.51}$$

in very close agreement.

For the $\phi - \Omega$ comparison, we need the $s\bar{s}$ P-state average energy, and here we have only two candidates [5], $f_1(1420\ \mathrm{MeV})$ which is $J^{PC} = 1^{++}$ and $f_2'(1525)$, $J^{PC} = 2^{++}$. Let us assume that they are not too far from the centre of gravity. Then we get, with $M_\phi = 1020$ MeV,

$$M_{\Omega^-} > 1659\ \mathrm{MeV} \tag{9.7.52}$$

in agreement with the experimental $M_{\Omega^-} = 1672$ MeV [5].

We can also make predictions for the masses of the ccc and bbb baryons. With $M_{J/\Psi} = 3095$ MeV and $M_{\chi_c}(\mathrm{triplet}) = 3520$ MeV, we obtain

$$M_{ccc} > 4762\ \mathrm{MeV}, \tag{9.7.53}$$

and,with $M_\Upsilon = 9460$ MeV and $M_{\chi_b}(\mathrm{triplet}) = 9900$ MeV,

$$M_{bbb} > 14314\ \mathrm{MeV}. \tag{9.7.54}$$

The observability of the ccc baryon is considered to be possible by Bjorken [9], and would be very interesting [10].

9.8 The case of unequal constituent masses

The extension of inequality (9.5.39) to baryons bearing different flavours is straightforward, but its practical consequences deserve some discussion.

One easily rewrites the kinetic energy as

$$\frac{\vec{p}_1^{\,2}}{2m_1} + \frac{\vec{p}_2^{\,2}}{2m_2} + \frac{\vec{p}_3^{\,2}}{2m_3} + = \frac{1}{2}\frac{(\vec{p}_1 + \vec{p}_2 + \vec{p}_3)^2}{m_1 + m_2 + m_3} + \frac{1}{2}\sum_{i<j}\frac{(m_j\vec{p}_i - m_i\vec{p}_j)^2}{(m_1 + m_2 + m_3)m_i m_j}. \tag{9.8.55}$$

Thus if one introduces

$$\begin{aligned} \vec{p}_{ij} &= \frac{m_j\vec{p}_i - m_i\vec{p}_j}{m_i + m_j} \\ \mu_{ij} &= \frac{m_i m_j}{m_i + m_j} \\ \tilde{\mu}_{ij} &= \mu_{ij}\frac{m_1 + m_2 + m_3}{m_i + m_j}, \end{aligned} \tag{9.8.56}$$

one can rewrite the reduced Hamiltonian of the baryon as

$$h_3 = \frac{1}{2}\sum_{i<j}\left[\frac{\vec{p}_{ij}^{\,2}}{\tilde{\mu}_{ij}} + v(r_{ij})\right] \tag{9.8.57}$$

leading to the lower limit

$$E_3(m_1, m_2, m_3; \frac{v}{2}) \geq \frac{1}{2}\sum_{i<j} E_2(\tilde{\mu}_{ij}, v), \tag{9.8.58}$$

which usually corresponds to a very good approximation. There are, however, some new features:

– the limit is not saturated anymore in the harmonic-oscillator case, $\sum r_{ij}^2$ with equal strengths, but it is for strengths proportional to the product of the masses, $\sum m_i m_j r_{ij}^2$ [86]

– the new limit (9.8.58) is not always better than the naïve limit (9.4.22).

Let us discuss this latter point in some detail, by considering two different masses, $m_1 = m_2 = m$, and $m_3 = M$. We have to compare the two inequalities

$$E_3(m,m,M;\frac{v}{2}) > \frac{1}{2}E_2(m,v) + E_2\left[\frac{2mM}{m+M},v\right], \tag{9.8.59}$$

$$E_3(m,m,M;\frac{v}{2}) > \frac{1}{2}E_2(\frac{m}{2}+\frac{M}{4},v) + E_2\left[\frac{mM(M+2m)}{(M+m)^2},v\right]. \tag{9.8.60}$$

For $M < 2m$, the constituent masses in the new inequality (9.8.60) are always lighter than in (9.8.59), resulting in a better limit. For very large M, the above inequalities give respectively

$$\begin{aligned} E_3 &> \frac{1}{2}E_2(m) + E_2(2m), \\ E_3 &> \frac{1}{2}E_2(\infty) + E_2(m), \end{aligned} \tag{9.8.61}$$

and the former is larger than the latter, because the ground-state energy E_2 is a concave function of the inverse reduced mass, as seen in Chapter 9. For a power-law potential, r^β, the limits (9.8.59) and (9.8.60) are proportional to

$$\begin{aligned} A &= \frac{1}{2} + (\frac{2x}{1+x})^\gamma, \\ B &= \frac{1}{2}(\frac{1}{2}+\frac{x}{4})^\gamma + \left[\frac{x(2+x)}{(1+x)^2}\right]^\gamma, \end{aligned} \tag{9.8.62}$$

respectively, where $\gamma = -\beta/(\beta+2)$ and $x = M/m$. For $x \geq 8.4$ in the Coulomb case $\beta = -1$, for $x \geq 12$ in the case of a smooth $r^{0.1}$ confinement, or for $x \geq 17.7$ in the harmonic-oscillator case, one has $A > B$, so that the old limit is better than the new one.

To illustrate the inequality (9.8.58), we choose in Table 9.3 several power–law potentials and the sets of constituent masses $(m_1, m_2, m_3) = (1, 1, 0.2)$ and $(1, 1, 5)$ which are representative of the mass ratios involved in double-charm or single-charm baryons.

9.9 Generalization to excited states

Extending the inequalities to excited states, or to the sum of the first energies does not appear as an easy task. The "minimax" principle [33] is not of immediate use here: for fixed $\vec{r}_3$, the wave function of a ground–state baryon, $\phi_0(\vec{r}_1,\vec{r}_2,\vec{r}_3)$ and that of an excited state, $\phi_1(\vec{r}_1,\vec{r}_2,\vec{r}_3)$ are not orthogonal with respect to integration over $\vec{r}_1$ and $\vec{r}_2$. For very special cases (harmonic oscillator, for instance) and for particular values of $\vec{r}_3$, ϕ_0 and ϕ_1 are not even linearly independent.

If one considers, however, our inequality (9.5.39) as relating the first symmetric level of the baryon spectrum and the first even level of the pseudomeson with quark mass

Table 9.3: Ground-state energy of qqQ compared with the lower limits of Eqs. (9.7.5) and (9.7.6) for some power-law potentials $\epsilon(\beta)r^\beta$ and quark mass ratios M/m. The exact result corresponds to a hyperspherical expansion pushed up to a grand orbital momentum $L = 8$.

	$m=1, M=0.2$			$m=1, M=5$		
β	$\frac{1}{2}\sum E_2(\mu_{ij})$	$\frac{1}{2}\sum E_2(\tilde{\mu}_{ij})$	Exact	$\frac{1}{2}\sum E_2(\mu_{ij})$	$\frac{1}{2}\sum E_2(\tilde{\mu}_{ij})$	Exact
-1	-0.2083	-0.1451	-0.1398	-0.5417	-0.4618	-0.3848
-0.5	-0.2083	-0.1451	-0.1398	-0.5417	-0.4618	-0.3848
0.1	1.9200	1.9432	1.9452	1.8239	1.8390	1.8436
1	4.5412	4.8982	4.9392	3.1411	3.3303	3.4379
2	6.6962	7.4498	7.5730	3.8238	4.1764	4.3729
3	8.3958	9.4978	9.7389	4.2712	4.7496	5.0166

$3m/4$, then a similar inequality holds between the first baryon with antisymmetric (A) spatial wave function and the first odd level of the pseudomeson

$$E_3(m,V,A) \geq \frac{3}{2}E_2(\frac{3}{4}m, 2V, l=1). \tag{9.9.63}$$

In the quark model this (A) state exists only for u and d quarks. A spin $\frac{1}{2}$ wave function and an isospin $\frac{1}{2}$ wave function, with mixed permutation symmetry, can be arranged in an antisymmetric spin–isospin wave function, which, in turn, can be combined to the colour wave function and this (A) spatial wave function in order to fulfil the Pauli principle. In the harmonic-oscillator model, this state with spatial wave function

$$\psi_A = (\vec{r}_2 - \vec{r}_1) \times (2\vec{r}_3 - \vec{r}_1 - \vec{r}_2) \exp -\alpha(r_{12}^2 + r_{23}^2 + r_{31}^2). \tag{9.9.64}$$

is referred to by specialists as the $[20, 1^+]$, $N = 2$ state. With anharmonic confinement, this (A) state occurs at the top of the multiplet of positive parity excitations, as seen in Chapter 8.

Chapter 10

BOUNDS ON SHORT-RANGE CORRELATIONS

10.1 Introduction

The probability of finding two constituents at the same position enters into the calculation of many properties of composite systems. This is the case for the hyperfine splittings in atoms, molecules, mesons or baryons, when one uses spin–spin forces of Breit–Fermi type, which have zero range. One may also mention some production rates or decay widths.

In this section, we review some properties [100, 101, 98] of the matrix elements

$$\delta_{ij} \equiv \left\langle \Phi \mid \delta^{(3)}(r_{ij}) \mid \Phi \right\rangle . \tag{10.1.1}$$

We already mentioned that, in the two-body case, the Schwinger rule (2.3.12), which can be rewritten as $4\pi\delta_{12} = \mu \langle V'(r) \rangle$, is very useful for constraining δ_{12} or for computing it in a reliable way. Its generalization to the 3-body case will lead to upper limits on δ_{12} for symmetric baryons.

10.2 Generalized Schwinger rule

For non-central forces or bound states containing more than two constituents, Eq. (2.3.12) is rewritten as [100, 101]

$$\delta_{12} = \frac{m}{4\pi} \left\langle \hat{r}_{12} \cdot \frac{\partial V_T}{\partial \vec{r}_{12}} - \frac{2\vec{l}^2}{m r_{12}^3} \right\rangle , \tag{10.2.2}$$

where V_T is the total potential energy. For a symmetric baryon bound by pairwise, central forces, this is $V_T = V(r_{12}) + V(r_{23}) + V(r_{31})$. If one introduces the Jacobi variables (3.4.18) then

$$\vec{r}_{12} = \vec{\rho}, \qquad \vec{r}_{23} = -\tfrac{1}{2}\vec{\rho} + \tfrac{\sqrt{3}}{2}\vec{\lambda}, \qquad \vec{r}_{31} = -\tfrac{1}{2}\vec{\rho} - \tfrac{\sqrt{3}}{2}\vec{\lambda}, \tag{10.2.3}$$

and the probability for quarks 1 and 2 to be on the top of each other is

$$\delta_{12} = \frac{m}{4\pi} \left\langle V'(r_{12}) - \tfrac{1}{2}\hat{r}_{23} \cdot \hat{r}_{12} V'(r_{23}) - \tfrac{1}{2}\hat{r}_{31} \cdot \hat{r}_{12} V'(r_{31}) - \frac{2\vec{l}_\rho^{\,2}}{m\rho^3} \right\rangle \tag{10.2.4}$$

This expression was already written down by Cohen and Lipkin [102] in a different context. They neglected the small orbital term, and, using the virial theorem, arrived at interesting conclusions on the mass dependence of the correlation coefficients, to which we shall come back in Chapter 11. Here, we shall use Eq. (10.2.4) to derive rigorous bounds on δ_{12}.

10.3 The case of linear confinement

Consider first a purely linear potential $V(r) = \frac{1}{2}br$. From the positivity of $\vec{l}_\rho^{\,2}$ and of $(\hat{r}_{12} + \hat{r}_{23} + \hat{r}_{31})^2$, which ensures that $\langle \hat{r}_{23} \cdot \hat{r}_{12} \rangle \geq -\frac{1}{2}$, when the average is taken for a symmetric wave function, one obtains

$$\delta_{12} \leq \frac{3}{16}\frac{mb}{\pi}. \tag{10.3.5}$$

For $m = b = 1$, the bound $\delta_{12} \leq 0.05968$ is not too far from the exact values obtained in Chapter 5, which are

$$\begin{aligned} &[56, 0^+] \ (n = 0) \qquad \delta_{12} = 0.05689, \\ &[56, 0^+]' \ (n = 1) \qquad \delta_{12} = 0.05664. \end{aligned} \tag{10.3.6}$$

Note that δ_{12} depends slightly on n, unlike in the 2-body case. The state with $n = 1$ contains more contributions from higher hyperspherical harmonics, or, say, from configurations with internal angular momenta $l_\rho = l_\lambda > 0$ (still coupled by $\vec{l}_\rho + \vec{l}_\lambda = 0$), and this reduces the value of δ_{12}. For a collective linear potential $V_T \propto (r_{12}^2 + r_{23}^2 + r_{31}^2)^{1/2}$, which is exactly hyperscalar, the correlation coefficient δ_{12} would be strictly independent of n.

10.4 Correlations for more general potentials

The result (10.3.5) can be generalized to any monotonically increasing potentials V such that $V'(r)/r$ is decreasing, in the form

$$\delta_{12} \leq \frac{m}{8\pi} \left\langle \sum_{i<j} V'(r_{ij}) \right\rangle . \tag{10.4.7}$$

The proof is given in Ref. [98], in a polished form due to A. Martin. Some comments are in order:

i) The inequality is saturated in the harmonic-oscillator case. This explains why, with general potentials, the actual value is not too far from the bound, as seen previously in the linear case.

ii) For a power-law potential $V = \frac{1}{2}Br^\beta$ with $1 \leq \beta \leq 2$, one can get a simple analytic bound on δ_{12} for the ground state by using the virial theorem and the variational principle. The sequence is

$$\begin{aligned}\delta_{12} &\leq \frac{m}{8\pi}\frac{3\beta B}{2}\left\langle r_{12}^\beta\right\rangle^{(\beta-1)/\beta} = \frac{m\beta}{8\pi}\left(\frac{3B}{2}\right)^{1/\beta}\langle V_T\rangle^{(\beta-1)/\beta} \\ &= \frac{m\beta}{8\pi}\left(\frac{3B}{2}\right)^{1/\beta}\left[\frac{2}{2+\beta}E\right]^{(\beta-1)/\beta} \leq \frac{m\beta}{8\pi}\left(\frac{3B}{2}\right)^{1/\beta}\left[\frac{2}{2+\beta}E_{\text{var}}\right]^{(\beta-1)/\beta}\end{aligned} \tag{10.4.8}$$

since the exact energy E is smaller than any variational approximation E_{var}. A trial wave function of Gaussian shape $\Psi(\vec{\rho},\vec{\lambda}) \propto \exp -\frac{1}{2}\alpha(\vec{\rho}^{\,2} + \vec{\lambda}^{\,2})$ leads to

$$E_{\text{var}} = \frac{3}{m}\frac{2+\beta}{\beta}\left[\frac{\beta}{2}mg\frac{\Gamma(\frac{3}{2}+\frac{\beta}{2})}{\Gamma(\frac{3}{2})}\right]^{2/(2+\beta)} \tag{10.4.9}$$

so, finally,

$$\delta_{12} \leq \frac{\beta}{8\pi}(mg)^{3/(2+\beta)}\left(\frac{6}{\beta}\right)^{(\beta-1)/\beta}\left(\frac{3}{2}\right)^{1/\beta}\left[\frac{\beta}{2}\frac{\Gamma(\frac{3}{2}+\frac{\beta}{2})}{\Gamma(\frac{3}{2})}\right]^{2(\beta-1)/\beta(2+\beta)} \tag{10.4.10}$$

iii) If the potential V grows faster than the harmonic oscillator, there are conflicting contributions from the centrifugal barrier in Eq. (10.2.4) and from the terms in V' whose expectation becomes larger than $m/8\pi\left\langle \sum V'(r_{ij})\right\rangle$. There are cases where the latter effect dominates. For instance, for $V = \frac{1}{2}Br^3$, the problem consists of comparing the zero-range correlation with the mean separation. From an accurate hyperspherical calculation, one gets for $m = B = 1$

$$\delta_{12} = 0.2263, \qquad \frac{9}{16\pi}\left\langle r_{12}^2\right\rangle = 0.2189. \tag{10.4.11}$$

Hence the inequality (10.4.7) is clearly violated.

iv) There are in fact good reasons to believe that the inequality (10.4.7) is inverted if $\mathrm{d}/\mathrm{d}r(V'/r) > 0$ everywhere. For perturbations around the harmonic oscillator, i.e. for $V = r^2 + \lambda w(r)$, one already has

$$\left\langle w'(r_{12}) - \tfrac{1}{2}\hat{r}_{23}\cdot\hat{r}_{12}w'(r_{23}) - \tfrac{1}{2}\hat{r}_{31}\cdot\hat{r}_{12}w'(r_{31})\right\rangle > \frac{1}{2}\left\langle\sum w'(r_{ij})\right\rangle \tag{10.4.12}$$

at first order, whereas the expectation value of $\vec{l}_\rho^{\,2}$ contributes only at second order. A numerical investigation shows that for $V = r^{2.1}$ or even $V = r^{2.01}$, one gets, indeed, the inequality $8\pi\delta_{12} > m\left\langle\sum V'(r_{ij})\right\rangle$.

Chapter 11

SOME APPLICATIONS TO BARYON SPECTROSCOPY

11.1 Introduction

In this chapter, we discuss some applications of accurate 3-body calculations to baryon spectroscopy. The selection is rather arbitrary: we come back on the Gell-Mann–Okubo mass formula and compute the quadrupole moment of the Ω^-, for instance, but do not discuss the magnetic moments. Anyhow, it is interesting to test how far one can push the NRQM to describe the baryon properties.

We shall use the handy notations

$$\begin{aligned}[q_1q_2q_3] &= \text{binding energy of } q_1, q_2, q_3, \\ (q_1q_2q_3) &= \text{mass of the baryon,} \\ (q_1q_2q_3) &= m_1 + m_2 + m_3 + [q_1q_2q_3].\end{aligned} \tag{11.1.1}$$

11.2 Ground-state baryons with central potentials

In the most elementary description of ground-state baryons, one would simply add the effective constituent masses, i.e. the masses would depend linearly upon the flavour numbers.

Now, if one introduces a central, flavour–independent potential and solves accurately the 3-body problem, one should hope to get something appreciably different. To measure to what extent this is true, let us define the scale-independent quantities

$$R_1 = \frac{2[qqq] + 2[qqs] - 4[ssq]}{[qqq] - [sss]} \tag{11.2.2}$$

and

$$R_2 = \frac{2[sss] + 2[ssq] - 4[qqs]}{[qqq] - [sss]}. \tag{11.2.3}$$

R_1 is relevant for possible deviations from the Gell-Mann–Okubo mass formula, R_1 and R_2 for the equal spacing rule of the decuplet.

R_1 and R_2 are expected to be negative, as shown in Section 8.3. The effect is of the order of 5–10% in magnitude for typical choices $m_s \lesssim m_q$, as seen in Fig. 11.1, where various power-law potentials r^β and quark mass ratios m_s/m_q are used. The ratios R_1 and R_2 were already displayed in Ref. [58] in a slightly different way. It is shown, in particular, that one hardly differentiates a 3-body Y-shape potential (see Eq. 9.3.14) from a genuinely additive linear potential.

In Fig. 11.2, we show the variations of the binding energy of qqQ as a function of the inverse of the mass m_Q of the heavy quark. The energy qqQ is almost linear in m_Q^{-1}, as conjectured in Ref. [87].

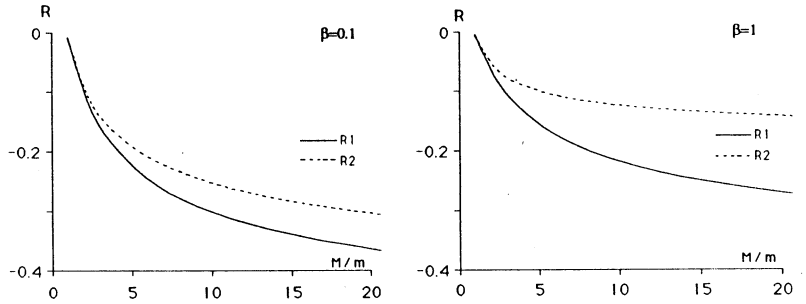

Figure 11.1: Scale independent ratios $R_1 = \{2[qqq]+2[qqQ]-4[QQq]\}/\{[qqq]-[QQQ]\}$ and $R_2 = \{2[QQQ]+2[QQq]-4[qqQ]\}/\{[qqq]-[QQQ]\}$ for the power-law potentials $\sum r_{ij}^\beta$ with $\beta = 0.1$ and $\beta = 1$, as a function of the quark mass ratio $x = M/m$.

11.3 Systematics of hyperfine splittings

If one adopts a spin–spin potential analogous to the Breit–Fermi contact term in atomic physics, namely [103]

$$V_{SS} = \frac{C}{2} \sum_{i<j} \frac{\vec{\sigma}_i \cdot \vec{\sigma}_j}{m_i m_j} \delta^{(3)}(r_{ij}) \tag{11.3.4}$$

and treats it at first order, one achieves a good phenomenological description of hyperfine splittings. In the approximation of $SU(3)_F$ flavour symmetry for the wave function, the correlation coefficients $\delta_{ij} \equiv \left\langle \delta^{(3)}(r_{ij}) \right\rangle$ are the same for all pairs in any ground-state baryon of the $SU(3)_F$ octet and decuplet, and one can derive amazing relations [103] such as

$$\begin{aligned} \Xi^* - \Xi &= \Sigma^* - \Sigma \\ 2\Sigma^* + \Sigma - 3\Lambda &= 2(\Delta - \mathrm{N}). \end{aligned} \tag{11.3.5}$$

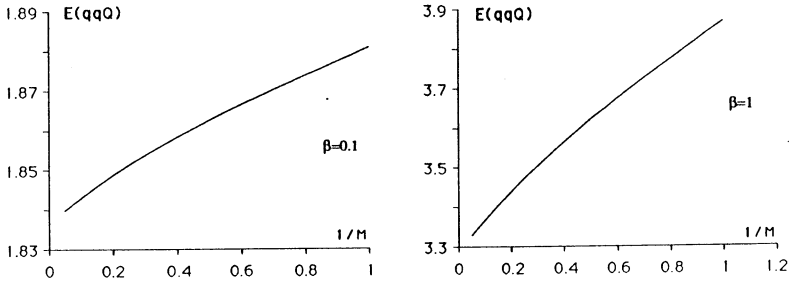

Figure 11.2: Binding energy of qqQ, as a function of the inverse mass m_Q^{-1} for the power–law potentials $\sum r_{ij}^\beta$ with $\beta = 0.1$ and $\beta = 1$.

Now, it is interesting to actually compute the correlation coefficients δ_{ij} and examine to what extent they depend on the quark i and j involved, and on the third quark.

To start with something simple, let us consider the ratio

$$R_3 = \frac{2\delta(\Omega^-)}{\Delta - N} = \frac{\delta_{ss}(sss)}{\delta_{qq}(qqq)} \left(\frac{m_q}{m_s}\right)^2 \tag{11.3.6}$$

that measures the ratio of the (non-observable) spin–spin shift $\delta(\Omega^-)$ of the Ω^- to the hyperfine splitting for ordinary baryons. Using the simple scaling laws (2.4.15), one gets

$$R_3 = \left(\frac{m_q}{m_s}\right)^{(1+2\beta)/(r2+\beta)} \tag{11.3.7}$$

For the small values $\beta \simeq 0.1$ mocking the combined effects of a Coulomb and a linear potential, the contraction of the wave function as m increases compensates a large part of the m^{-2} dependence of the spin–spin operator.

We now turn to more elaborate calculations where one has to account for the disymmetry of the wave function. First, we consider the $\Sigma - \Lambda$ mass difference, a longstanding problem in baryon spectroscopy. The ratio

$$R_4 = \frac{\Sigma - \Lambda}{\Sigma^* - \Sigma} \tag{11.3.8}$$

is experimentally $R_4 \simeq 0.41$. In the model (11.3.4), it is

$$R_4 = 2\frac{\delta_{12} - \delta_{13}(m_q/m_s)}{3\delta_{13}(m_q/m_s)} \tag{11.3.9}$$

and, as seen in Fig. 11.3, it is slightly lower than the experimental value $R_4 \simeq 0.41$, if one adopts standard values $m_s \lesssim m_q$ for the constituent masses. Note that pionic loops might improve the situation [104].

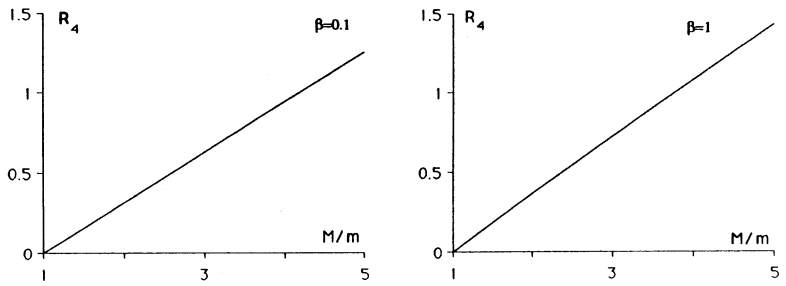

Figure 11.3: Ratio $R_4 = (\Sigma - \Lambda)/(\Sigma^* - \Sigma)$ for the power-law potentials $\sum r_{ij}^{\beta}$ with $\beta = 0.1$ and $\beta = 1$, as a function of the quark mass ratio $x = M/m$

On the other hand, the ratio

$$R_5 = \frac{2\Sigma^* + \Sigma - 3\Lambda}{2\Delta - 2\mathrm{N}} = \frac{\delta_{qq}(qqs)}{\delta_{qq}(qqq)} \tag{11.3.10}$$

which focuses on the comparison of qq correlations in qqs and qqq systems, is reasonably well reproduced. For harmonic confinement, $R_5 = 1$ since the ρ and λ oscillators decouple exactly. As seen in Fig. 11.4, with a smooth potential r^{β}, $\beta \simeq 0.1$, one accounts for the experimental value $R_5 = 1.04$ [5], whose departure from 1 was noticed by Cohen and Lipkin [102].

Similarly, the ratio

$$R_6 = \frac{\Xi^* - \Xi}{\Sigma^* - \Sigma} = \frac{\delta_{sq}(ssq)}{\delta_{sq}(qqs)} \tag{11.3.11}$$

turns out to be $R_6 \simeq 1.16$ experimentally, while a strict equality is implied by SU(6) symmetry. In the harmonic oscillator, this ratio is close to 1 but not exactly equal to 1. With a smooth confinement, one gets a larger value, as seen in Fig. 11.4. Further evidence for the Cohen–Lipkin effect is shown in Ref. [105].

11.4 Hyperfine splitting of heavy baryons

We now come back to the $\Sigma - \Lambda$ and $\Sigma^* - \Sigma$ splittings and examine how they behave if the mass of the strange quark is increased. In Fig. 11.5, we plot the value of

$$R_7 = \frac{\Sigma_Q - \Lambda_Q}{\Sigma_\infty - \Lambda_\infty}. \tag{11.4.12}$$

as a function of the ratio $x = m_Q/m_q$. In the simple model (11.3.4), it is

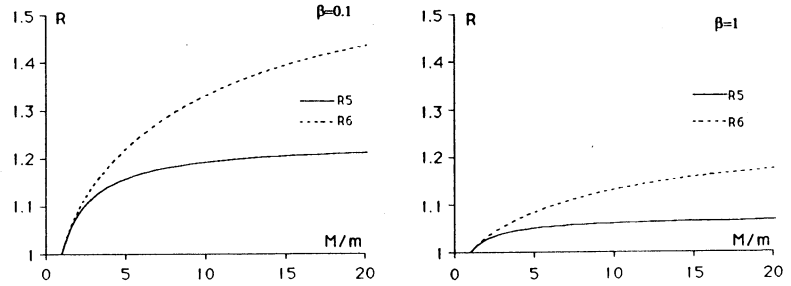

Figure 11.4: Ratios $R_5 = (2\Sigma^* + \Sigma - 3\Lambda)/(2\Delta - 2\mathrm{N})$ and $R_6 = (\Xi^* - \Xi)/(\Sigma^* - \Sigma)$ for the power-law potentials $\sum r_{ij}^{\beta}$ with $\beta = 0.1$ and $\beta = 1$, as a function of the quark mass ratio M/m

$$R_7 = \frac{M\delta_{qq}(qqQ) - m\delta_{qQ}(qqQ)}{\delta_{qq}(qq\infty)}. \tag{11.4.13}$$

The sharp variation is responsible for the observed increase from $\Sigma - \Lambda = 77$ MeV to $\Sigma_c - \Lambda_c = 168$ MeV. The Σ_b should also be unstable, thanks to its pionic decay to Λ_b.

On the other hand, the ratio

$$R_8 = \frac{\Sigma_Q^* - \Sigma_Q}{\Sigma_\infty - \Lambda_\infty} = \frac{3m}{2M}\frac{\delta_{qQ}(qqQ)}{\delta_{qq}(qq\infty)}, \tag{11.4.14}$$

where the latter expression refers to model (11.3.4), goes to zero as the quark mass m_Q increases. Thus, the decay mode $\Sigma_Q^* \to \Sigma_Q + \pi$ becomes forbidden for heavy flavours and the experimental disentangling of Σ_Q and Σ_Q^* is difficult. The value of R_8 is shown in Fig. 11.5 for simple models.

The analysis is rather simple for doubly-flavoured baryons QQq . The light quark has a reduced mass close to m_q, so that its wave function is almost independent of m_Q. It experiences the potential of a localized diquark of spin 1. Hence, one expects

$$m_Q \to \infty \quad \Longrightarrow \quad \Xi_{QQ}^* - \Xi_{QQ} \propto m_Q^{-1} \tag{11.4.15}$$

Already, Fleck [73, 7], with a central potential $V \propto r^{0.1}$ and a contact interaction (11.3.4), obtained

$$\frac{\Xi_{cc}^* - \Xi_{cc}}{\Xi^* - \Xi} \simeq 0.52, \tag{11.4.16}$$

not too far from the quark mass ratio $m_s/m_c \simeq 0.32$ which she used. The agreement would be much better for the comparison of Ξ_{cc} and Ξ_{bb}. More hyperfine splittings have been analysed recently by Anselmino et al.[105].

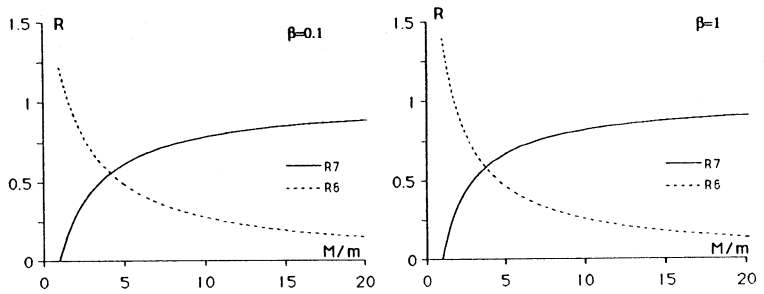

Figure 11.5: Ratios $R_7 = (\Sigma_Q - \Lambda_Q)/(\Sigma_\infty - \Lambda_\infty)$ and $R_8 = (\Sigma_Q^* - \Sigma_Q)/(\Sigma_\infty - \Lambda_\infty)$ for the power-law potentials $\sum r_{ij}^\beta$ with $\beta = 0.1$ and $\beta = 1$, as a function of the quark mass ratio M/m

11.5 Electromagnetic mass differences

In the constituent-quark model, the isospin breaking of hadron masses results from several contributions, namely

i) the quark mass difference $\delta m = m_d - m_u$;

ii) the induced change δE of the binding energy;

iii) the change in strength of the chromomagnetic interaction, that is proportional to $(m_i m_j)^{-1}$ and the variation of the correlation coefficient $\delta_{ij} = \left\langle \delta^{(3)}(r_{ij}) \right\rangle$ (more generally, the variations of the wave function, when hyperfine effects are treated beyond first order);

iv) the electromagnetic interactions between the charged quarks.

In several cases, these contributions tend to cancel each other out. This implies that they have to be computed carefully. Besides this technical aspect, this also means that the model dependence will be much amplified in the selected cases where the cancellation does not occur. For instance, Lane and Weinberg [106] have predicted much smaller splitting among Σ_c's than did de Rújula et al.[103] who used a simpler ansatz to extrapolate matrix elements from ordinary to charmed hadrons.

When comparing the above contributions *i)* and *ii)*, one is reminded that the non-relativistic approximation is never worse than for open flavours. Likewise, the electron is more relativistic in hydrogen than in positronium. If $\delta E + \delta m < 0$ when the u quark is replaced by d (contributions *iii)* and *iv)* being provisionally forgotten), we are in a paradoxal regime were the resulting hadron mass decreases as the mass of one of the constituents is increased. This is a warning that relativistic corrections are required [107].

To be specific, consider the neutron-to-proton mass difference. To zeroth order, n and p are degenerate, with a symmetric spatial wave function. If now the mass difference δm and electromagnetic interaction are switched on, small mixed-symmetry components are allowed, that can be treated perturbatively, exactly as the non-potential harmonics of Section 5.5 (the usual source of inaccuracy in this type of calculations consists of selecting *a priori* a few neighbouring states of the unperturbed Hamiltonian that are believed to mix with the main component; the Sternheimer equations of Section 5.5 are by far more powerful [50]). One can even optimize the starting point by adopting an inverse constituent mass $m^{-1} = (2m_u^{-1} + m_d^{-1})/3$ for the proton and $m^{-1} = (2m_d^{-1} + m_u^{-1})/3$ for the neutron, before implementing the corrections *i)–iv)*.

In the hyperspherical formalism, the wave function is expanded as

$$\Psi(\vec{\rho}, \vec{\lambda}) = \Psi_1 + \Psi_2 = \sum_{[L]\in S_1} \frac{u_{[L]}(\xi)}{\xi^{5/2}} \mathcal{Q}_{[L]}(\Omega_5) + \sum_{[K]\in S_2} \frac{v_{[K]}(\xi)}{\xi^{5/2}} \mathcal{P}_{[K]}(\Omega_5). \qquad (11.5.17)$$

The set S_1 contains the symmetric HH and S_2 those of mixed symmetry. The problem is first solved with S_1 only, as in Chapter 5, and then the effect of S_2 is studied by means of inhomogeneous equations similar to Eqs. (5.5.23) and (5.5.24).

Richard and Taxil [107] consider, among others, the following model

$$V = \tfrac{1}{2}\sum_{i<j}(A + Br_{ij}^\beta) \qquad (11.5.18)$$

supplemented by the spin–spin term of Eq. (11.3.4), treated perturbatively. They obtained a good fit of ground-state baryons with the parameters (all units are appropriate powers of GeV)

$$\begin{aligned} \beta = 0.1, \quad A = -8.337, \quad B = 6.9923, \quad C = 2.572, \\ m_q = 0.300 \quad m_s = 0.600, \quad m_c = 1.895. \end{aligned} \qquad (11.5.19)$$

Then SU(2) is explicitly broken by using different constituent masses for u and d, $m_u = 0.300$ and $m_d = 0.313$ GeV, with the results displayed in Table 11.1. Also

Table 11.1: Various contributions (in MeV) to the neutron-to-proton mass difference in two non-relativistic models

β	δm	Central δE	Chromomag.	Electrostatic	Magnetic	Total
0.1	13	−8.5	−2.7	−0.7	0.2	1.3
1.0	2	−0.2	−0.4	−0.3	0.002	1.2

shown are the values obtained with a linear potential model ($\beta = 1$), for which the fit of experimental splittings suggested a much smaller δm. These two models predict very similar $m_n - m_p$ but differ widely in the charm sector. The situation for charmed baryons is analysed by Capstick [106] with references to earlier works.

11.6 The charge radius of the neutron

So far, the applications of the spin–spin potential (11.3.4) were restricted to mass splittings such as Δ–N. We now look at the effect of the hyperfine interactions on the wave function of the neutron. The spin–spin potential pushes the d quarks apart a little. In more technical terms, some mixed-symmetry components are introduced into the wave function.

The wave-function decomposition of Eq. (11.5.17) is now extended as

$$\Psi = \Psi_1 + \Psi_2 + \Psi_3. \tag{11.6.20}$$

The components Ψ_1 and Ψ_2 are associated with a symmetric spin–isospin wave function. The dominent component Ψ_1 is also symmetric in space variables, whereas Ψ_2 is of mixed symmetry and thus vanishes as $\delta m = m_d - m_u$ goes to zero. The third component Ψ_3 is induced by the spin–spin interaction. It is symmetric, with both space and spin–isospin parts of mixed symmetry, as per eq. (3.5.34). It produces a small difference between the r.m.s. radii $\langle r_d^2\rangle$ and $\langle r_u^2\rangle$ and thus a non-vanishing charge radius squared

$$R_n^2 = \left\langle \sum_i e_i r_i^2 \right\rangle. \tag{11.6.21}$$

If one neglects here isospin breaking, it is given by

$$R_n^2 = \frac{e}{6}\left\langle \vec{\lambda}^{\,2} - \vec{\rho}^{\,2} \right\rangle. \tag{11.6.22}$$

At first approximation, Ψ_1 is dominated by its hyperscalar componenent $\pi^{-3/2}u_0(\xi)/\xi^{5/2}$, and Ψ_3 by its lowest hyperspherical harmonics with grand orbital momentum $L = 2$

$$\Psi_3 = \frac{w_2(\xi)}{\xi^{5/2}}\mathcal{P}_2(\Omega_5), \tag{11.6.23}$$

where $\mathcal{P}_2(\Omega_5)$ denotes the mixed-symmetry pair made out of $2\pi^{-3/2}(\vec{\lambda}^{\,2} - \vec{\rho}^{\,2})/\xi^2$ and $4\pi^{-3/2}(\vec{\lambda}\cdot\vec{\rho})/\xi^2$ appropriately combined with the spin and isospin wave functions. This gives

$$R_n^2 = \frac{e}{6\sqrt{2}}\int_0^\infty u_0(\xi)\xi^2 w_2(\xi)d\xi, \tag{11.6.24}$$

and, when the spin–spin interaction (11.3.4) is treated at first order,

$$w_2''(\xi) - \frac{63}{4}\frac{w_2(\xi)}{\xi^2} + m\left[E_0 - V_{0,0}(\xi)\right] = 12\sqrt{2}\pi^{-2}C\frac{u_0(\xi)}{m\xi^3}. \tag{11.6.25}$$

Once again, equations of this type are not equivalent to a mixing between closest neighbours of the unperturbed Hamiltonian.

With the model given in Eqs. (11.5.18) and (11.5.19), one obtains $R_n^2 = -0.047$ e.fm^2 and slightly larger values with sharper confinement. The experimental value [5], which is $R_n^2 = -0.10$ e.fm^2, probably receives contributions from other effects. For instance, in chiral bag models [14, 104], the neutron often consists of a proton-like core surrounded by a π^- cloud.

11.7 The quadrupole moment of the Omega

In fact the spin–spin potential (11.3.4) which we repeatedly used throughout this chapter is only a part of the chromomagnetic interaction

$$v_{\text{c.m.}} = V_{\text{SS}}\vec{\sigma}_1\cdot\vec{\sigma}_2 + V_{\text{T}}S_{12}, \tag{11.7.26}$$

where $S_{12} = 3\vec{\sigma}_1\cdot\hat{r}\vec{\sigma}_2\cdot\hat{r} - \vec{\sigma}_1\cdot\vec{\sigma}_2$ is the tensor operator. The tensor component V_{T} plays a role for orbital momenta $l > 0$. In any potential model that includes only a vector-exchange piece V_{V} and a scalar-exchange piece V_{S}, the ratio of tensor to spin–spin is well defined. In the particular one-gluon model [103] for equal masses

$$\begin{aligned} V_{\text{SS}} &= \frac{C}{2m^2}\sum_{i<j}\vec{\sigma}_i\cdot\vec{\sigma}_j\delta^{(3)}(r_{ij}) \\ V_{\text{T}} &= \frac{3}{8\pi}\frac{C}{2m^2}\sum_{i<j}\frac{S_{ij}}{r_{ij}^3} \\ C &= \frac{8\pi\alpha_s}{9}. \end{aligned} \tag{11.7.27}$$

In Ref. [108] are listed the tests of chromomagnetism in baryon spectroscopy. Let us discuss here one example, the quadrupole deformation of Ω^-.

The effect was first mentioned by Goldhaber and Sternheimer [109], who speculated on the fine and hyperfine structure of exotic atoms consisting of an atomic nucleus and an Ω^-. The splitting pattern would provide a measurement of the quadrupole moment as well of the magnetic moment of the Ω^-. In Ref. [109], a quadrupole moment $Q = 1\,\text{fm}^2$ was assumed for numerical illustration, on the grounds that the Ω^- has a mass comparable to that of the deuteron and hence might also have Q of the same order of magnitude. In fact much smaller values of Q are obtained from current quark models [108, 110].

Let us adopt the same familiar notation $^{2S+1}\ell_J$ as in quarkonium spectroscopy. The analogue of expansions (11.5.17) and (11.6.20) is [110]

$$\Psi = \sum_n \frac{u^{(n)}(\xi)}{\xi^{5/2}}\mid {}^4\text{S}^{(n)}{}_{3/2}\rangle + \sum_p \frac{w^{(p)}(\xi)}{\xi^{5/2}}\mid {}^4\text{D}^{(p)}{}_{3/2}\rangle + \sum_q \frac{u^{(q)}(\xi)}{\xi^{5/2}}\mid {}^2\text{S}^{(q)}{}_{3/2}\rangle, \tag{11.7.28}$$

where n, p and q denote the successive hyperspherical harmonics of given spin and orbital momentum content. For an Ω^- with spin $S_z = 3/2$, one needs only

$$\mid {}^4\text{S}^{(0)}{}_{3/2}\rangle = \pi^{-3/2}\mid \tfrac{3}{2},\tfrac{3}{2}\rangle, \tag{11.7.29}$$

where the spin 3/2 wave function is given in Section 3.6, and

$$\begin{aligned} \mid {}^4\text{D}^{(0)}{}_{3/2}\rangle = \frac{\sqrt{12}}{\pi^{3/2}\xi^2}\Big[&\sqrt{\tfrac{2}{5}}(\rho_+^2 + \lambda_+^2)\mid \tfrac{3}{2},-\tfrac{1}{2}\rangle \\ &- \sqrt{\tfrac{4}{5}}(\rho_+\rho_3 + \lambda_+\lambda_3)\mid \tfrac{3}{2},\tfrac{1}{2}\rangle \\ &+ \sqrt{\tfrac{2}{15}}(\rho_3^2 + \rho_+\rho_- + \lambda_3^2 + \lambda_+\lambda_-)\mid \tfrac{3}{2},\tfrac{3}{2}\rangle\Big], \end{aligned} \tag{11.7.30}$$

where $\rho_\pm = \mp(\rho_x \pm \rho_y)/\sqrt{2}$ and $\rho_3 = \rho_z$ are the usual standard components of $\vec{\rho}$. Indeed, the unperturbed wave function is dominated by its hyperscalar component and the quadrupole operator

$$Q_{zz} = \sum_i e_i(3z_i^2 - r_i^2) = \frac{e_s}{2}(3\rho_3^2 - \vec{\rho}^{\,2} + 3\lambda_3^2 - \vec{\lambda}^{\,2}) \qquad (11.7.31)$$

connects $|\,^4S^{(0)}_{3/2}\rangle$ only with $|\,^4D^{(0)}_{3/2}\rangle$. We end with equations very similar to those involved for the neutron charge radius

$$\begin{aligned} Q_\Omega &= \langle Q_{zz}\rangle = \frac{e_s}{\sqrt{10}}\int_0^\infty u_0\xi^2 w_0 \mathrm{d}\xi \\ w_0'' &- \frac{63}{4\xi^2}w_0 + m_s\,[E_0 - V_{0,0}]\,w_0 = \frac{C}{m_s}\frac{96\sqrt{2}}{\pi^2\sqrt{5}}\frac{u_0(\xi)}{\xi^3}. \end{aligned} \qquad (11.7.32)$$

Restricting the quadrupole deformation to a mixing of closest unperturbed states is exact for harmonic confinement, but leads us to underestimate Q_Ω by 20% for a smooth potential $\beta = 0.1$. The latter model, with the parameters (11.5.19), gives $Q_\Omega = 0.004\,\mathrm{fm}^2$.

Note that the dependence on the exponent β is rather simple, if one restricts oneself to power-law potentials of the type (11.5.18). The strength of confinement, B, is determined from any excitation energy, for instance the orbital splitting $E \equiv E(2^+) - E(0^+)$, while the strength of hyperfine corrections is measured by the mass shift $\Delta M = \langle 3V_{SS}\rangle$ of the ground state. One can easily show [110] that Q_Ω scales as $\Delta M/(E^2 m_s)$ (and, in turn, ΔM is related by scaling to measurable mass shifts like $\Delta - \mathrm{N}$). In other words, choosing a confining potential fixes the reduced quadrupole moment $q_\Omega = Q_\Omega E^2 m_s/\Delta M$, and q_Ω varies by less than a factor of 2 when going from a very smooth to a very sharp confinement. The phenomenological uncertainties come mainly from the choice of strengths B and C, i.e. from different adjustments of excitation energies and hyperfine splittings. The same scaling laws also hold for the charge radius of the neutron.

11.8 Outlook

As already said, some of the applications presented in this review are probably too detailed with regard to the crudeness of the non-relativistic model which is assumed. On the other hand, some qualitative conclusions very likely will hold beyond the NRQM, for instance the regularities of the mass spectrum in flavour space, a consequence of the universality of the interquark potential.

Beyond ordinary mesons and baryons, a key issue in hadron spectroscopy is the existence of multiquark states. The main difficulty lies in extrapolating the interquark forces from the $q\bar{q}$ and qqq sectors to more complicated systems. Another difficulty will be to treat correctly the 4-body (or 5-, or 6-body) problem, with, in particular,

a proper account for the coupling to the dissociation channels. It is hoped that this introduction to 3-body techniques will serve as a training ground for checking or improving multiquark calculations, in the same way as the recent refinements on the 2-body systems have been a source of progress for the 3-body problem.

Acknowledgements

I would like to thank many colleagues for enlightening discussions on baryon spectroscopy during recent years: J.L. Ballot, S. Boukraa, M. Fabre de la Ripelle, D. Gromes, N. Isgur, G. Karl, D.B. Lichtenberg, E. Predazzi, J. Stubbe, A. Turbiner, and many others, with a special mention to my collaborators, who have elaborated most of the results presented here: J.-L. Basdevant, W.N. Cottingham, S. Fleck, C. Gignoux, H. Grosse, P. Hasenfratz, H. Høgaasen, R. Horgan, J. Kuti, A. Martin, B. Silvestre-Brac, P. Taxil, K. Tsu, and S. Zouzou. I have a deep gratitude to A. Martin for his advice on rigorous methods, to C. Gignoux for his decisive help on the Faddeev equations, to Sonia Fleck for her careful reading of the manuscript and many suggestions, and to Susan Leech O'Neale for her assistance in improving the english and the typography of the manuscript. Finally, I thank the members of the Theory Division at CERN, and, in particular J. Ellis, for their warm hospitality during the academic year 1990/91.

Bibliography

[1] See for example the Proceedings of the last *Few-Body Conferences* for reviews and further references:
Eugene (Oregon) 1980: *The Few-Body Problem*, ed. F.S. Levin, *Nucl. Phys.* **A353** (1981);
Karlsruhe (Germany) 1983: *Few-Body Problems in Physics*, ed. B. Zeitnitz, *Nucl. Phys.* **A416** (1984);
Tokyo and Sendai (Japan) 1987: *Few-Body Systems in Particle and Nuclear Physics*, ed. T. Sasakawa et al., *Nucl. Phys.* **A463** (1987);
Dubna (USSR) 1987: *Int. Conf. on the Theory of Few-Body and Quark Hadronic Systems*, JINR, Dubna (1987);
Vancouver (Canada) 1989: *Few-Body Problems in Physics*, ed. H.W. Fearing, *Nucl. Phys.* **A508** (1990).

[2] T.K. Lim, in Proc. Karlsruhe 1983, *op. cit.*.

[3] See for example J.J.J. Kokkedee, *The Quark Model* (Benjamin,N.Y.,1964);
M. Gell-Mann and Y. Ne'eman, *The Eightfold Way* (Benjamin, N.Y.,1964);
D. Flammm and F. Schöberl, *An Introduction to the Quark Model of Elementary Particles* (Gordon and Breach, N.Y., 1983).

[4] O.W. Greenberg, *Phys. Rev. Lett.* **13** (1964) 598.

[5] Particle Data Group, *Review of Particle Properties*, *Phys. Lett.* **B239** (1990).

[6] A.J.G. Hey and R.L. Kelly, *Phys. Rep.* **96** (1986) 71.

[7] S. Fleck and J.-M. Richard, *Progr. Theor. Phys.* **82** (1989) 760.

[8] S. Fleck and J.-M. Richard, *Part. World* **1** (1990) 67.

[9] B.J. Bjorken, in *Proc. Int. Conf. on Hadron Spectroscopy*, College Park, 1985, ed. S. Oneda (A.I.P., 1985).

[10] A. Martin, in *Heavy Flavours and High Energy Collisions in the 1–100 TeV Range*, Proc. Erice Workshop (1988), ed. A. Ali and L. Cifarelli (Plenum, N.Y. 1989).

[11] For a review and references, see for example
P. Kroll, in *The Elementary Structure of Matter*, Proc. Les Houches Workshop, ed. J.-M. Richard et al. (Springer Verlag, Berlin, 1988);
S. Fleck, *ibidem*;
A. Martin, in *Proc. Workshop on Diquarks*, Turin, 1988, ed. M. Anselmino and E. Predazzi (World Scientific, Singapore, 1989).

[12] W. Gloeckle, *The Quantum Mechanical Few-Body Problem* (Springer, Berlin, 1983);
E.W. Schmid and H. Ziegelmann, *The Quantum Mechanical 3-body Problem*, (Pergamon Press, Oxford, 1974).

[13] W. Lucha, F. Schöberl and D. Gromes, *Phys. Rep.* **203** (1991) 127.

[14] P. Hasenfratz and J. Kuti, *Phys. Rep.* **42** (1978) 75;
C.E. DeTar and J.F. Donoghue, *Ann. Rev. Nucl. Part. Sci.* **33** (1983) 235.

[15] L.J. Reinders, H.R. Rubinstein and S. Yazaki, *Phys. Rep.* **127** (1985) 1;
S. Narison, *QCD Spectral Sum Rules*, World Scientific Lecture Notes in Physics, **vol. 43** (Singapore, 1989).

[16] See, e.g., *Lattice 88*, Proc. 1988 Symp. on Lattice Field Theory, Fermilab, ed. A.S. Kronfeld and P.B. Mackenzie, North-Holland (*Nucl. Phys. B*, Proc. Suppl. **9**, 1989);
Lattice 89, Proc. 1989 Symp. on Lattice Field Theory, Capri, ed. N. Cabbibo et al., North-Holland (*Nucl. Phys. B*, Proc. Suppl. **17**, 1990).

[17] C. Quigg and J.L. Rosner, *Phys. Rep.* **56** (1979) 167.

[18] H. Grosse, A. Martin, *Phys. Rep.* **60** (1979) 341.

[19] A. Martin, in *Proc. Int. Universitätswochen für Kernphysik*, Schladming, Austria, 1986, ed. H. Latal and H. Mitter (Springer–Verlag, Berlin, 1987).

[20] H. Grosse and A. Martin, book in preparation.

[21] See for example A. Messiah, *Mécanique Quantique* (Dunod, Paris,1972).

[22] See for example R. Courant and D. Hilbert, *Methods of Mathematical Physics* (Wiley, N.Y., 1953).

[23] C. Quigg and J.L. Rosner, *Comments Nucl. Part. Phys.* **8** (1978) 11.

[24] References can be traced back from recent contributions:
R.S. Friedman, M.J. Jamieson and S.C. Preston, *Comput. Phys. Commun.* **58** (1990) 17;
F. Salviat and R. Mayol, *ibidem* **62** (1991)65;
U. Larsen, *Phys. Lett.* **105A** (1984) 179.

[25] D.R. Hartree, *The Calculation of Atomic Structures* (Wiley, N.Y., 1957).

[26] S. Boukraa and J.-L. Basdevant, *J. Math. Phys.* **30** (1989) 1060.

[27] K.J. Miller and M.G. Olsson, *Phys. Rev.* **D25** (1982) 2383.

[28] M. Abramowitz and I.A. Stegun (eds.), *Handbook of Mathematical Functions with Formulas, Graphs and Mathematical Tables* (Dover, N.Y., 1964).

[29] See for example K. Yang and M. de Liano, *Am. J. Phys.* **57** (1989) 57;
H. Grosse and A. Martin, Ref. [20].

[30] M. Baumgartner, H. Grosse and A. Martin, *Phys. Lett.* **146B** (1984) 363;
Nucl. Phys. **B254** (1985) 528.

[31] A.K. Common and A. Martin, *Europhys. Lett.* **4** (1987) 1349;
A. Martin and J. Stubbe, *ibidem* **14** (1991) 287.

[32] A. Martin, J.-M. Richard and P. Taxil, *Nucl. Phys.* **B329** (1990) 327.

[33] See, e.g., W. Thirring, *A Course in Mathematical Physics*, **Vol. 3** (Springer Verlag, 1981).

[34] R.H. Dalitz, in *High Energy Physics*, Proc. École d'Été de Physique Théorique, ed. C. DeWitt and M. Jacob (Gordon and Breach, N.Y.,1965);
R.H. Dalitz, in *Baryon Resonances 73*, Proc. Purdue Conf., 1973, ed. E.C. Fowler (Purdue University, West Lafyette, Indiana, 1973).

[35] R.R. Horgan and R.H. Dalitz, *Nucl. Phys.* **B66** (1973) 135; **B71** (1974) 546;
R.R. Horgan *Nucl. Phys.* **B71** (1974) 514;
M. Jones, R.R. Horgan and R.H. Dalitz, *Nucl. Phys.* **B129** (1977) 45;
R.R. Horgan, in *Proc. Topical Conf. on Baryon Resonances*, Oxford, 1976, ed. R.T. Ross and D.H. Saxon (Rutherford Lab., Chilton, U.K., 1976).

[36] N. Isgur and G. Karl, *Phys. Lett.* **72B** (1977) 109; **74B** (1978) 353;
Phys. Rev. **D18** (1978) 4187.

[37] D. Gromes and I.O. Stamatescu, *Z. Phys.* **C3** (1979) 43.

[38] R.E. Cutkosky and R.E. Hendrick, *Phys. Rev.* **D16** (1977) 793; **D16** (1977) 793; **D16** (1977) 2902.

[39] D. Faiman and D.E. Plane, *Nucl. Phys.* **B50** (1972) 379;
D. Faiman and A. Hendry, *Phys. Rev.* **180** (1969) 1609.

[40] Yu.A. Simonov, *Sov. J. Nucl. Phys.* **3** (1966) 461; **7** (1968) 722.

[41] For recent reviews on QCD, see for example:
A. Peterman, *Phys. Rep.* **53** (1979) 157;
A.H. Mueller, *Phys. Rep.* **73** (1981) 237;
A.J. Buras, *Phys. Rep.* **52** (1980) 199;
G. Altarelli, *Phys. Rep.* **81** (1982) 1;
F.J. Yndurain, *QCD* (Springer–Verlag, N.Y., 1982).

[42] T.A. Brody and M.A. Moshinsky, *Tables of Transformation Brackets for Nuclear Shell Model Calculations* (2^{nd} edit.) (Gordon and Breach, 1967);
see also, R.D. Lawson, *Theory of the Nuclear Shell Model* (Oxford University Press, 1980), and references therein.

[43] J. Raynal, *Nucl. Phys.* **A259** (1976) 272.

[44] B. Silvestre-Brac, *J. de Phys. (Paris)* **46** (1985) 1087.

[45] R.R. Horgan, *J. Phys. G* **2** (1976) 625.

[46] M.A. Abdel-Raouf, *Phys. Rep.* **84** (1982) 163.

[47] S. Zouzou et al., *Z. Phys.* **32** (1982) 427;
L. Heller, in *The Elementary Structure of Matter*, Proc. Les Houches Workshop, 1987, ed. J.-M. Richard et al.(Springer–Verlag, Berlin, 1988);
H.J. Lipkin, *Phys. Lett.* **B172**, 242 (1986).

[48] V. Fock, *Z. Phys.* **63** (1930) 855;
see, also, J. Dias de Deus, A.B. Henriques and J.M.R. Pulido, *Z. Phys.* **C7** (1981) 157.

[49] M. Moshinsky, *The Harmonic Oscillator in Modern Physics : from Atoms to Quarks* (Gordon and Breach, N.Y., 1969).

[50] A. Turbiner, private communication.

[51] N. Papanicolaou and N. Spathis, *J. Phys.* **G11** (1985) 149.

[52] L.M. Delves, *Nucl. Phys.* **9** (1959) 391; **20** (1962) 268.

[53] J.L. Ballot and M. Fabre de la Ripelle, *Ann. Phys. (N.Y.)* **127** (1980) 62;
M. Fabre de la Ripelle and J. Navarro, *Ann. Phys. (N.Y.)* **123** (1979) 185;
M. Fabre de la Ripelle, *Ann. Phys. (N.Y.)* **147** (1983) 281;
M. Fabre de la Ripelle, *Few–Body Systems* **1** (1986) 181.

[54] M.I. Haftel and V.B. Mandelzweig, *Ann. Phys. (N.Y.)* **150** (1983) 48;
Phys. Lett. **120A** (1987) 232; *Phys. Rev.* **A38** (1988) 5995;
N. Barnea and V.B. Mandelzweig, *Phys. Rev.* **A41** (1990) 5209;
V.B. Mandelzweig, *Phys. Lett.* **80A** (1980) 361.

[55] A.B. Guimares, H.E. Coehlo and R. Chanda, *Phys. Rev.* **D24** (1981) 1343;
A.T. Aerts and L.H. Heller, *Phys. Rev.* **D23** (1981) 185; **D25** (1982) 1365;
Phys. Lett. **221B** (1989) 194;
E.V. Inopin and A.E. Inopin, *Sov. J. Nucl. Phys.* **51** (1990) 300;
J.-L. Basdevant and P. Boukraa, *Z. Phys.* **C30** (1986) 103;
P. Hasenfratz et al., Ref. [70]
J.-M. Richard, Ref. [90];
J.-M. Richard and P. Taxil, Ref. [58];
A.M. Badalyan, *Phys. Lett.* **199B** (1987) 267.

[56] C. Müller, *Spherical Harmonics*, Lecture Notes in Mathematics, vol.**17** (Springer Verlag, Berlin, 1966).

[57] W. Zickendraht, *Ann. Phys. (N.Y.)* **35** (1965) 38;
J.M. Levy-Leblond and M. Levy-Nahas, *J. Math. Phys.* **6** (1965) 1571.

[58] J.-M. Richard and P. Taxil, *Ann. Phys. (N.Y.)* **150** (1983) 267.

[59] For a review on Faddeev equations, see E. Hadjimichael, *Int. Rev. of Nucl. Phys.* (World Scientific, Singapore) **3** (1985) 1.

[60] J. Giraudoux, *La guerre de Troie n'aura pas lieu* (Grasset, Paris).

[61] B. Silvestre-Brac, C. Gignoux, *Phys. Rev.* **D32** (1985) 743.

[62] H.P. Noyes, in *Three-Body Problem in Nuclear and Particle Physics*, ed. J.C.S. MacKee and P.M. Rolph (North-Holland, Amsterdam, 1970);
H.P. Noyes and H. Fiedeldey, in *Three-Particle Scattering in Quantum Theory*, ed. J. Gillespie and J. Nuttall (Benjamin, N.Y., 1968).

[63] S.P. Merkuriev, *Nucl. Phys.* **A233** (1974) 395;
C. Gignoux, A. Laverne and S.P. Merkuriev, *Phys. Rev. Lett.* **33** (1974) 1350;
S.P. Merkuriev, C. Gignoux and A. Laverne, *Ann. Phys. (N.Y.)* **99** (1976) 30.

[64] C. Gignoux and A. Laverne, *Phys. Rev. Lett.* **29** (1972) 436; *Nucl. Phys.* **A203** (1973) 597.

[65] R. Omnes, in *Les Réactions Nucléaires à Trois Corps*, $9^{ième}$ Cours de Perfectionnement de l'Association Vaudoise des Chercheurs en Physique, Zermatt, April 1967 (Institut de Physique Nucléaire, Lausanne, 1967).

[66] C. Gignoux, private communication.

[67] *A European Hadron Facility*, Proc. Mainz Conf., ed. Th. Walcher, *Nucl. Phys.* **B279** (1987);
Proc. of a Workshop on Science at the KAON Factory, July 90, ed. D.R. Gill (Triumf, Vancouver, 1991).

[68] D.B. Lichtenberg, W. Namgung, E. Predazzi and J.G. Wills, *Phys. Rev. Lett.* **48** (1982) 1653.

[69] A. Martin, *Z. Phys.* **C32** (1986) 359.

[70] H.G. Dosch and V.F. Müller, *Nucl. Phys.* **B116** (1976) 470;
D. Gromes and I.O. Stamatescu, Ref. [37];
P. Hasenfratz et al., *Phys. Lett.* **94**(1980) 401;
J. Carlson, J. Kogut and V.R. Pandharipande, *Phys. Rev.* **D27** (1983) 233;
D28 (1983) 2807.

[71] S. Fleck, B. Silvestre–Brac and J.-M. Richard, *Phys. Rev.* **D38** (1988) 1519.

[72] J.L. Ballot, M. Fabre de la Ripelle and J.S. Levinger, *Phys. Rev.* **C26** (1982) 2301.

[73] S. Fleck, Thesis, Université Joseph Fourier, Grenoble (1988).

[74] E. Eichten and K. Gottfried, *Phys. Lett.* **66B** (1977) 286.

[75] K.L. Bowler et al., *Phys. Rev.* **D24** (1981) 197.

[76] R.H. Dalitz, R.R. Horgan and L.J. Reinders, *J.Phys.G* **3** (1977) L195.

[77] D. Gromes and I.O Stamatescu, *Nucl.Phys.* **B112** (1976) 213.

[78] N. Isgur and G. Karl, *Phys.Rev.* **D19** (1979) 2653.

[79] J.-M. Richard and P. Taxil, *Nucl. Phys.* **B329** (1990) 310.

[80] H. Grosse, A. Martin, J.-M. Richard and P. Taxil, in *Proc. 23rd Int. Conf. High Energy Physics*, Berkeley, 1986, ed. S.C. Loken (World Scientific, Singapore, 1987).

[81] K.C. Bowler and B.F. Tynemouth, *Phys. Rev.* **D27** (1983) 662.

[82] H. Høgaasen and J.-M. Richard, *Phys. Lett.* **B124** (1983) 520.

[83] J.-P. Ader, J.-M. Richard and P. Taxil, *Phys.Rev.* **D25** (1982) 2370.

[84] S. Nussinov *Phys. Rev. Lett.* **51** (1983) 2081.

[85] J.-L. Basdevant, A. Martin and J.-M. Richard, *Nucl. Phys.* **343** (1990) 60.

[86] J.-L. Basdevant, A. Martin and J.-M. Richard, *Nucl. Phys.* **343** (1990) 69.

[87] A. Martin, *Phys. Lett.* **103B** (1981) 51.

[88] S. Nussinov, *Phys. Rev. Lett.* **52** (1984) 966;
J.-M. Richard and P. Taxil, *Phys. Rev. Lett.* **54** (1985) 847;
E. Lieb, *Phys. Rev. Lett.* **54** (1985) 1987;
A. Martin, J.-M. Richard and P. Taxil, *Phys. Lett.* **176B** (1986) 224.

[89] O.W. Greenberg and H.J. Lipkin, *Nucl. Phys.* **A370** (1981) 349.

[90] J.-M. Richard, *Phys.Lett.* **100B** (1981) 515.

[91] J.-M. Richard, *Phys. Lett.*, **B139** (1984) 408.

[92] A. Martin and J.-M. Richard, *Phys. Lett.* **B185** (1987) 426.

[93] J.-M. Richard and P. Taxil, *Phys. Lett.* **B128** (1983) 453.

[94] M. Maltman and N. Isgur, *Phys. Rev.* **D22** (1980) 1701.

[95] R.L. Hall and H.R. Post, *Proc. Phys. Soc.* **90**(1967) 381.

[96] A. Martin, *Helv. Phys. Acta* **63** (1990) 616.

[97] H.J. Lipkin, *Phys. Lett.* **B171** (1986) 293.

[98] J.-M. Richard, *Phys. Lett.* **B255** (1991) 435.

[99] R.A. Bertlmann and A. Martin, *Nucl. Phys.* **B168**(1980) 111.

[100] J. Hiller, J. Sucher and G. Feinberg, *Phys. Rev.* **A18** (1978) 2399.

[101] M. Hoffmann–Ostenhof, T. Hoffman–Ostenhof and W. Thirring, *J. Phys.* **B11** (1978) L571.

[102] I. Cohen and H.J. Lipkin, *Phys. Lett.* **B106** (1981) 119.

[103] A. de Rújula, H. Georgi and S.L. Glashow, *Phys. Rev.* **D12** (1975) 2060.

[104] W.N. Cottingham, K. Tsu and J.-M. Richard, *Nucl. Phys.* **B179** (1981) 541
F. Myhrer, G.E. Brown and Z. Xu, *Nucl. Phys.* **A362** (1981) 317.

[105] M. Anselmino, D.B. Lichtenberg and E. Predazzi, *Z. Phys.* **C48** (1990) 605.

[106] S. Coleman and S.L. Glashow, *Phys. Rev. Lett.* **6** (1961) 423;
K Lane and S. Weinberg, *Phys. Rev. Lett.* **37** (1976) 717;
N. Isgur, *Phys. Rev.* **D21** (1980) 779;
W.Y.P. Hwang and D.B. Lichtenberg, *Phys. Rev.* **D35** (1987) 3526;
S. Capstick, *Phys. Rev.* **D36** (1987) 2800;
W. Lucha et al.Ref. [13].

[107] W. Celmaster, *Phys. Rev. Lett.* **34** (1976) 1042;
D. Flamm, F. Schöberl and H. Uemats, *Phys. Rev.* **D36** (1987) 2176;
J.-M. Richard and P. Taxil, *Z. Phys.* **C26** (1984) 421.

[108] N. Isgur, G. Karl and R. Koniuk, *Phys. Rev.* **D25** (1982) 2394.

[109] R.M. Sternheimer and M. Goldhaber, *Phys. Rev.* **A8** (1973) 2207.

[110] J.-M. Richard, *Z. Phys.* **12** (1982) 369.

Contents

List of Figures

List of Tables

Imprimé au CERN. Prix : 3.00 Fr.